$$(30) \qquad \bar{\psi} - \bar{\psi}_o \geq (\rho_m - \rho_B)gd + \frac{\pi G'd}{D}$$

The implementation of this employs the dimensionless graph

$$(31) \qquad \Delta P_D = \frac{4\pi Kh}{q\mu}(\bar{\psi} - \bar{\psi}_o) = -\,Ei(-\frac{r_D^2}{4})$$

as

$$\Delta P_D \quad \text{versus} \quad r_D = \quad \phi_o \mu c r^2/Kt$$

as shown in Figure 7.

The step-by-step process is as follows:

Step 1

In field units, defined below, calculate the value of

$$(32) \qquad \Delta P_D = \frac{Kh}{2+20.6q\mu}(0.052(\rho_m - \rho_B)d + 3.33 \times 10^{-3}\frac{G'd}{D})$$

using 8.6 lb/gal for ρ_m, 8.4 lb/gal for ρ_B, 10 lb/100 ft^2 for G', 11 inches for D, and design values for all other parameters.

Step 2

Draw a horizontal line at this value of ΔP_D on the graph of Figure 7 and read off the value of r_D at the intersection of this line and the curve. This defines a value of r_D where

$$(33) \qquad r_D = \sqrt{\phi_o \mu c r^2/Kt}$$

Step 3

Using the numerical value of r_D found in Step 2 compute the initial estimate for r by solving Eq.(33) for r

$$(34) \qquad r = r_D \cdot \sqrt{2.31Kt/\phi_o \mu c}$$

along with design values for other parameters. This is the preliminary radius of investigation. Here the symbols and units are:

q = injection rate (gpm)

ϕ_o = injection zone porosity (fraction)

μ = brine viscosity (cp)

c = effective rock/fluid compressibility (psi^{-1})

K = effective permeability (md)

t = design lifetime of injection well (at rate q) (years)

r = radius from well (ft.)

h = injection zone thickness (ft)

ρ_m = minimum mud density (8.6 lb/gal)

ρ_B = brine density (8.4 lb/gal) (mean)

G' = effective minimum gel strength (assumed) 10 $lb/(100ft^2)$

d = depth to injection zone (ft)

D = largest hole diameter (assumed) 11 inches

Now this assigns a radius value, r_{1A}, (in feet) and we then must seek out records on every abandoned well within this circle. If it is ascertained that all such holes were rotary drilled with mud then we should assign a new effective gel strength of 400 $lb/(100ft^2)$ and use actual hole diameters to recompute ΔP_D. In this calculation we can use the reported mud density from the well record if the depth of the abandoned hole is not much greater than the depth, d, of the injection zone. This is because even though segregation of heavier solids to near bottom hole has occurred, there is still nearly the full weight of the column above the injection zone. However, if the abandoned well depth is much greater than depth to injection zone only bentonite mud remains in the hole above the injection zone level and we retain 8.6 lb/gal as mud weight in our calculation for ΔP_D.

If any well located by this record search was drilled with cable tools, or air-rotary, this well must be put on the list for plugging if adequate proof of plugging is not established.

Now out of the list of new ΔP_D values, computed as just described, we select the smallest and again draw a line on the P_D vs r_D graph at this value of ΔP_D. This will intersect the curve at a new, smaller value of r_D. This is used in Eq.(34) to compute a new value of $r = r_{2A}$. Now every well within this "radius of endangered influence" must be examined for record of adequate plugging. Of course, where adequate plugging is not clearly demonstrated, these wells must be re-entered and plugged.

Thus, the pre-construction area of review process we propose differs little from that described by Barker (1981). However, we stress that values we assign for mud density and effective gel strength in abandoned holes differ significantly from those identified by Barker.

Post Construction Area of Review

The post construction area of review process we propose is designed to exploit the pressure-flow rate transient history of the injection well to define values for all pertinent injection zone parameters. Ideally, we would propose use of a simulator, such as that constructed for this study, and carry out a history match of injection well bottom-hole pressure versus time, for the recorded injection rate history over a long period of time, by adjusting parameters in the simulator.

Such techniques are widely used in the petroleum industry and are often complemented with short-term pressure transient testing. For example, Payne (1985) describes a technique for identifying effects of "no-flow" boundaries on pressure transient data when a well is shut-in and Yaxley (1985) provides similar procedures for partially-sealing faults.

If such a history match is successfully carried out, then the simulator can be used to forecast the onset of leaking of abandoned wells just as we have in our case studies. This reassessment may call for re-evaluation of abandoned wells previously considered to be outside the region of endangering influence.

We caution that a major limitation is that these history matching or pressure transient testing methods are "non-directional" when carried out with data from only one well. Thus, we might ascertain that a partially-sealing fault exists at a certain apparent distance from the well but neither the direction nor the nearest distance to the fault would be determined. Thus in assigning the new area of review, every direction would have to be considered as a possibility. If several injection wells, or monitor wells, are completed near the subject well in the same aquifer, then pressure transient interference tests are capable of determining not only $\sqrt{K_x K_y}$ but also K_x/K_y and therefore the orientation of the axes of permeability anisotropy. (Elkins and Skov, 1960; Pollock and Bennett, 1983)

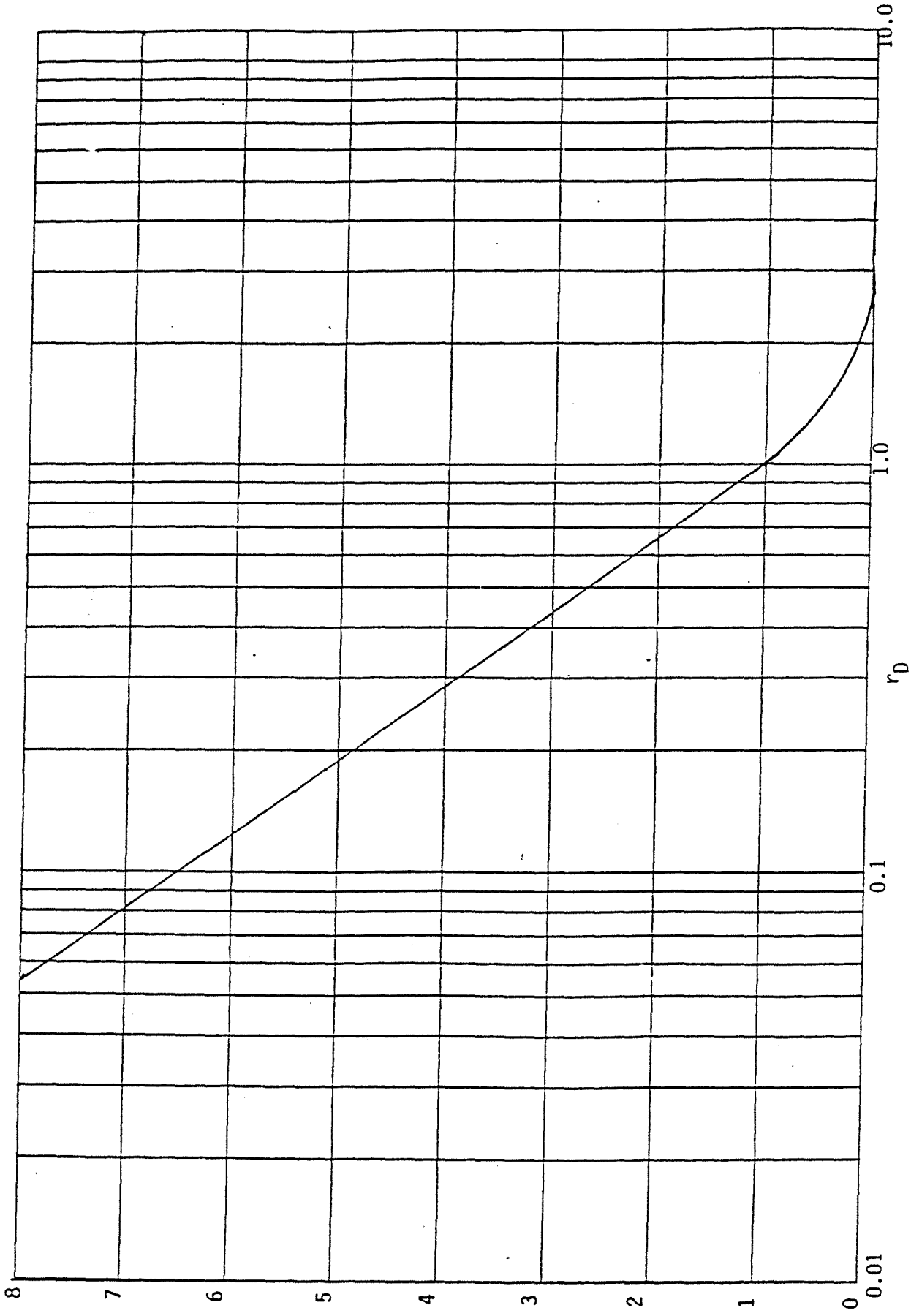

TYPE CURVE FOR INFINITE RESERVOIR
FIGURE 7.

THIS PAGE

INTENTIONALLY

LEFT BLANK

BIBLIOGRAPHY

Annis, M.R.: "High Temperature Properties of Water-Base Drilling Fluids", J. Pet Tech., p. 1074, Aug. (1976)

Arnold, D.M. and Paap, H.J.: "Quantitative Monitoring of Water Flow Behind and in Wellbore Casing", J. Pet Tech., Jan. (1979) p. 121 - 130

Barker, S.E.: "Determining The Area of Review for Industrial Waste Disposal Wells", M.S. Thesis (Supervised by R. E. Collins), Univ. of Texas at Austin (1981)

N.L. Baroid Company, Manual of Drilling Fluids Technology, N.L. Industries, Inc., Houston, Texas (1979)

Bebout, D.G., Weise, B.R., Gregory, A.R. and Edwards, M.B.: "Wilcox Sandstone Reservoirs in the Deep Subsurface Along the Texas Gulf Coast", Report of Invest. 117, Bureau of Econ. Geol., The University of Texas at Austin (1982)

Brace, W.F., Walsh, J.B. and Frangos, W.T.: "Permeability of Granite Under High Pressure", J. Geophy. Res., 73, p. 2225, March (1968)

Braunstein, Jules and O'Brian, Gerald D.: Diapirism and Diapirs, Am. Association of Pet. Geol. Bull., v. 57 (1973) p. 878 - 886

Brooks, C.S. and Purcell, W.R.: Trans AIME, 195, p. 289 (1952)

Bruce, C.J.: "Pressurized Shale and Related Sediment Deformation; Mechanism for Development of Regional Contemporaneous Faults", Am. Assoc. Pet. Geol. Bull., 57, p. 879 (1973)

Carslaw, H.S. and Jaeger, J.C.: Conduction of Heat In Solids; Oxford; Clarendon Press, Great Britain, Second Ed. (1973)

Chen, B., Herrera, I.: "Numerical Treatment of Leaky Aquifers in The Short Time Range", Water Resources Research, 18, No. 3, p. 557 (1982)

Chenevert, M.E.: "Shale Control with Balanced Activity Oil-Continuous Muds", J. Pet Tech., p. 1309, Oct. (1970)

Chenevert, M.E.: Private Communication to R.E. Collins concerning field experiences on re-entering abandoned wells (1986)

Collins, R.E.: Mathematical Models for Physicists and Engineers, Reinhold Book Co., New York (1968)

Collins, R.E.: Flow of Fluids Through Porous Materials, 1st Printing, Reinhold Pub. Co., New York (1961), Reprint, PennWell Pub. Co. Tulsa, OK (1978)

Collins, R.E.: "A New Solution for the Leaky Shale Problem", Submitted to Water Resources Research (1986)

Cooke, C.E., Jr., Kluck, M.P. and Medrano, R.: "Field Measurement of Annular Pressure and Temperature During Primary Cementing", J. Pet. Tech., p. 1429, Aug. (1983)

Cooke, C.E., Kluck, M.P. and Medrano, R.: "Annuluar Pressure and Temperature Measurements Diagnose Cementing Operations", J. Pet. Tech., p. 2181, Dec. (1984)

Davis, K.E. and Sengelmann, G.D.: "Factors Affecting the Area of Review for Hazardous Waste Disposal Wells", Proc. Int. Conf. Underground Injection, New Orleans, LA., March (1986)

Edwards, M.B.: "The Live Oak Delta Complex: An Unstable Shelf-Edge Delta in the Deep Wilcox Trend of South Texas", Gulf Coast Assoc. of Geol. Soc. Trans., 30, No. 1, p. 54 (1982)

Elkins, L.F. and Skov, A.M.: "Determination of Fracture Orientation From Pressure Interference", Pet.Trans AIME, 219, p. 301, (1960)

Engineering Enterprises, Inc.: Guidance Document for the Area of Review Requirement, Norman, Oklahoma, May (1985)

Ewing, T.E.: "Decollement Zones for Texas Gulf Coast Growth Fault Trends", Abstracts and Programs GSA, 14, No. 7, p. 486 (1982)

Galloway, W.E., Finley, R.J. and Henry, C.D.: "South Texas Uranium Province Geologic Perspective", Guide Book 18, Bur. Econ. Geol., The Univ. of Texas at Austin, (1979)

Garrison, A.D.: "Surface Chemistry of Clays and Shales", Pet. Trans. AIME, 132, p. 191, (1939)

Gray, G.R. and Darley, H.C.H.: Composition and Properties of Oil Well Drilling Fluids, 4th Ed., Gulf Pub. Co., Houston, TX. (1981)

Green, C.J.: "Underground Injection Control Technical Assistance Manual", Texas Dept. of Water Resources, April (1983)

Hall, C.W. and Ballentine, R.K.: "U.S. Environmental Protection Agency Policy on Subsurface Implacement of Fluids by Well Injection", Underground Waste Management and Artificial Recharge (1973)

Han, J.H.: "Genetic Stratigraphy and Associated Growth Structures of The Vicksburg Formation, South Texas", Ph.D. Dissertation, The Univ. of Texas at Austin, (1981)

Hantush, M.S. and Jacob, C.E.: "Non-steady Radial Flow in an Infinite Leaky Aquifer", Trans. Am. Geophy. Union, 36, p. 95 (1955)

Hantush, M.S.: "Modification of The Theory of Leaky Aquifers", J. Geophy. Res., 65, No. 1, p. 3713 (1960)

Herrera, I.: "Theory of Multiple Leaky Aquifers", Water Resources Research, 6, No. 1, p. 185 (1970)

Illinois State of Rules and Regulations, Title 35, Subtitle G, Chapter I, section 730.106, "Area of Review", March 1, (1984)

Kozeny, J.: S.-Ber. Wiener Akad. Abt. IIa, 136, p. 271 (1927)

McCarthy, D.G. and Barfield, E.C.: "The Use of High Speed Computers for Predicting Flood-Out Patterns", Pet. Trans AIME, 213, P. 139 (1958)

McKinley, R.M.: "Production Logging", SPE 10035, 1982 SPE International Petroleum Exhibition, Bejing, China, March 18 - 26 (1982)

Miller, C., Fischer, T.A. II., Clark, J.E., Porter, W.M., Hales, C.H. and Tilton, J.R.: "Flow and Containment of Injected Wastes", Int. Conf. on Underground Injection, New Orleans, LA., March (1986)

National Archives of The United States, Code of Federal Regulations, Protection of Environment, 40, parts 100 - 149, 146.6, "Area of Review", revised as of July 1 (1985)

Payne, R.E.: "A Method to Identify the Effects of No-Flow Boundaries Upon Pressure Build-Up Data", SPE 14312, Annual Meeting SPE, Las Vegas, NV., Sept. (1985)

Pollack, C.B. and Bennett, C.O.: "An Eight-Well Interference Test in The Anschutz Ranch East Field", SPE 11968, Annual Fall Meeting SPE, San Francisco, Oct 5 - 8 (1983)

Price, W.H.: "The Determination of Maximum Injection Well Pressure for Effluent Disposal Wells", M.S. Thesis, Univ. of Texas (1971)

Schlumberger: Production Log Interpretation, pub. by Schlumberger Limited (1973)

Steed, W.C.: "Well Plugging in Texas", Abandoned Wells Conference, The University of Oklahoma, May (1984)

Suman, John R.: Petroleum Production Methods, Gulf Publishing Company, Houston (1923)

Theis, C.V.: "The Relation of The Lowering of the Piezometric Surface and The Rate and Duration of Discharge of a Well Using Ground Water Storage", Trans. Am. Geophy. U., p. 519, Aug. (1935)

Warner, D.L., Koederitz, L.F., Simon, A.D. and Yow, M.G.: Radius of Pressure Influence of Injection Wells, Prepared for the Robert S. Kerr Environmental Research Laboratory, Office of Research & Development USEPA, 600/2-99-170 (1979)

Weintritt, P.J. and Hughes, R.G.: "Factors Involved in High Temperature Drilling Fluids", J. Pet. Tech., p. 707, June (1965)

Williams, B.B., Gidley, John L. and Schechter, R.S.: Acidizing Fundamentals, SPE Monograph, Soc. of Pet. Engr. of AIME, Dallas (1979)

Yaxley, L.M.: "The Effect of a Partially Communicating Fault on Transient Pressure Behavior", SPE 14311, Presented at Annual SPE Conf. in Las Vegas, NV., Sept. (1985)

APPENDIX A

MATHEMATICAL MODELS FOR AREA OF REVIEW STUDY

APPENDIX A

Mathematical Models For Area of Review Study

The injection zone is here treated as a sedimentary deposit of uniform thickness, porosity and permeability bounded above and below by shale layers. There are two versions of the model described here, one in which the bounding shale layers above and below are both impermeable aquicludes and one in which one, or both of these have small, but non-zero permeability to brine.

For flow of brine and/or injected fluid, we neglect any differences in density and viscosity and assume a homogeneous, slightly compressible fluid flowing in the formation having density ρ depending on pressure, P, as

$$\rho = \rho_o e^{c_f(P-P_o)} \tag{A1}$$

where ρ_o is density at reference pressure P_o and c_f is the constant compressibility of the fluid. This is to be used in the equation of continuity for conservation of fluid mass

$$\frac{\partial}{\partial x}(\rho v_x) + \frac{\partial}{\partial y}(\rho v_y) + \frac{\partial}{\partial z}(\rho v_z) = - \frac{\partial}{\partial t}(\rho \phi) \tag{A2}$$

where ϕ is formation porosity fraction and v_x, v_y and v_z are the rectangular components of volume flux density of fluid flow in the formation. For these, we have from Darcy's law

$$v_x = - \frac{K_x}{\mu} \left(\frac{\partial P}{\partial x} + \rho g \frac{\partial H}{\partial x}\right) \tag{A3}$$

$$v_y = - \frac{K_y}{\mu} \left(\frac{\partial P}{\partial y} + \rho g \frac{\partial H}{\partial y}\right)$$

$$v_z = - \frac{K_z}{\mu} \left(\frac{\partial P}{\partial z} + \rho g \frac{\partial H}{\partial z}\right)$$

where H(x,y,z) is vertical height above a datum plane, g is the acceleration of gravity and μ is fluid viscosity. Here K_x, K_y and K_z are the principal values of the anisotropic formation permeability tensor and it is assumed that the coordinate axes are selected to coincide with the principal axes of permeability. The above expressions are to be <u>approximated</u> by replacing ρ in the gravity term by ρ_o. Also we note that $\partial H/\partial x$ is cos θ_x, $\partial H/\partial y$ is cos θ_x

and cos θ_z is similarly defined with θ_x, θ_y, θ_z being the direction angles of the vertical relative to the coordinate axes. Then $\cos^2\theta_x + \cos^2\theta_y + \cos^2\theta_z$ is unity.

This three-dimensional flow problem is reduced to a two-dimensional flow problem by defining average mass fluxes in the formation plane over the thickness, h, of the formation; thus, for example,

$$\overline{\rho v_x} = \frac{1}{h}\int_o^h \rho v_x \, dz \tag{A4}$$

Thus, Eq.(A2) is expressed as

$$\frac{\partial}{\partial x}(\overline{\rho v_x}) + \frac{\partial}{\partial y}(\overline{\rho v_y}) + \frac{1}{h}\left[(\rho v_z)_h - (\rho v_z)_o\right] = -\frac{\partial(\overline{\rho\phi})}{\partial t} \tag{A5}$$

with a bar denoting average value over $0 < z < h$.

In the version of the model with sealed, impermeable aquiclude above and below both v_z terms are zero and we deal with

$$\frac{\partial}{\partial x}(\overline{\rho v_x}) + \frac{\partial}{\partial y}(\overline{\rho v_y}) = -\frac{\partial(\rho\phi)}{\partial t} \tag{A6}$$

The term on the right is simplified to account for compressible rock and fluid using

$$\frac{\partial(\rho\phi)}{\partial t} = \rho \frac{d\phi}{dP}\frac{d\rho}{\partial t} + \phi \frac{d\rho}{dP}\frac{\partial P}{\partial t} \tag{A7}$$

which is equivalent to

$$\frac{\partial(\rho\phi)}{\partial t} = \rho\phi\,(c_\phi + c_f)\frac{\partial P}{\partial t} = \rho\phi c \frac{\partial P}{\partial t} \tag{A8}$$

where c_f is defined in Eq.(A1) and

$$c_\phi = \frac{1}{\phi}\frac{d\phi}{dP} \tag{A9}$$

is the pore compressibility of the formation. In the analysis to follow, it will be assumed that both c_ϕ and c_f are small so that the product $\rho\phi$ in the right member of Eq.(A8) can be approximated as $\rho_o\phi_o$; the values at $P = P_o$.

We next observe that when we insert Darcy's law for v_x and v_y in Eq.(A6), together with Eq.(A1) for ρ we obtain terms such as

$$(A10) \qquad \frac{1}{h}\int_o^h \frac{\partial}{\partial x}\left(\frac{K_x}{\mu}\rho_o e^{c_f(P-P_o)}\left(\frac{\partial P}{\partial x}+\rho g\frac{\partial H}{\partial x}\right)\right) dz$$

In this, we see that

$$(A11) \qquad \rho_o e^{c_f(P-P_o)}\frac{\partial P}{\partial x} = \frac{1}{c_f}\frac{\partial \rho}{\partial x}$$

and then for <u>small</u> c_f we have from Eq.(A1) to <u>first order in</u> $c_f(P-P_o)$

$$(A12) \qquad \rho - \rho_o \simeq c_f \rho_o (P - P_o)$$

so that

$$(A13) \qquad \frac{1}{c_f}\frac{\partial \rho}{\partial x} \simeq \frac{\partial P}{\partial x}$$

Therefore, if we approximate ρ as ρ_o in the gravity term in Eq. (A10) above, we have the form

$$(A14) \qquad \frac{1}{h}\int_o^h \frac{\partial}{\partial x}\left[\frac{K_x}{\mu}\rho_o\left(\frac{\partial P}{\partial x}+\rho_o g\frac{\partial H}{\partial x}\right)\right] dz$$

Therefore defining

$$(A15) \qquad \bar{\psi} = \frac{1}{h}\int_o^h (P + \rho_o g H)\, dz$$

we have the expression in Eq.(A10) as

$$(A16) \qquad \rho_o \frac{\partial}{\partial x}\left(\frac{K_x}{\mu}\frac{\partial \bar{\psi}}{\partial x}\right)$$

and then, with Eqs.(A8) and (A15), Eq.(A6) becomes

$$(A17) \qquad K_x \frac{\partial^2 \bar{\psi}}{\partial x^2} + K_y \frac{\partial^2 \bar{\psi}}{\partial y^2} = \phi_o \mu c \frac{\partial \bar{\psi}}{\partial t}$$

This follows because H is independent of t so $\partial\bar{\rho}/\partial t$ and $\partial\bar{\psi}/\partial t$ are equivalent. Now Eq.(A15) is the general form of our "working" differential equation for K_x and K_y uniform throughout the formation. In this case, we introduce the coordinate substitutions

$$(A18) \qquad x' = x\sqrt{\frac{K}{K_x}} \quad , \quad y' = y\sqrt{\frac{K}{K_y}} \quad , \quad K = \sqrt{K_x K_y}$$

to obtain the isotropic form,

$$(A19) \qquad \frac{\partial^2 \bar{\psi}}{\partial x'^2} + \frac{\partial^2 \bar{\psi}}{\partial y'^2} = \frac{\phi_o \mu c}{K} \frac{\partial \bar{\psi}}{\partial t}$$

This basic equation then describes both isotropic ($K_x = K_y$) and anisotropic ($K_x \neq K_y$) formations with uniform ϕ_o, h, c and K and small c_f. The reservoir need not be horizontal, nor for that matter "flat"; the function H(x',y') in the expression

$$(A20) \qquad \bar{\psi} = \bar{P}(x', y', t) + \rho_o g \bar{H}(x', y')$$

need only be specified.

Since Eq.(A19) describes both isotropic and anisotropic cases, we will delete primes on coordinates in all subsequent analysis with it understood that, for example, x is either just x or it is $x \cdot \sqrt{K/K_x}$ as appropriate to the system.

Returning now to the case of the "leaky" aquifer in which the shale aquiclude above and/or below the formation of interest has non-zero permeability. In this case, our analysis begins with Eq.(A5) rather than Eq.(A6). The only difference is in the presence of the terms in v_z. For simplicity, we describe the case in which v_z is zero at z = 0 (the bottom of the formation) but $v_z \neq 0$ at z = h.

Now

$$(A21) \qquad (v_z)_{z=h} = -\frac{K_{zs}}{\mu}\left(\frac{\partial P}{\partial z} + \rho_g \frac{\partial H}{\partial z}\right)_{z=h} = -\frac{K_{zs}}{\mu} \frac{\partial \psi_s}{\partial z}$$

where K_{zs} is permeability of the shale in the z direction (normal to the layer) and $(\partial\psi_s/\partial z)$ is the potential gradient in the shale at the shale-formation interface. Here we approximate this as the "instantaneous steady-state", linear form,

$$(A22) \qquad -\frac{\partial\psi_s}{\partial t} \simeq \frac{\bar{\psi} - \bar{\psi}_o}{h_s}$$

where $\bar{\psi}$ is the mean ψ in the injection formation at this location, $\bar{\psi}_o$ is the value of ψ in a permeable aquifer above the shale and h_s is the shale thickness. With this approximation, and $\rho \simeq \rho_o$ in the term (ρv_z) at $z = h$, we then see all other treatments of Eq.(A4) are being applicable to Eq.(A3), so there results

$$(A23) \qquad \frac{\partial^2 \bar{\psi}}{\partial x^2} + \frac{\partial^2 \bar{\psi}}{\partial y^2} - \alpha(\bar{\psi}-\bar{\psi}_o) = \frac{\phi_o \mu c}{K} \frac{\partial \bar{\psi}}{\partial t}$$

describing the aquifer formation with a "leaky" aquiclude on top. Here

$$(A24) \qquad \alpha = \frac{K_{zs}}{Khh_s}$$

and $\bar{\psi}_o$ is assumed as a uniform, constant value for ψ in the aquifer overlying the aquiclude. Furthermore, this must also be the uniform <u>initial</u> value for ψ in the formation of interest since these aquifers were initially in hydrostatic equilibrium. Observe that if <u>both</u> upper and lower aquicludes are "leaky", then α is replaced by the sum, $\alpha_u + \alpha_L$, of the α values of upper and lower shale bodies.

Now the above description of the leaky shales in terms of an <u>instantaneous steadv-state</u> potential gradient within the shale, Eq.(A22), is admittedly a crude approximation. An extensive body of literature (see bibliography) is available which treats "leaky aquifers" in terms of transient, compressible flow in this shale. Unfortunately, these more sophisticated forms do not yield solution forms amenable to evaluation in the context of a practical configuration of wells. The form we have obtained on the other hand, Eq.(A23), will be shown to yield a <u>very</u> practical and useful solution form. Furthermore, this can be shown to be an approximation for another "leaky shale" system as follows.

In the case of a very thick shale laver, or other rock of low permeability, overlying the aquifer as aquiclude we can insert another approximation for $\partial\psi_s/\partial z$ at $z = h$ in Eq.(A21) in lieu of the steady-state form in Eq.(A22). We assume flow in the thick shale to be purely vertical and neglect all horizontal flow. Then the boundary value problem for ψ_s is

$$\text{(A25)} \qquad \frac{\partial^2\psi_s}{\partial z^2} = \frac{\phi_s \mu c_s}{K_{zs}} \frac{\partial \psi_s}{\partial t}; \qquad \begin{aligned} &\psi_s = \bar{\psi}_o, \ t = 0 \\ &\psi_s \to \bar{\psi}_o, \ z \to \infty \\ &\psi_s = \bar{\psi}(x,y,t), \ z = h \end{aligned}$$

From the solution for this boundary value problem given by Carslaw and Jaeger (1973, p. 62) we have

$$\text{(A26)} \qquad \psi_s(z,t) - \bar{\psi}_o = \sum_{j=1}^{n} \Delta\bar{\psi}(x,y,t_j) \ \mathrm{erfc}\left(\frac{z - h}{2\sqrt{\gamma(t-t_j)}}\right)$$

where γ denotes $K_{zs}/\phi_s \mu c_s$, $\Delta\bar{\psi}(x,y,t_j)$ is the increase in $\bar{\psi}(x,y,t) - \bar{\psi}_o$ occurring at time $t = t_j$ and erfc denotes the complimentary error function.

Here the continuous variation in $\bar{\psi}(x,y,t)$ in time has been approximated as a step-wise variation. We then find for $\partial\psi_s/\partial z$ at $z = h$ the result

$$\text{(A27)} \qquad \left(\frac{\partial\psi_s}{\partial z}\right)_{z=h} \approx -\sum_{j=1}^{n} \frac{\Delta\bar{\psi}(x,y,t_j)}{\sqrt{\pi\gamma(t-t_j)}} = -\int_o^t \frac{\partial\bar{\psi}(x,y,\lambda)}{\partial\lambda} \frac{d\lambda}{\sqrt{\pi\gamma(t-\lambda)}}$$

with the integral form being the result for continuous variation in $\bar{\psi}(x,y,t)$. If we then approximate the sum by a single term as

$$\text{(A28)} \qquad \left(\frac{\partial\psi_s}{\partial z}\right)_{z=h} = -\frac{\psi(x,y,t) - \psi_o}{\sqrt{\pi\gamma\Delta\tau}}$$

with $\Delta\tau$ a constant parameter we see this as having the same form as Eq.(A22) with the "effective thickness", h_s being given as $\sqrt{\pi\gamma\Delta\tau}$.

An order of magnitude for $\Delta\tau$ to be inserted here can be estimated from another analytical solution given by Carslaw and Jaeger (1973) in Figure 11 on page 101; there the solution is plotted for a layer of finite thickness with a unit

step change at one surface. This indicates a variable $\Delta\tau$ would be required but for $\gamma t/h_s^2$ between 0 and .05 an <u>average</u> value of $1/\sqrt{\pi\gamma\Delta\tau}$ is seem to be 2.0.

Of course, these approximations are not rigorous and we could employ the integral form in Eq.(A27) in lieu of our Eq.(A22) as an almost exact description for the effect of a thick shale of finite permeability, but this yields an integro-differential equation for $\bar{\psi}$. Thus in all our analysis of "leaky" shales we employ Eq.(A23).

ANALYTICAL SOLUTIONS OF EQUATIONS OF FLOW

For the cases in which the disposal zone is approximated as a uniform aquifer having uniform values of ϕ_o, K_x, K_y, h, μ and c throughout, with a simple class of boundaries, to be described below, analytical solutions for the equation of flow, Eq.(A23), can be constructed for both the "leaky", $\alpha \neq 0$, and "sealed", $\alpha = 0$, cases. These solutions can accommodate any number of injection wells in the common aquifer each having any arbitrary variable rate history.

The Sealed Aquifer

The method of solution is illustrated first for the case of the sealed aquifer, $\alpha = 0$. The method employs a "line source" solution to represent an injection well of constant rate in an aquifer of infinite areal extent and exploits the fact that the differential equation for $\bar{\psi}$, Eq.(A23), is a <u>linear</u> equation so that solutions can be <u>added</u> to construct other solutions. Thus, solutions for "wells" of various rates, starting at various times can be "superposed" (added) with the wells at the <u>same location</u> to represent one well at that location with a variable rate history. Also "image" wells, identical to such a well, can be placed throughout the infinite aquifer to create <u>lines of symmetry</u> in the resulting areal array of wells which appear as no-flow plane boundaries in the aquifer.

The single, constant rate, line source in an infinite aquifer case is first solved by the method of Boltzman by placing the origin of coordinates at the well and writing the differential equation in polar coordinates, thus;

$$\text{(A29)} \qquad \frac{1}{r}\frac{\partial}{\partial r}\left(r\frac{\partial\bar{\psi}}{\partial r}\right) + \frac{1}{r^2}\frac{\partial^2\bar{\psi}}{\partial\theta^2} - \alpha\,(\psi-\psi_o) = \frac{\phi_o\mu c}{K}\frac{\partial\bar{\psi}}{\partial t}$$

Then, by symmetry, flow is uniformly radial from the origin and does not depend upon θ, hence

$$\text{(A30)} \qquad \frac{1}{r}\frac{\partial}{\partial r}\left(r\frac{\partial \bar{\psi}}{\partial r}\right) - \alpha(\bar{\psi}-\bar{\psi}_o) = \frac{\phi_o \mu c}{K}\frac{\partial \bar{\psi}}{\partial t}$$

For the case $\alpha = 0$, we then assume a solution with $\bar{\psi}$ a function only of the variable

$$\text{(A31)} \qquad \zeta = \frac{\phi_o \mu c r^2}{4Kt}$$

and this yields (see Dake [1980])

$$\text{(A32)} \qquad \bar{\psi} = A\int_{\zeta}^{\infty} \frac{e^{-\zeta}}{\zeta}\, d\zeta + B$$

with A and B being constants. Now as $r \to \infty$ we have $\zeta \to \infty$ and the integral must vanish. This also holds as $t \to 0$. Thus, we see that the constant B must be the initial value $\bar{\psi}_o$ of $\bar{\psi}$ and this is also the uniform value at infinite distance from the well for all finite time.

Next, note that the flow rate across the cylindrical shell of radius r and height h, concentric to the well is, from Eq.(A32)

$$\text{(A33)} \qquad q = \left(-2\pi r h \frac{K}{\mu}\frac{\partial \bar{\psi}}{\partial r}\right)_r = A\,\frac{4\pi K h}{\mu}\, e^{-\frac{\phi_o \mu c r^2}{4kt}}$$

which yields for $r \to 0$

$$\text{(A34)} \qquad A = \frac{q\mu}{4\pi K h}$$

where q is the flow rate from the line source at the origin. This also holds in the anisotropic case where K is $\sqrt{K_x K_y}$. Thus the line source solution is the familiar form

$$\text{(A35)} \qquad \bar{\psi} = \bar{\psi}_o + \frac{q\mu}{4\pi K h}\left\{-Ei\left(-\frac{\phi_o \mu c r^2}{4Kt}\right)\right\}$$

where

$$(A36) \qquad -Ei(-\zeta) = \int_{\zeta}^{\infty} \frac{e^{-\lambda}}{\lambda}\, d\lambda$$

is the well known exponential integral function. We note the approximation

$$(A37) \qquad -Ei(-\zeta) = -\ln\gamma\zeta, \quad \zeta < .01$$

often applied with high accuracy. Here

$$(A38) \qquad \ln \gamma = 0.5772, \quad \gamma \simeq 1.781$$

is Euler's Constant.

By shifting the origin of coordinates so that the well (line source) is located at x_w , y_w instead of the origin, we have in the above solution

$$(A39) \qquad r^2 = (x-x_w)^2 + (y-y_w)^2$$

with x, y any point at which $\bar{\psi}$ is evaluated, and this solution is a solution of the general two-dimensional equation, Eq.(A19), or Eq.(A23) with $\alpha = 0$.

For a well with the variable rate history, (a step-rate history)

$$(A40) \qquad q = \sum_{j=1}^{n} \Delta q_j, \qquad t_n < t < t_{n+1}$$

we simply add solutions like that above for multiple wells superposed at the same location, x_w, y_w, having rates Δq_j, j = 1, 2, ... with well number j coming on stream at time t_j. Thus the solution is

$$(A41) \qquad \bar{\psi} = \bar{\psi}_o + \sum_{j=1}^{n} \frac{\Delta q_j \mu}{4\pi Kh} \{-Ei(-\frac{\phi_o \mu c r^2}{4K(t-t_j)})\}$$

Note that $t_1 = 0$ is usually the case with $q = \Delta q_1$ being the initial rate of the well and of course, r^2 is in general defined by Eq.(A39). Also observe that as t increases beyond t_{n+1}, then another term is added to the series, i.e. a term with Δq_{n+1} and t_{n+1} appearing as the last term for $t_{n+1} < t < t_{n+2}$, etc.

We can exploit additivity of solutions to represent aquifers with straight lateral boundaries as described above. Two particular cases are formulated, one the finite rectangular domain and the other a semi-infinite domain bounded by two straight boundaries intersecting at the origin. The latter case is described first.

The domain of the aquifer is represented as shown in Figure A1.1 as the hatched region with <u>one</u> well. To achieve the effect of the two boundaries shown, the lines shown are drawn by symmetry in 45° segments with additional wells then "inserted" as marked by x's. These are image wells. In order for this symmetry to exist, the angle, θ_T , between the two boundaries at the origin must be an <u>even</u> integral fraction of 2π, i.e.

(A42) $$\theta_T = \frac{2\pi}{2n_T} , \quad n_T = 1, 2, 3, \ldots$$

Then image wells are located such that the total collection of wells in the <u>infinite</u> reservoir are located at

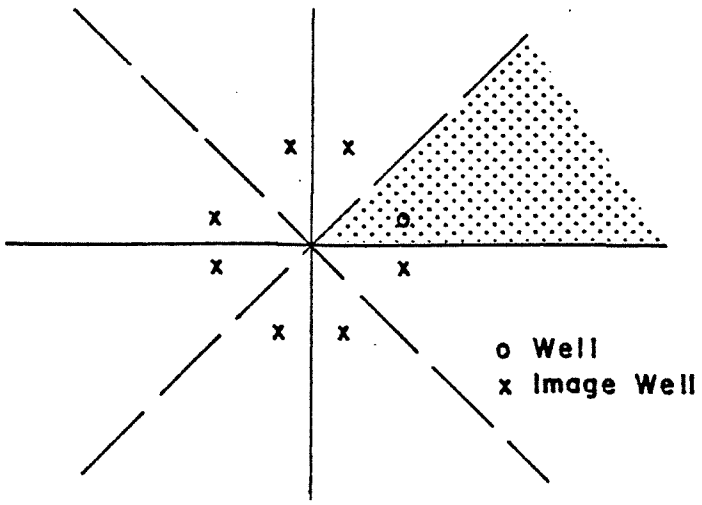

FIGURE A1.1

(A43)
$$\begin{aligned} x_{wn1} &= R_w \cos(2(n-1)\theta_T + \theta_w) \\ y_{wn1} &= R_w \sin(2(n-1)\theta_T + \theta_w) \\ x_{wn2} &= R_w \cos(2(n-1)\theta_T - \theta_w) \\ y_{wn2} &= R_w \sin(2(n-1)\theta_T - \theta_w) \qquad n=1,2,\ldots n_T \end{aligned}$$

where n_T is defined by Eq.(A40) and

$$R_w = (x^2_w + y^2_w)^{\frac{1}{2}} \tag{A44}$$

$$\theta_w = \sin^{-1}(y_w/R_w)$$

with x_w, y_w the actual coordinates of the original well.

Then if these wells are ordered and labeled by a single index i = 1, 2,... we can write the solution for one well with variable rate, as described above, in the bounded domain as

$$\bar{\psi} - \bar{\psi}_o = \sum_i \sum_{j=1}^{n} \frac{\Delta q_j \mu}{4\pi Kh} \{-Ei(-\frac{\phi_o \mu c r_i^2}{4K(t-t_j)})\} \tag{A45}$$

where r_i is the distance from the i^{th} well to the point x, y in the bounded domain where $\bar{\psi}$ is evaluated. Note that all of the wells here have an identical rate history. This is readily generalized to represent any number of actual wells in the bounded domain simply by adding a similar double sum on the right for each such well.

Observe a special case of "one" plane boundary when $\theta_T = 180^o$; then there is only one image well for each actual well, i.e. $n_T = 1$.

The other bounded case treated is the rectangular domain. In this case, we have for one well in the domain, the infinite array of lines of symmetry and image wells as shown in Figure A1.2.

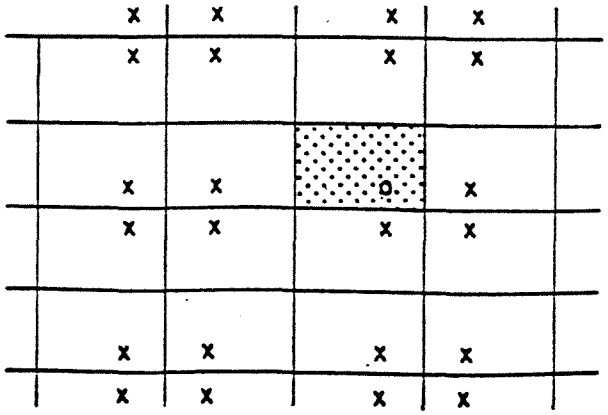

FIGURE A1.2

In this case, the original well located at $x = a$, $y = b$ is now replaced by the two-dimensional, infinite array with wells located at

$$
\begin{aligned}
x_{wn1} &= 2nL - (L-a) = (2n-1)L + a \\
y_{wn1} &= 2mw - (w-b) = (2m-1)w + b \\
x_{wn2} &= (2n-1)L - a \\
y_{wn2} &= (2m-1)w - b
\end{aligned}
\qquad
\begin{aligned}
n &= \pm 1, \pm 2, \ldots \\
m &= \pm 1, \pm 2, \ldots
\end{aligned}
\tag{A46}
$$

Again, we can put these wells in correspondence with a single integer index, $i = 1, 2, \ldots$ and Eq.(A45) is then the form of the solution for <u>one well</u> with variable rate history in the rectangular domain. The addition of a similarly structured double sum on the right in Eq.(A45) for each additional well in the rectangular aquifer yields the solution form for multiple wells.

In practice of course, the <u>infinite</u> array of wells shown above is truncated to include only wells <u>near enough</u> to the rectangular domain of interest to contribute <u>significantly</u> to the value of $\bar{\psi}$.

<u>The Leaky Aquifer</u>

In the case of the leak-off of brine into a shale aquiclude, we begin with the case of a single line source (well) at the origin and hence must solve Eq.(A30). We seek a solution in terms of the dependent function

$$U = e^{\frac{\alpha}{\beta} t} (\bar{\psi} - \bar{\psi}_o) \tag{A47}$$

where α is defined by Eq.(A24) and β is defined as

$$\beta = \frac{\phi_o \mu c}{K} \tag{A48}$$

Thus Eq.(A30) becomes

$$\frac{1}{r} \frac{\partial}{\partial r} \left(r \frac{\partial U}{\partial r} \right) = \beta \frac{\partial U}{\partial t} \tag{A49}$$

which has the same structure as Eq.(A30) with $\alpha = 0$. Therefore, there is a

solution in terms of U, defined by Eq.(A31), of the same <u>form</u> as obtained for $\bar{\psi}$ in Eq.(A32); that is,

$$(A50) \qquad U = A \int_{\zeta}^{\infty} \frac{e^{-\zeta}}{\zeta} d\zeta + B$$

which yields, with $U \to 0$ as $\zeta \to \infty$, and the quantity q defined by

$$(A51) \qquad q = \lim (-2\pi rh \frac{K}{\mu} \frac{\partial U}{\partial r}) = A \frac{4\pi Kh}{\mu}$$

the form

$$(A52) \qquad e^{\frac{\alpha}{\beta} t} (\bar{\psi} - \bar{\psi}_o) = \frac{qu}{4\pi Kh} \{-Ei(- \frac{\phi_o \mu c r^2}{4Kt})\}$$

Clearly, this does <u>not</u> correspond to a well with constant flow rate at the origin. This situation is simply remedied by using <u>superposition</u> of solutions in the manner already described, namely replacing Eq.(A45) by the form

$$(A53) \qquad e^{\frac{\alpha}{\beta} t} (\bar{\psi}-\bar{\psi}_o) = \sum_j \frac{\Delta q_j \mu}{4\pi Kh} \{-Ei(- \frac{\phi_o \mu c r^2}{4K(t-t_j)})\}$$

for $t_j < t < t_{j+1}$. Then, in the limit, $t_{j+1} - t_j \to 0$, for all j, this has the limiting form

$$(A54) \qquad e^{\frac{\alpha}{\beta} t} (\bar{\psi}-\bar{\psi}_o) = \frac{q(o)\mu}{4\pi Kh} \{-Ei(-\frac{\phi_o \mu c r^2}{4Kt})\} + \int^t \frac{\mu}{4\pi Kh} \frac{dq(\tau)}{d\tau} \{-Ei(-\frac{\phi_o \mu c r^2}{4K(t-\tau)})\} \frac{\alpha}{\beta} d\tau$$

Now using

$$(A55) \qquad q_a = \lim_{r \to 0} (-2\pi rh \frac{K}{\mu} \frac{\partial \bar{\psi}}{\partial r})$$

as the equation defining the actual rate of the well at the origin, there results upon using Eq.(A54) for $\bar{\psi}$ the form,

$$(A56) \qquad q_a = e^{-\frac{\alpha}{\beta}t}\left[\int_o^t \frac{dq(\tau)}{d\tau}\,d\tau + q(o)\right] = e^{-\frac{\alpha}{\beta}}\,q(t)$$

This then requires the form,

$$(A57) \qquad q(t) = q_a e^{\frac{\alpha}{\beta}t}$$

in Eq.(A54) to yield the form for $\bar{\psi}$ for a well of constant rate q_a at the origin. Thus the solution of Eq.(A23) corresponding to a well of constant rate q_a at the origin, in an infinite reservoir, is

$$(A58) \qquad \bar{\psi} - \bar{\psi}_o = \frac{q_a\mu}{4\pi Kh}\left[e^{-\frac{\alpha}{\beta}t}\{-Ei(-\frac{\phi_o\mu cr^2}{4Kt})\} + \int_o^t e^{-\frac{\alpha}{\beta}(t-\tau)}\{-Ei(-\frac{\phi_o\mu cr^2}{4K(t-\tau)})\}\frac{\alpha}{\beta}d\tau\right]$$

or, with λ for $t - \tau$

$$(A59) \qquad \bar{\psi} - \bar{\psi}_o = \frac{q_a\mu}{4\pi Kh}\left[e^{-\frac{\alpha}{\beta}t}\{-Ei(-\frac{\phi_o\mu cr^2}{4Kt})\} + \int_o^t e^{-\frac{\alpha}{\beta}\lambda}\{-Ei(-\frac{\phi_o\mu cr^2}{4K\lambda})\}\frac{\alpha}{\beta}d\lambda\right]$$

Of course, the form in Eq.(A55) for q(t) can be inserted into Eq.(A51) to yield the approximate form for the solution in Eq.(A53)

$$(A60) \qquad \bar{\psi} - \bar{\psi}_o = \frac{q_a\mu}{4\pi Kh}\left[e^{-\frac{\alpha}{\beta}t}\{-Ei(-\frac{\phi_o\mu cr^2}{4Kt_n})\}\right.$$

$$\left. + \frac{q_a\mu}{4\pi Kh}e^{-\frac{\alpha}{\beta}t_n}\sum_{j=1}^{n-1}(e^{\frac{\alpha}{\beta}t_j} - e^{\frac{\alpha}{\beta}t_{j-1}})\{-Ei(-\frac{\phi_o\mu cr^2}{4(t_n-t_j)})\}\right.$$

for $\bar{\psi} - \bar{\psi}_o$ at time t_n.

Since Eq.(A23) for the "leaky" shale aquiclude is linear we may again add solutions of the form in Eq.(A59), or Eq.(A60), to create solutions for multiple wells, wells of variable rate and wells in domains bounded by plane fault boundaries using images. Hence all of the analysis given for the non-leaky aquifer can be generalized to the leaky aquifer.

Effects of Transmissibility Variations: Applications of Pseudo Steady-State Analysis

The primary simulator used in this study incorporates effects of fault boundaries, leaky shale aquicludes and multiple, variable-rate injection wells, although our basic study has focused upon a single, constant-rate injection well. In this primary simulator, the disposal zone was represented as having uniform, homogeneous porosity, permeability and thickness, so we now employ some analytical methods to assess the impact of variability in permeability, or transmissibility, on the spatial distribution of pressure build-up in the injection zone.

In the analysis to follow we will show that if we examine fluid flow in the aquifer in the pseudo steady-state approximation then we can exploit a method from potential theory to estimate the effect of plane discontinuities in permeability, transecting the aquifer, on pressure build-up in the aquifer.

The Non-Leaky Aquifer; Pseudo Steady-State

For the non-leaky aquifer, we have used superposition of solutions of the equation of diffusion type (Eq.A19),

$$\frac{\partial^2 \bar{\psi}}{\partial x^2} + \frac{\partial^2 \bar{\psi}}{\partial y^2} = \frac{\phi_o \mu c}{K} \frac{\partial \bar{\psi}}{\partial t} \tag{A61}$$

corresponding to a single constant-rate injection well in an infinite reservoir to describe various types of boundary configurations. This solution is of the form

$$\bar{\psi} - \bar{\psi}_o = \frac{q\mu}{4\pi Kh} \{-Ei(-\frac{\phi_o \mu c r^2}{4Kt})\} \tag{A62}$$

with r the distance from the injection well at time t after start of injection at rate q. For large values of t such that

$$\frac{\phi_o \mu c r^2}{4Kt} < 0.01 \qquad \text{(A63)}$$

this solution is well approximated by the pseudo steady-state form (see Magnus and Oberhettinger [1949])

$$\bar{\psi} - \bar{\psi}_o \simeq \frac{q\mu}{4\pi Kh} \{-\ln \frac{\gamma \phi_o \mu c r^2}{4Kt}\} \qquad \text{(A64)}$$

where $\gamma = 1.781$.

Now this functional form is in fact a solution of the LaPlace Equation

$$\frac{\partial^2 \bar{\psi}}{\partial x^2} + \frac{\partial^2 \bar{\psi}}{\partial y^2} = 0 \qquad \text{(A65)}$$

which is the steady-state form of Eq.(A61). Thus we infer that for large injection times we can use techniques applicable to solving this equation to evaluate long-term pressure distributions in disposal aquifers having sealed aquicludes. Observe that for the typical values:

$$\phi_o = .2, \quad \mu = 1 \text{ cp.}, \quad c = 5 \times 10^{-6} \text{ psi}^{-1} \quad K = 300 \text{ md}$$

with r in thousands of feet and t in years, the above inequality becomes,

$$\frac{r^2}{t} < 27.6 \frac{(\text{thousands of ft.})^2}{\text{years}} \qquad \text{(A66)}$$

Thus for r on the order of 10 thousand feet, this gives

$$\frac{10^2}{t} < 27.6 \qquad \text{(A67)}$$

or

$$t > 3.62 \text{ years} \qquad \text{(A68)}$$

Hence for injection times in excess of 3.62 years, the pressure (or flow potential) distribution out to distances on the order of 10,000 feet, or more, has the same form as in a steady-state condition. For t on the order of 36

years, this holds out to distances of 32,000 feet, or about six miles, from the injection well.

Clearly the above time criterion will vary with spatial location in an inhomogeneous reservoir in which ϕ_o and K are not uniform but a lower bound on time to reach this "steady-state" condition can be estimated.

A consequence of this result is that techniques of potential theory (solutions of LaPlace's Equation) can be applied to access effects of non-uniform permeability on the distribution of pressure build-up in the disposal reservoir.

The Leaky Aquifer; Pseudo Steady-State

In the case of the leaky aquifer, we have employed superposition of solutions of the diffusion type equation with losses,

$$\frac{\partial^2 \bar{\psi}}{\partial x^2} + \frac{\partial^2 \bar{\psi}}{\partial y^2} - \alpha(\psi - \psi_o) = \frac{\phi_o \mu c}{K} \frac{\partial \bar{\psi}}{\partial t} \tag{A69}$$

of the form

$$\bar{\psi} - \bar{\psi}_o = \frac{q_a \mu}{4\pi Kh} \left[e^{-\frac{\alpha}{\beta}t} \{-Ei(-\frac{\beta r^2}{4t})\} + \int_o^t e^{-\frac{\alpha}{\beta}\lambda} \{-Ei(-\frac{\beta r^2}{4\lambda})\} \frac{\alpha}{\beta} \, d\lambda \right] \tag{A70}$$

corresponding to a single well of constant rate q_a in an infinite, uniform, plane aquifer. We construct an approximate form of this solution valid for large t by the following device. We write the integral in Eq.(A70) as

$$\int_o^t f \, d\lambda = \int_o^\infty f \, d\lambda - \int_t^\infty f \, d\lambda \tag{A71}$$

where $f(\lambda)$ is the integrand appearing there. Then for the first integral on the right, we use the closed form (see Collins [1968] p. 127)

$$\int_o^\infty e^{-\frac{\alpha}{\beta}\lambda} \{-Ei(-\frac{\beta r^2}{4\lambda})\} \frac{\alpha}{\beta} \, d\lambda = 2 K_o (\sqrt{\alpha} \, r) \tag{A72}$$

where K_o is the modified Bessel function of the second kind, (a tabulated

function) while for the second integral on the right, we use the approximate form

$$(A73) \qquad \int_t^\infty e^{-\frac{\alpha}{\beta}\lambda} \{-Ei(-\frac{\beta r^2}{4\lambda})\}\frac{\alpha}{\beta}\, d\lambda \simeq \int_t^\infty e^{-\frac{\alpha}{\beta}\lambda} \{\ln \frac{4\lambda}{\gamma\beta r^2}\}\frac{\alpha}{\beta}\, d\lambda$$

with $\ln \gamma$ being Euler's constant as introduced earlier. This requires that $\beta r^2/Kt$ be sufficiently small as specified in Eq.(A63). Finally, this integral is evaluated using integration by parts to yield as the pseudo steady-state solution for a single well in a leaky aquifer

$$(A74) \qquad \bar{\psi} - \bar{\psi}_o = \frac{q_a \mu}{4\pi Kh} [2\, K_o(\alpha r) - e^{-\frac{\alpha}{\beta}t} \ln \frac{\gamma\beta r^2}{4Kt} + \{-Ei(-\frac{\alpha}{\beta}t)\}]$$

Here, just as for the sealed aquifer, we find that this is a solution of a steady-state equation; in this case Eq.(A74) is a solution of

$$(A75) \qquad \frac{\partial^2 \psi}{\partial x^2} + \frac{\partial^2 \psi}{\partial y^2} - \alpha(\bar{\psi} - \bar{\psi}_o) = 0$$

valid for $\phi_o \mu c r^2/4Kt$ specified as in Eq.(A60). Thus, all of our analysis given above for the sealed aquifer, concerning the radius r of the circle within which this solution is approximately valid, for a given t, is applicable here.

We note that as $t \to \infty$, the solution in Eq.(A74) approaches

$$(A76) \qquad \psi - \psi_o = \frac{q_a \mu}{2\pi Kh} K_o(\alpha r)$$

which is the steady-state solution for a single well of rate q_a in a uniform leaky aquifer given by Hantush and Jacob (1955).

A Discontinuity in Permeability

The first case we consider is that of a reservoir approximated as having two regions of distinctly different permeability. This gives insight into the effect of a trend, or gradient in transmissibility on the spatial distribution in pressure build-up.

We have the potential problem as shown in Figure A1.3.

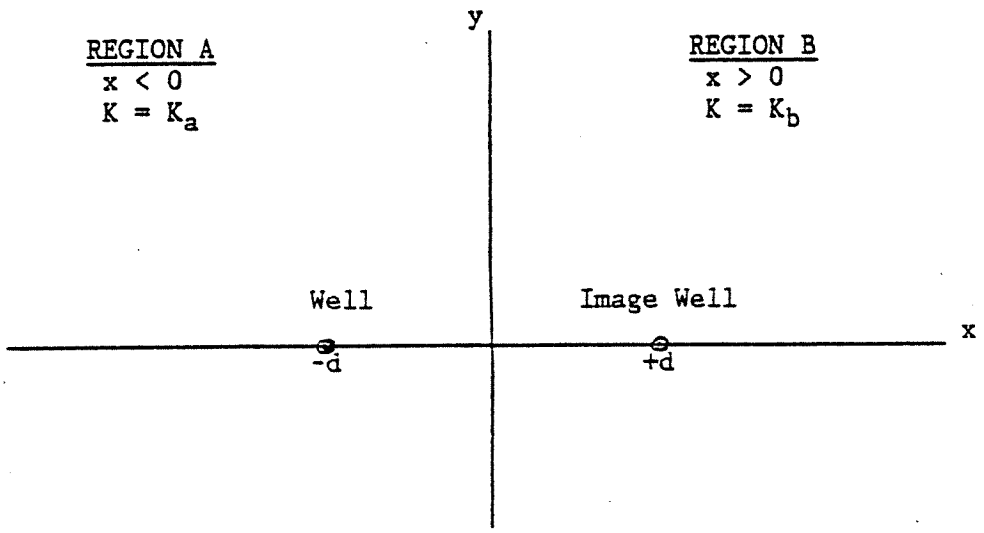

FIGURE A1.3

In Region A, the solution is written as

(A77) $$\bar{\psi}_a - \bar{\psi}_o = - \frac{q\mu}{4\pi K_a h} \left[\ln \frac{\gamma\phi_o\mu c[(x+d)^2 + y^2]}{4K_a t} + A \ln \frac{\gamma\phi_o\mu c[(x-d)^2 + y^2]}{4K_a t} \right]$$

while in Region B, it is

(A78) $$\bar{\psi}_b - \bar{\psi}_o = - \frac{q\mu}{4\pi K_a h} \left[B \ln \frac{\gamma\phi_o\mu c[(x+d)^2 + y^2]}{4K_a t} + A \ln \frac{\gamma\phi_o\mu c[(x-d)^2 + y^2]}{4K_a t} \right]$$

where A and B are constants to be determined by the boundary conditions on the separating plane at x = 0,

(A79)
$$\bar{\psi}_a = \bar{\psi}_b$$
$$K_a \frac{\partial \bar{\psi}_a}{\partial x} = K_b \frac{\partial \bar{\psi}_b}{\partial x}$$

These give

(A80)
$$A = \frac{1 - \frac{K_b}{K_a}}{1 + \frac{K_b}{K_a}}$$

(A81)
$$B = \frac{2}{1 + \frac{K_b}{K_a}}$$

With these constants inserted for A and B in the above expressions for ψ_a and ψ_b, we then have an approximate prediction formula for $\bar{\psi}$ everywhere for large injection times. This can be extended to include fault boundaries and permeability discontinuities by images, but here we use this result simply to compare the "ultimate" increase in pressure at an abandoned well in an injection zone having such a discontinuity in permeability with that which would exist in the absence of this discontinuity.

We have at the abandoned well at position x,y in Region B, the pressure increase for this inhomogeneous case

(A82)
$$\Delta P_{IH} = - \frac{2}{1 + \frac{K_b}{K_a}} \frac{qu}{4\pi K_a h} \ln \frac{\phi_o \mu c[(x+d)^2 + y^2]}{4K_a t}$$

due to the injection well at position x = -d, y = 0 in Region A. This is to be compared to the increase

(A83)
$$\Delta P_H = - \frac{qu}{4\pi K_a H} \ln \frac{\gamma \phi_o \mu c[(x + d)^2 + y^2]}{4K_a t}$$

in the homogeneous case. This gives

$$\frac{\Delta P_{IH}}{\Delta P_H} \simeq \frac{2}{1 + \frac{K_b}{K_a}} \qquad \text{(Region B)} \tag{A84}$$

Thus if $K_b > K_a$, the pressure build-up at an abandoned well in Region B is less than would occur in a homogeneous reservoir while for $K_b < K_a$, the pressure build-up is greater than in the homogeneous reservoir.

If the abandoned well at x,y is located in Region A, we find, in a similar manner, from the above solutions:

$$\frac{\Delta P_{IH}}{\Delta P_H} \simeq 1 + \frac{1 - \frac{K_b}{K_a}}{1 + \frac{K_b}{K_a}} \frac{\ln \frac{4Kt}{\gamma \phi_o \mu c r r_z^2}}{\ln \frac{4Kt}{\gamma \phi_o \mu c r^2}} \tag{A85}$$

where r is the distance from the injection well to the abandoned well, while r_I is the distance from the image well to the abandoned well. Since both logarithms are positive and $r_I > r$, this ratio is less than unity for all time and any location in Region A.

Denoting the ratio of the two logarithms here by ε_t, we note that $0 < \varepsilon_t < 1$, with the upper bound of unity being achieved only as $t \to \infty$. Then the above equation appears as:

$$\frac{\Delta P_{IH}}{\Delta P_H} \simeq 1 + \varepsilon \frac{1 - \frac{K_b}{K_a}}{1 + \frac{K_b}{K_a}} \tag{A86}$$

which shows that for any ε_t, in Region A

$$\frac{\Delta P_{IH}}{\Delta P_H} < 1 \quad \text{for} \quad K_b > K_a \tag{A87}$$

and

$$(A88) \qquad \frac{\Delta P_{IH}}{\Delta P_H} > 1 \qquad \text{for } K_b > K_a$$

Now these results show that if an injection well is located in a higher permeability region of the reservoir, $K_a > K_b$, with reservoir permeability of lower value to the east, in Region B, then all abandoned wells to either the east or west, of the injection well, but lying in Region A, experience greater pressure build-up than would occur in a homogeneous reservoir. By contrast, if the injection well is located in a lower permeability region, $K_a < K_b$, with permeability of higher value in region B, then all abandoned wells to either east or west of the injector, but in region A, experience less pressure build-up than would occur in a homogeneous reservoir.

This result is more firmly established by examining the two limiting extremes for K_b, either $K_b = 0$ or $K_b \to \infty$. In these cases, exact solution of the diffusion type equation, Eq. (A61) by the method of images is possible.

For $K_b = 0$, the line $x = o$ is a no-flow "fault" boundary for Region A. There is no build-up in Region B but at any well in Region A, (by image)

$$(A89) \qquad \Delta P_{IH} = \frac{q\mu}{4\pi K_a h}\left[-Ei\left(-\frac{\phi_o \mu c r^2}{4K_a t}\right) - Ei\left(\frac{\phi_o \mu c r_I^2}{4K_a t}\right)\right]$$

or

$$(A90) \qquad \frac{\Delta P_{IH}}{\Delta P_H} = 1 + \frac{-Ei\left(-\frac{\phi_o \mu c r_I^2}{4K_a t}\right)}{-Ei\left(-\frac{\phi_o \mu c r^2}{4K_a t}\right)}$$

with r and r_I as defined above. This is clearly in complete accord with Eq. (A85) with $K_b \to 0$.

For Region B, Eq. (A84) would forecast a value of 2.0 for $K_b \to 0$ but this is inaccurate; the exact result for Region B in this case is forecast by a condition extracted from the differential equation, Eq. (A61), applied to Region B. Thus

$$(A91) \qquad \frac{\partial \bar{\psi}_b}{\partial t} = \frac{K_b}{\phi_o \mu c} \nabla^2 \psi_b$$

so for a finite value of $\nabla^2 \psi_b$, we see that as $K_b \to 0$, $\partial \psi_b / \partial t \to 0$ and of course there is no build-up of pressure in Region B.

The other extreme, $K_b \to \infty$, is also evaluated exactly using images. In this case, we have in Region A

$$(A92) \qquad \Delta P_{IH} = \frac{q\mu}{4\pi K_a h} \left[-Ei\left(-\frac{\phi_o \mu c r^2}{4K_a t}\right) + Ei\left(-\frac{\phi_o \mu c r_I^2}{4K_a t}\right) \right]$$

or

$$(A93) \qquad \frac{\Delta P_{IH}}{\Delta P_H} = 1 - \frac{-Ei\left(-\frac{\phi_o \mu c r_I^2}{4K_a t}\right)}{-Ei\left(-\frac{\phi_o \mu c r^2}{4K_a t}\right)}$$

which again is in complete accord with Eq. (A85), but in this case for $K_b \to \infty$. Here, of course, the line $x = 0$ acts as an equipotential boundary at original reservoir potential and the entire Region B remains always at original potential. There can be no potential gradients in Region B when $K_b \to \infty$. Thus in Region B, $x > 0$,

$$(A94) \qquad \frac{\Delta P_{IH}}{\Delta P_H} = 0$$

which is in complete accord with Eq. (A84) as $K_b \to \infty$.

We can summarize these various cases in the following table. In this table we consider the injection well always located in region A and examine the effect of the discontinuity in permeability on pressure buildup at an abandoned well which may be located in either region A or region B. The symbolic notations ↑, ↓, - indicate increase, decrease or no change in pressure buildup at the abandoned relative to a homogeneous reservoir case, caused by the discontinuity in permeability.

Effect of Permeability
Discontinuity on Pressure Buildup
(Injector in Region A)

Case	Location of Abandoned Well	Effect on Pressure Buildup at Abandoned Well
$K_A > K_B$	A	↑
$K_A > K_B$	B	↑
$K_A < K_B$	A	↓
$K_A < K_B$	B	↓

Partially-Sealing Faults

In all analyses thus far described, faults have been treated as totally sealing plane boundaries; here we examine effects of partially-sealing faults on the temporal history of the potential distribution in the injection zone. Specifically, we consider the problem of one linear, partially-sealing fault transecting a uniform, infinite aquifer. Yaxley (1985) has solved this problem for a single well of constant rate using the LaPlace transform in the time domain and the Fourier transform in the space domain. Here we describe his solution in terms of the same coordinate geometry employed earlier for other fault problems.

The nature of a partially-sealing fault is displayed in Figure A1.4.

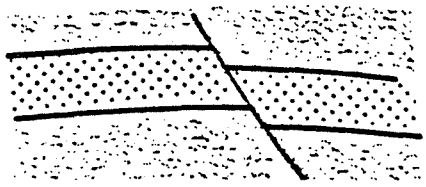

FIGURE A1.4

The "narrowed" flow pathway indicated at the fault is equivalent to a "thin" domain of lower permeability as shown in Figure A1.5.

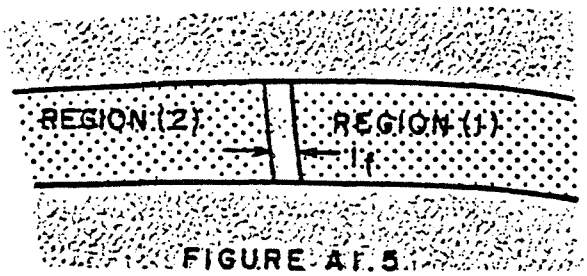

FIGURE A1.5

with the thickness ℓ_f being very small. Thus, the mathematical description of the problem takes the form as seen in Figure A1.6.

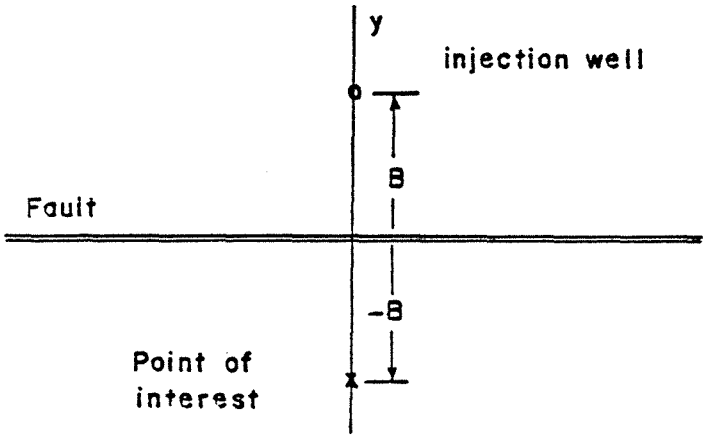

FIGURE A1.6

Then:

$$\frac{\partial^2 \bar{\psi}_2}{\partial x^2} + \frac{\partial^2 \bar{\psi}_2}{\partial y^2} = \frac{\phi_o \mu c}{K} \frac{\partial \bar{\psi}_2}{\partial t} \tag{A95}$$

$$\frac{\partial^2 \bar{\psi}_1}{\partial x^2} + \frac{\partial^2 \bar{\psi}_1}{\partial y^2} = \frac{\phi_o \mu c}{K} \frac{\partial \bar{\psi}_1}{\partial t} \tag{A96}$$

$$\lim_{\frac{x^2 + y^2}{t} \to \infty} \bar{\psi}_1 = \bar{\psi}_o \; ; \quad y > 0 \tag{A97}$$

$$\lim_{\frac{x^2 + y^2}{t} \to \infty} \bar{\psi}_2 = \bar{\psi}_o \; ; \quad y < 0 \tag{A98}$$

and there is a <u>point singularity</u> in $\bar{\psi}_1$, at the point (B,0) corresponding to a

line source of constant rate q in the reservoir of unique thickness, h. Also, at the fault, x = 0, we have

(A99) $$\frac{K}{\mu}\frac{\partial \bar{\psi}_2}{\partial y} = \frac{K}{\mu}\frac{\partial \bar{\psi}_1}{\partial y} = \frac{K_f}{\mu}\frac{\bar{\psi}_1 - \bar{\psi}_2}{\ell_f} \quad ; y = 0$$

Thus, there is a <u>discontinuity</u>, $\bar{\psi}_1 - \bar{\psi}_2$, at the fault, i.e. we let $\ell_f \to 0$ with also $K_f \to 0$ such that the ratio K_f/ℓ_f is finite and non-zero in the limit.

The solution of this boundary value problem is given by Yaxley (1985) as:

<u>For y > 0:</u>

(A100) $$\Delta P_D = -Ei\left(-\frac{(y_D - 1)^2 + x_D^2}{4t_D}\right) - Ei\left(-\frac{(y_D + 1)^2 + x_D^2}{4t_D}\right)$$

$$-2\pi\alpha_f e^{[2\alpha_f(|y_D| + 1)]} \int_0^{t_D} e^{\left(4\alpha_f^2\mu - \frac{x_D^2}{4\mu}\right)}$$

$$\cdot \operatorname{erfc}\left[2\alpha_f\sqrt{\mu} + \frac{|y_D| + 1}{2\sqrt{\mu}}\right] \frac{du}{\sqrt{\mu}}$$

<u>For y < 0:</u>

(A101)

$$\Delta P_D = 2\pi\alpha_f e^{[2\alpha_f(|y_D| + 1)]} \int_0^{t_D} e^{\left(4\alpha_f^2\mu - \frac{x_D^2}{4\mu}\right)}$$

$$\cdot \operatorname{erfc}\left[2\alpha_f \mu + \frac{|y_D| + 1}{2\sqrt{\mu}}\right] \frac{du}{\sqrt{\mu}}$$

where we define dimensionless quantities as

(A102) $$\Delta P_D = \frac{4\pi Kh}{q\mu}(\bar{\psi} - \bar{\psi}_o), \qquad x_D = \frac{x}{B}, \; y_D = \frac{y}{B}$$

$$t_D = \frac{Kt}{\phi_o \mu c B^2}, \qquad \alpha_f = \frac{K_f B}{K\ell_f}$$

The reader should note that our definition for ΔP_D is precisely $2 \cdot P_D$ where P_D is the dimensionless pressure defined by Yaxley and generally used in the petroleum engineering literature.

Both of the above forms for ΔP_D involve the function defined as

$$(A103)\quad I(\alpha_f, |y_D|, x_D, t_D) = 2\pi\alpha_f e^{2\alpha_f[|y_D+1|]} \int_0^{t_D} e^{\left(4\alpha_f^2\mu - \frac{x_D^2}{4\mu}\right)} \cdot \operatorname{erfc}\left[2\alpha_f\mu + \frac{|y_D|+1}{2\sqrt{\mu}}\right] \frac{du}{\sqrt{\mu}}$$

In fact, for $y_D < 0$, this is precisely ΔP_D. The integral here cannot be evaluated in closed form so numerical evaluation is necessary. Yaxley carried out such evaluations to provide results for limited cases but only one set of these results is applicable to problems of interest here. In Figure A1.7 his results are shown for $x_D = 0$ and $y_D = -1$. This places the "observation well", or an abandoned well in our study, at a point on the line normal to the fault at the same distance as is the injection well on the opposite side of the fault.

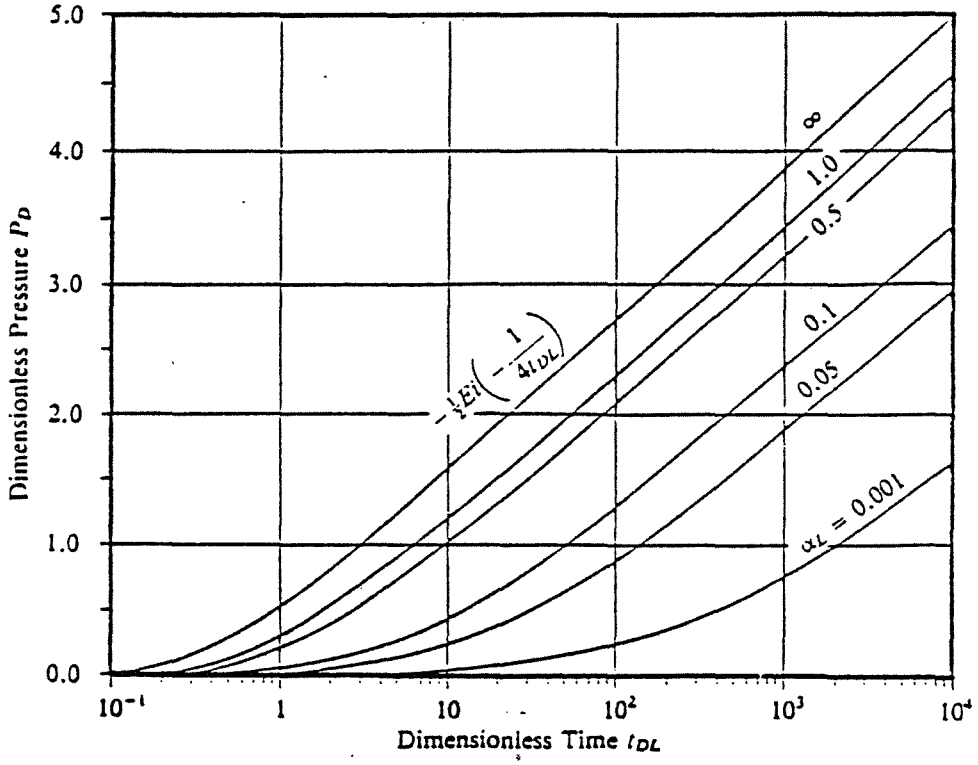

FIGURE A1.7

In Figure A 1.7, P_D is $\Delta P_D/2$, α_L is $2\alpha_f$ and t_{DL} is $t_D/4$ because Yaxley employed L = 2B in defining the dimensionless time and α_L for this calculation.

Note that for large values of time, and any value of α_L, the curve for P_D, (or ΔP_D), are all parallel to the curve for $\alpha_L = \infty$. This curve is simply the P_D vs t_{DL} that exists in the total absence of the fault. Thus, for large time, ΔP_D is simply shifted by an additive constant determined by α_f. This is very useful information but unfortunately it is applicable only to <u>one</u> abandoned well location; therefore, we have evaluated this solution for a general range of values for x_D, y_D, t_D and α_f. These results are described in the body of this report.

APPENDIX B

ON THE EFFECT OF BOREHOLE GEOMETRY ON APPARENT GEL STRENGTH OF DRILLING MUD IN ABANDONED WELLS

APPENDIX B

On The Effect of Borehole Geometry on Apparent Gel Strength of Drilling Mud In Abandoned Wells

ABSTRACT

A series of small scale experiments was carried out to determine the effectiveness of old, gelled drilling mud in abandoned wellbores in preventing brine from migrating up abandoned wells from a fluid injection zone driven by pressure build-up. It was found that in general the critical pressure for initiation of brine entry into the mud-filled wellbore is composed of two parts, one due to the weight of the mud column and the other due to the gel strength of the mud. For typical water-base bentonite muds and smooth, straight, uniform diameter holes, these contributions are comparable in magnitude. However, for holes of irregular shape, as with shale wash-outs, the contribution due to gel strength may be increased by five-fold or more.

Experimental Objectives

These small-scale experiments were conducted to determine criteria for brine entry into an abandoned, mud-filled bore hole from an aquifer due to increase in pressure from fluid injection into the aquifer. Specifically, we wish to define a critical pressure, P_{crit}, in the aquifer at the abandoned well which, if exceeded, will allow brine entry to the abandoned well.

General Description of Apparatus and Procedure

This study actually includes nine different experiments using the same basic apparatus with only minor alterations. Figure 1 shows the general configuration of laboratory equipment. A core was epoxied into a nipple and then attached to a pipe joint below the core which in turn was attached to a line carrying brine from a salt water reservoir. The pressure at the salt reservoir was recorded using a gauge or mercury manometer. Pressure was supplied to the brine using compressed nitrogen and a pressure regulator. Brine was pushed through the brine delivery system until no air existed in the lines and the rock was saturated with the brine. At this point, a pipe was attached to the core nipple and a column of bentonite mud (20 ppb bentonite with 3 ppb salt in run 1 and 30 ppb bentonite in all other runs) was placed in the pipe over the core.

A sample of this mud was also placed in a Fann viscometer cup to remain quiescent. A small diameter transparent tube was attached to the top of the mud column and filled with brine so that when the mud column moved, fluid movement could be noted at the top of the column. The mud was allowed to gel for approximately 12 hours, at which time, pressure was slowly applied to the brine delivery system until fluid movement was noted in the viewing tube at the top of the column. Concurrently, the gel strength of the mud sample in the viscometer cup was measured using a Fann V-G meter. Note that the relevant distances to calculate pressures are indicated by A, B, and C in

Figure 1. All physical dimensions of this apparatus are given in the appendix together with physical properties of fluids used.

Specific Description of Runs

Runs 1 & 2
The geometries for the various experimental runs are shown in Figure 2. In the first two runs, the pipe size was small (refer to Appendix). Two 1/16 inch shoulders were located along the length of the pipe, one just above the core and one midway up the length of the pipe. In addition, a fairly severe constriction occurred at the top of the column where the viewing tube was substantially smaller (diameter = 1/8") than the pipe itself and mud actually extended into this tube. Therefore, three constrictions existed along the mud column. The 1/16 inch shoulders were fairly large relative to the total diameter of the pipe.

Run 3
A large pipe was substituted for the small pipe (see Appendix). The pipe contained only one 1/8" shoulder located above the core. The adapter with brine viewing tube on top was used as shown in inset of Figure 2.

Run 4
The same set-up as run 3 was used; however, the pipe had an oily film over its entire surface. No specific data was collected since fluid flow responded immediately to changes in hydrostatics and no apparent gel strength was observed.

Run 5
Run 5 was similar to run 3 except that an additional constriction was placed o the mud column and the mud column extended into the smaller pipe on top and into the brine viewing tube. (see Figure 2 inset)

Run 6 & 7
Runs 6 & 7 were identical. These runs were identical to run 3 but instead of a smooth pipe being used, a series of five joints and nipples (in addition to the one located above the core mentioned in 3) were located along the length of the pipe. (see Figure 2)

Run 8
This rum employed the small pipe as in Run 1 and 2 but in this case the mud did not extend into the small viewing tube initially. The mud level was in the 5/8" ID pipe.

Run 9
This run was intended to test behavior in a pipe of uniform dimensions with no constrictions anywhere. A PVC pipe was mounted into the core containing the nipple used in Runs 3 and 4 with the pipe inserted flush to the core plug face. Thus no "shoulders" were present in the mud-filled pipe. The adapter with the brine-filled viewing tube was mounted on top but the mud level was in the uniform diameter pipe.

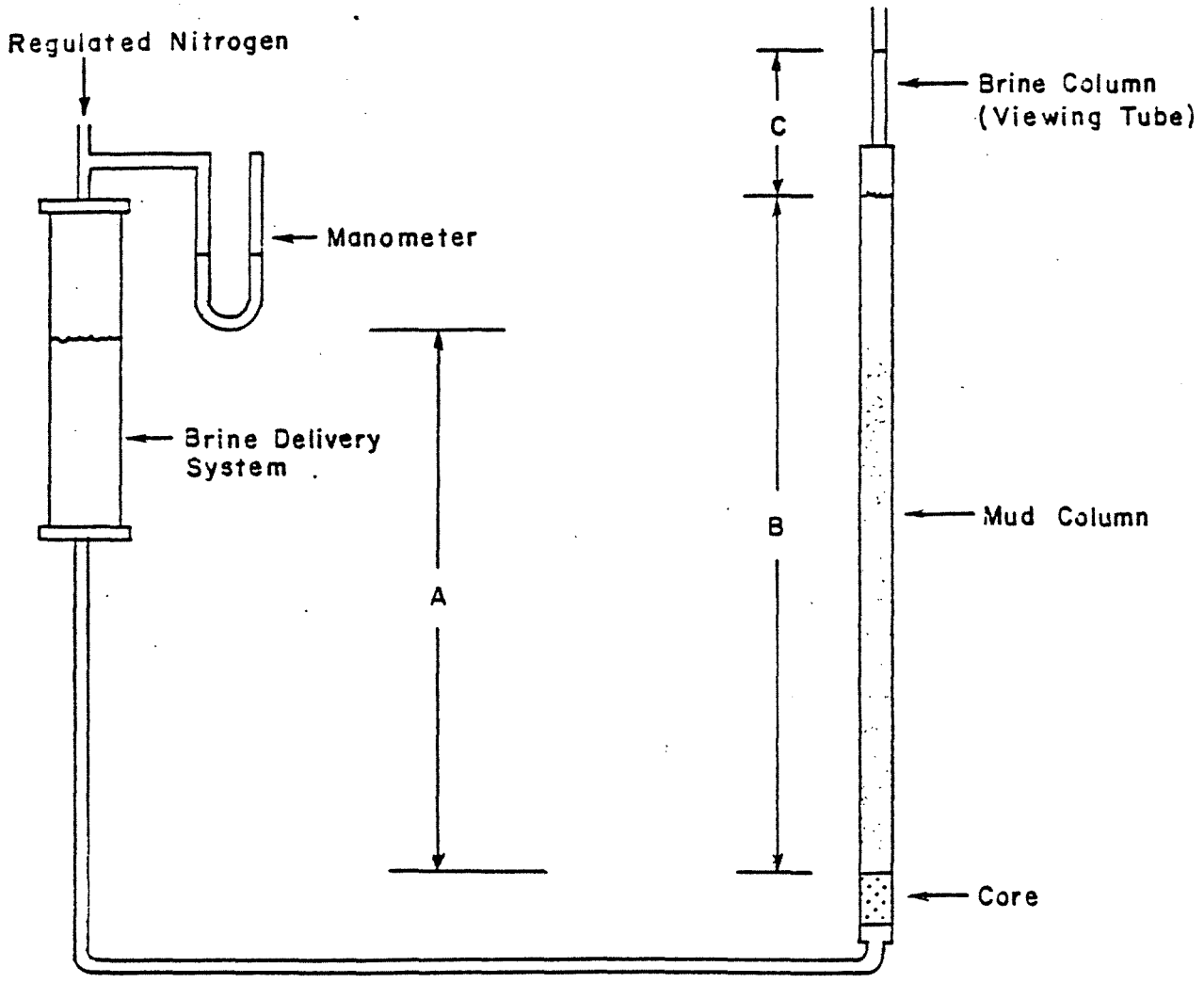

FIGURE I. General Description of Equipment

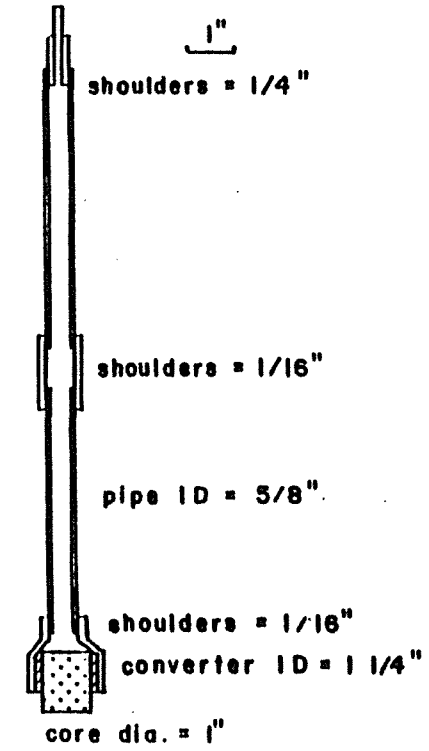

Runs 1, 2 and modified for Run 8

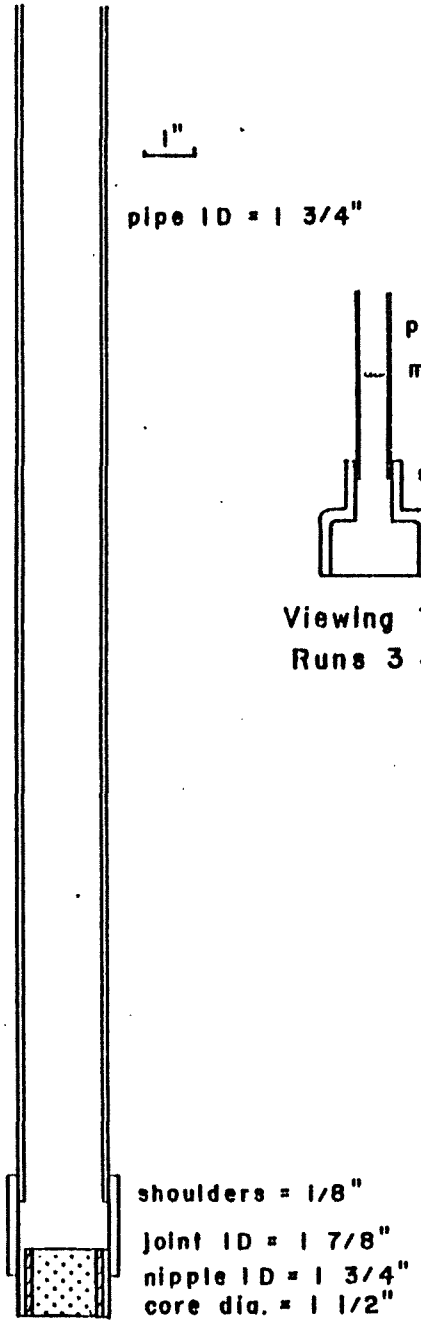

Runs 3, 4 and modified for Runs 5 and 9

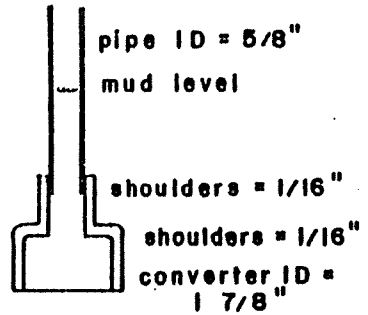

Viewing Tube
Runs 3 - 9

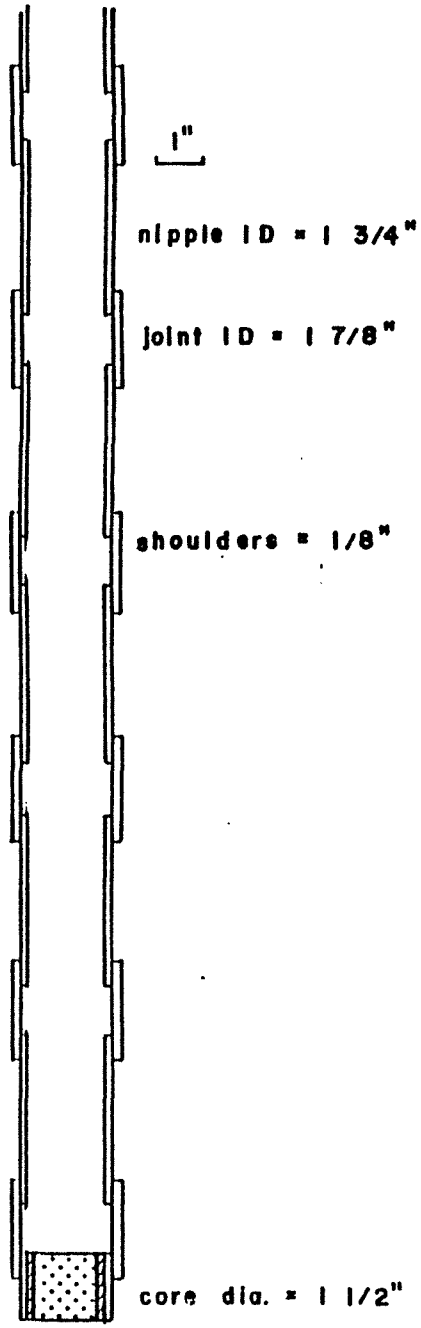

Runs 6 and 7

FIGURE 2

Calculations and Results

The apparent gel strength, G', of the mud in column is defined using the force balance on the mud column formulated as for a uniform cylindrical column of the same vertical height, B, as the actual column and the same diameter as the inside diameter of the pipe used in the experiment. Note that this computation explicitly excludes allowances for non-uniformity in diameter at nipple joints, etc.

The pressure of brine at the face of the core plug against the mud column is given by (gauge value)

$$(1) \qquad P_c = P_m + \rho_b g A$$

where P_m is manometer reading of pressure on brine in the reservoir. The hydrostatic pressure of the mud column and brine on top of the mud is (gauge value)

$$(2) \qquad P_h = \rho_m g B + \rho_B g C$$

Then the force balance criterion for on-set of movement of the mud column by shearing of the gel at the cylindrical wall of the column is

$$(3) \qquad \pi r_p^2 (P_c - P_h) \geq 2\pi r_p A G'$$

where G' is the apparent gel strength. Thus we calculate G' from the experimental data using

$$(4) \qquad G' = \frac{r_p}{2A} (P_c - P_h)$$

The calculated apparent gel strength G' was compared to the Fann gel strength G as a ratio R, where

$$R = G' / G$$

A summary of results is given in Table 1.

Run #	1	2	3	4	5	6	7	8	9
R	5.11	5.05	1.68	0.0	2.77	3.83	3.61	5.76	1.99

TABLE 1. R Values For All Runs

Discussion of Results

The results of Runs 1 and 2 indicate non-uniform geometry profoundly influences the apparent gel strength. Apparently the relative size of diameter constrictions in relation to the cylinder in which the mud stands produced the larger increases in apparent gel strength observed in Runs 1 and 2 as compared to other runs.

In Run 3, the one shoulder in the large pipe produced, approximately, a 68% increase in apparent gel strength over the measured Fann measured value. In Runs 6 and 7, it would be reasonable to assume that the increase in apparent gel strength should be about six times the 68% value observed in Run 3 since 6 shoulders are present. This would produce an R value of 1 + (0.68 * 6) or 5.08 which is larger than the apparent values actually observed in Runs 6 and 7.

Run 5 provides further evidence that geometric irregularities produce increases in apparent gel strength. With the constriction on the top of the pipe (along with the shoulder of Run 3), the apparent gel is increased by nearly three-fold over the Fann measured value.

Run 4 demonstrates that when the mud column is detached from the pipe structure by an oily film, either the brine flows up the pipe around the mud column or the column provides little or no gel strength since it is, in effect, not bonded to the pipe.

Run 8 was to test whether the very large value of G observed in Runs 1 and 2 was due in part to the fact that mud extended into the small diameter viewing tube at the top of the 5/8" ID pipe. Since the observed value of R in Run 8 was even larger, this is not the case.

The objective in Run 9 was to determine whether a tube free of any non-uniformities in diameter of the mud column would yield a G value comparable to that measured in the Fann viscometer. Since the apparent G value in this case was almost double the Fann determined value, this is not the case. Thus, there are other factors involved besides non-uniform diameter of hole which cause the high apparent G values.

We can speculate on the implications of the data obtained in the above experiments:

(1) There is clearly an increase in the contribution of mud gel strength to the threshold pressure for brine entry arising from constrictions or non-uniformities in pipe (simulated borehole) diameter. A factor of about 2 - 5 was observed.

(2) There is another contribution to threshold brine entry pressure not associated with hole geometry. We speculate that this may be due to an "interfacial tension" effect as brine tries to enter gelled mud from the small pores in the core plug.

This interfacial tension effect would contribute a ΔP to the threshold entry pressure as

$$\Delta P = \frac{2\gamma}{r}$$

where r is the radius of the hemispherical bubble of brine entering the mud while γ is an effective interfacial tension. The value of r should be the average of the largest pores open on the core plug face. Thus for the same brine and mud we could see a difference in ΔP for the two core plugs used in our experiments. Also it is possible that upon standing with mud pressure on the core plug, some particulates could enter the larger pores of the core plug so r might be reduced in later experiments using the same core plug. This might account for the results in Runs 8 and 9.

Future Research

Clearly, we have not answered all questions concerning the criteria for brine entry into a mud-filled abandoned well but we have shown that the critical pressure for brine entry is given by an equation of the form (P_{crit} in psi)

$$P_{crit} = \Delta P + 0.052\ \rho_{mud} d + 3.33 \times 10^{-3}\ \frac{G'd}{D}$$

where

ρ_{mud} = mud weight (lb/gal)

G' = apparent gel strength of mud (lb/100 ft^2)

d = total depth to disposal aquifer (ft)

D = mean diameter of abandoned well (inches)

ΔP = possible brine-mud interfacial tension contribution (psi)

In order to fully quantify this equation, more experimentation is required. We propose doing experiments using larger diameter simulated boreholes with a variety of well-defined non-uniformities in diameter, with fluid entry through rock circumferentially as in a real well. We also will design an experiment to directly measure the contribution to P_{crit} defined above as ΔP.

In closing this preliminary report, we note the significance of the results thus far obtained. For a borehole of 5000 ft. depth filled with mud of minimal weight (P_{mud} = 8.16 lb/gal) and minimal gel strength (G' = 50 lb/100 ft^2) we compute for a 9 inch diameter hole,

$$P_{crit} = \Delta P + 2236 + 8.34$$

but if, as indicated by our data, the last term due to gel is increased four-fold by hole irregularities, this is

$$P_{crit} = \Delta P + 2236 + 33.37$$

Now, since normal static aquifer pressure at 5000 ft. is about .437 x 5000 = 2185, we see that mud weight alone gives a tolerable pressure increase in the aquifer of 2236 - 2185 = 51 psi and the gel adds more than half this amount to the critical entry pressure. If this were a typical salt mud, G' would be five times greater and the gel contribution, with hole irregularities, would be about 167 psi or more than three times the mud weight contribution.

Data and Results

Run 1

	in.	cm.
Core Radius	0.5	1.27
Pipe Radius	0.3125	0.7438
Length A	24.409	62.0
Length B	11.5	29.2
Length C	4.53	11.5

	psi	in. Hg
Pm	3.0	
Ps	+0.8937	+ 1.8
Ph	0.5966	1.2
Pc	3.89	7.9

	psi	lbs/100 sq. ft (12 hours)
G		125.0
G'	0.04475	644.0

$G'/G = R = 5.11$

Run 2

	in.	cm.
Core Radius	0.5	1.27
Pipe Radius	0.3125	0.7438
Length A	14.6	37.0
Length B	12.0	30.5
Length C	3.94	10.0

	psi	in. Hg
Pm	7.859	16.0
Ps	-0.533	-1.1
Ph	0.5966	1.2
Pc	7.326	14.9

	psi	lbs/100 sq. ft (12 hours)
G		250.0
G'	0.08763	1262.0

$G'/G = R = 5.05$

10B

Run 3

	in.	cm.
Core Radius	0.75	1.91
Pipe Radius	0.8125	2.06
Length A	11.4	29.0
Length B	26.0	66.0
Length C	6.5	16.5

	psi	in. Hg
Pm	3.438	7.0
Ps	-0.418	-0.851
Ph	1.218	2.48
Pc	3.02	6.15

	psi	lbs/100 sq. ft (12 hours)
G		250.0
G'	0.02816	405.0

$G'/G = R = 1.68$

Run 5

	in.	cm.	
Core Radius	0.75	1.91	
Pipe Radius	0.8125	2.06	small pipe
Length A	12.2	31.0	radius =
Length B	33.9	86.0	0.3125 inch
Length C	3.54	9.0	(see sketch)

	psi	in. Hg
Pm	4.91	10.0
Ps	-0.4476	-0.91
Ph	1.4059	2.86
Pc	4.4643	9.1

	psi	lbs/100 sq. ft (12 hours)
G		210.0
G'	0.04042	582.0

$G'/G = R = 2.77$

Run 6

	in.	cm.
Core Radius	0.75	1.91
Pipe Radius	0.8125	2.06
Length A	13.8	35.0
Length B	26.0	66.0
Length C	6.3	16.0

	psi	in. Hg
Pm	3.93	8.0
Ps	-0.5044	-1.28
Ph	1.21	2.46
Pc	3.425	6.97

	psi	lbs/100 sq. ft (12 hours)
G		130.0
G'	0.03460	498.0

$G'/G = R = 3.83$

Run 7

	in.	cm.
Core Radius	0.75	1.91
Pipe Radius	0.8125	2.06
Length A	13.8	35.0
Length B	26.0	66.0
Length C	6.3	16.0

	psi	in. Hg
Pm	4.13	8.4
Ps	-0.5044	-1.28
Ph	1.21	2.46
Pc	3.6214	7.373

	psi	lbs/100 sq. ft (12 hours)
G		150.0
G'	0.03768	542.0

$G'/G = R = 3.61$

Run 8 Small Pipe - no top constriction

	in.	cm.
Core Radius	0.5	1.27
Pipe Radius	0.3125	0.7938
Length A	21.65	55.0
Length B	9.84	25.0
Length C	3.05	7.75

	psi	in. Hg
Pm	6.1886	12.6
Ps	-0.7925	-1.6135
Ph	0.4827	0.9828
Pc	5.396	10.98

	psi	lbs/100 sq. ft (12 hours)
G		195.0
G'	0.078	1123.0

G'/G = R = 5.76

Run 9

	in.	cm.
Core Radius	0.75	1.91
Pipe Radius	0.75	1.91
Length A	20.866	53.0
Length B	22.441	57.0
Length C	5.906	15.0

	psi	in. Hg
Pm	3.438	7
Ps	-0.7637	-1.555
Ph	1.062	2.162
Pc	2.674	5.444

	psi	lbs/100 sq. ft (12 hours)
G		195.0
G'	0.02694	388.0

G'/G = R = 1.99

FLUID PROPERTIES

	Density (g/cc)	lb/gal	psi/ft	psi/in	psi/cm
Salt	1.0147	8.45	0.4394	0.0366	0.01441
Mud (Run 1)	1.0396	8.65	0.4498	0.0375	0.01476
Mud (Runs 2-7)	1.0444	8.70	0.4520	0.0377	0.01484

Mud Composition:
Run 1: 20 ppb bentonite, 3 ppb salt
Runs 2-9: 30 ppb bentonite

NOMENCLATURE

A,B,C	Vertical dimensions of experimental set-up
r_c	Core Radius
r_p	Pipe Radius
h_p	Pipe Length
Pm	Manometer pressure
Ps	Hydrostatic pressure of brine reservoir
Ph	Hydrostatic head of mud/brine over core
Pc	Pressure at core face

THIS PAGE

INTENTIONALLY

LEFT BLANK

APPENDIX C

CASE STUDIES

FOR ALL CASES

DEPTH = 5000 FT.

INITIAL PRESSURE = P_o = 2200 PSI

CASE I

EFFECTS OF SEALING FAULT BOUNDARIES AND WELL LOCATIONS

Group 1, Only boundaries are varied

Group 2, Same as Group 1 but with different injection well location

Group 3, Same as Group 1 and 2 but with yet another injection well location

Group 4, Same as Group 2 but with different K and h

Group 5, Same as Group 1 but with K and h of Group 4

Group 6, Complete pressure histories for all abandoned wells for run Case I, Group 1, No. 2

CASE I GROUP 1

PROPERTIES OF THE DISPOSAL ZONE

COMPRESSIBILITY = 0.500E-05 1/PSI
PERMEABILITY = 300.000 MD
VISCOSITY = 1.000 CP
THICKNESS = 50.0 FT
POROSITY =0.200

PROPERTIES OF ABANDONED HOLES

ABAN WELL	DIAM IN	DEPTH TO DISP ZONE FT	DEPTH TO H2O ZONE FT	MUD DENSITY LB/GAL	GEL STRENGTH LB/100FT2	CRITIC PRESSU PSI
1	9.6	5000.00	600.0	9.000	100.00	2513.16
2	9.6	5000.00	600.0	9.000	100.00	2513.16
3	9.6	5000.00	600.0	9.000	100.00	2513.16
4	9.6	5000.00	600.0	9.000	100.00	2513.16
5	9.6	5000.00	600.0	9.000	100.00	2513.16
6	9.6	5000.00	600.0	9.000	100.00	2513.16
7	9.6	5000.00	600.0	9.000	100.00	2513.16
8	9.6	5000.00	600.0	9.000	100.00	2513.16
9	9.6	5000.00	600.0	9.000	100.00	2513.16
10	9.6	5000.00	600.0	9.000	100.00	2513.16

COORDINATES OF THE ABANDONED WELLS

WELL #	X FT.	Y FT.
1	5000.000	1500.000
2	3000.000	1000.000
3	4400.000	3600.000
4	6000.000	4000.000
5	6500.000	2500.000
6	8000.000	4000.000
7	9000.000	2000.000
8	7800.000	6400.000
9	9000.000	6000.000
10	8000.000	7000.000

COORDINATES OF THE INJECTION WELL

X= 4000.000 Y= 2000.000 FT.
INJECTION RATE =5000. BBL/DAY

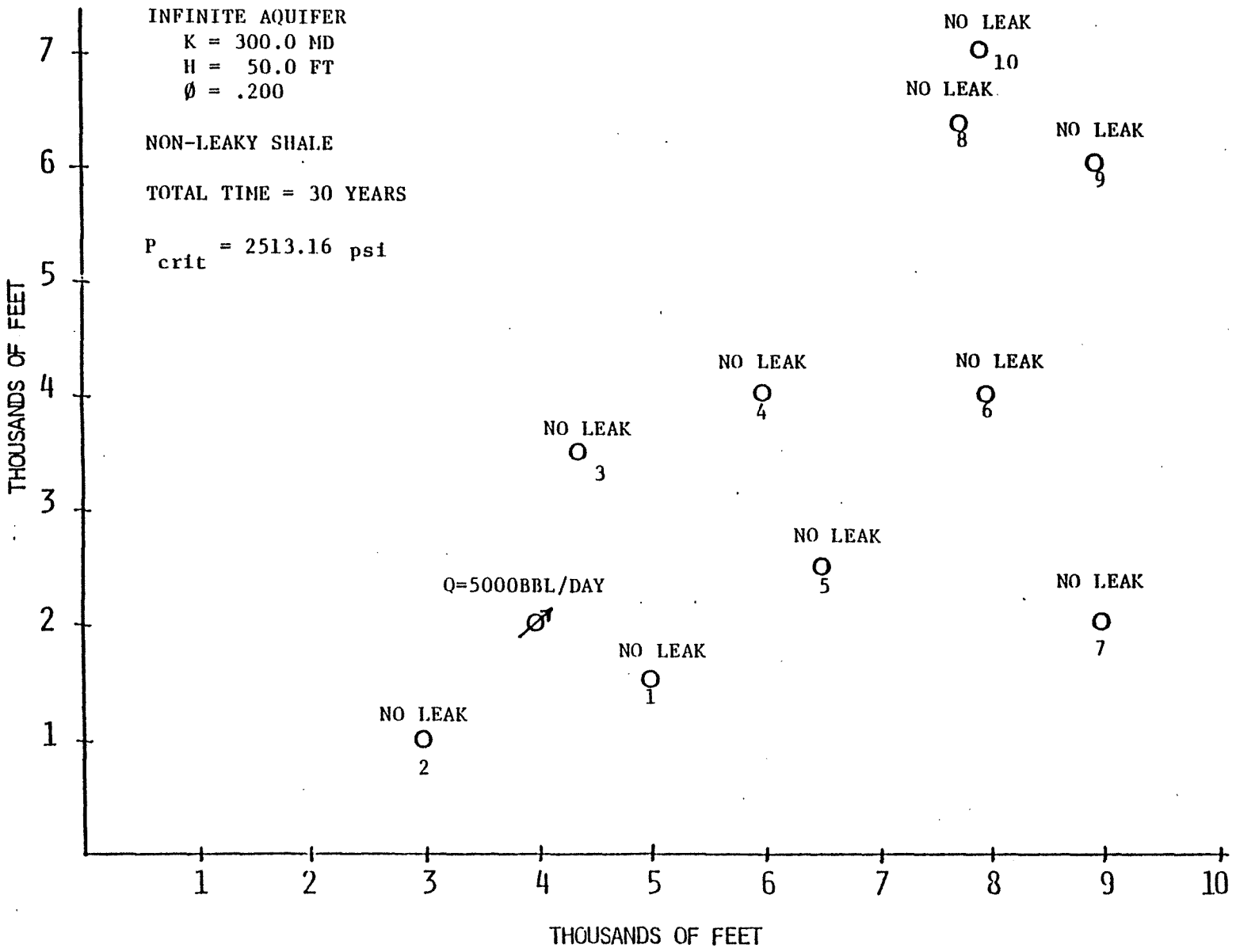

CASE 1, GROUP 1, NO. 1

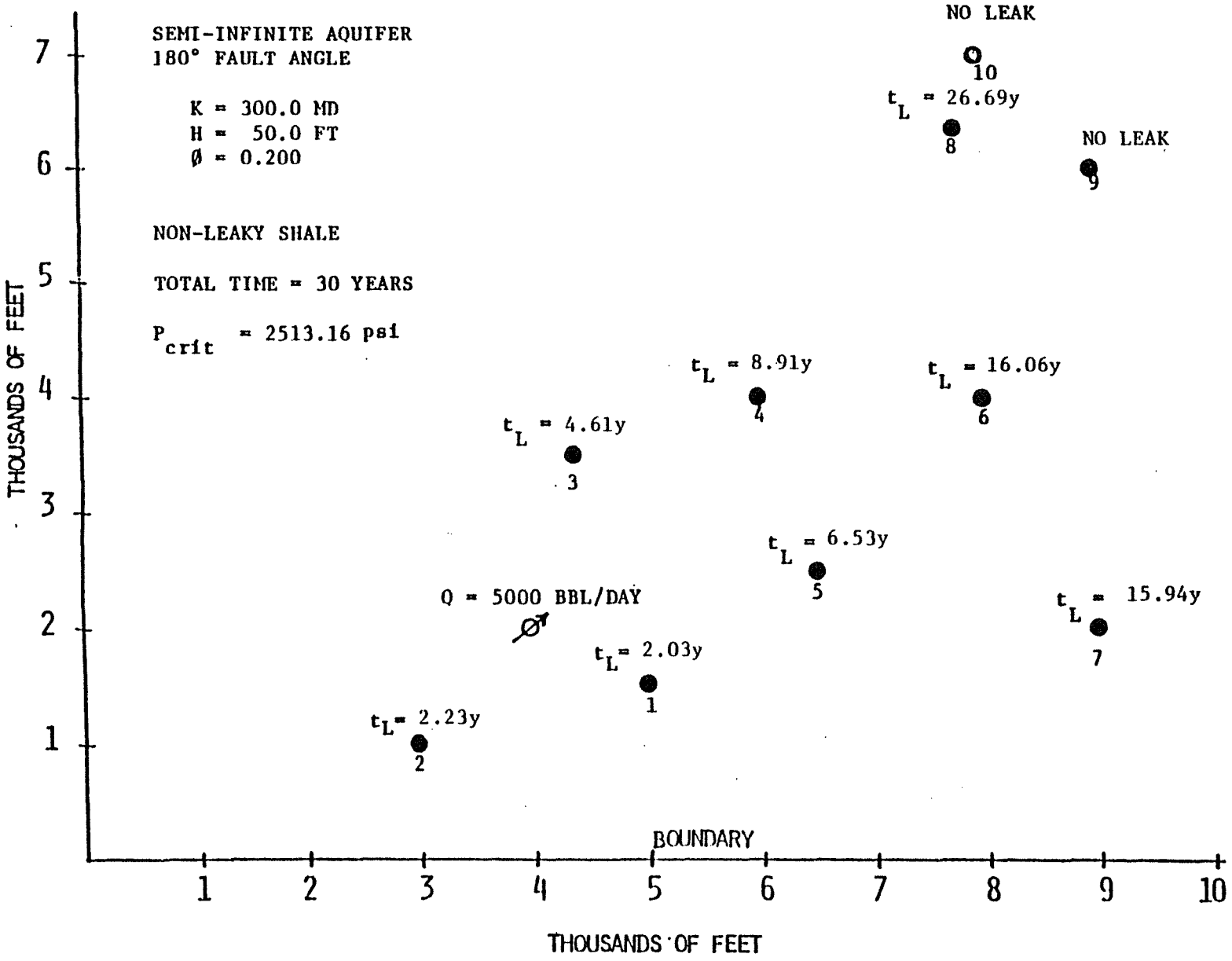

CASE I, GROUP 1, NO. 2

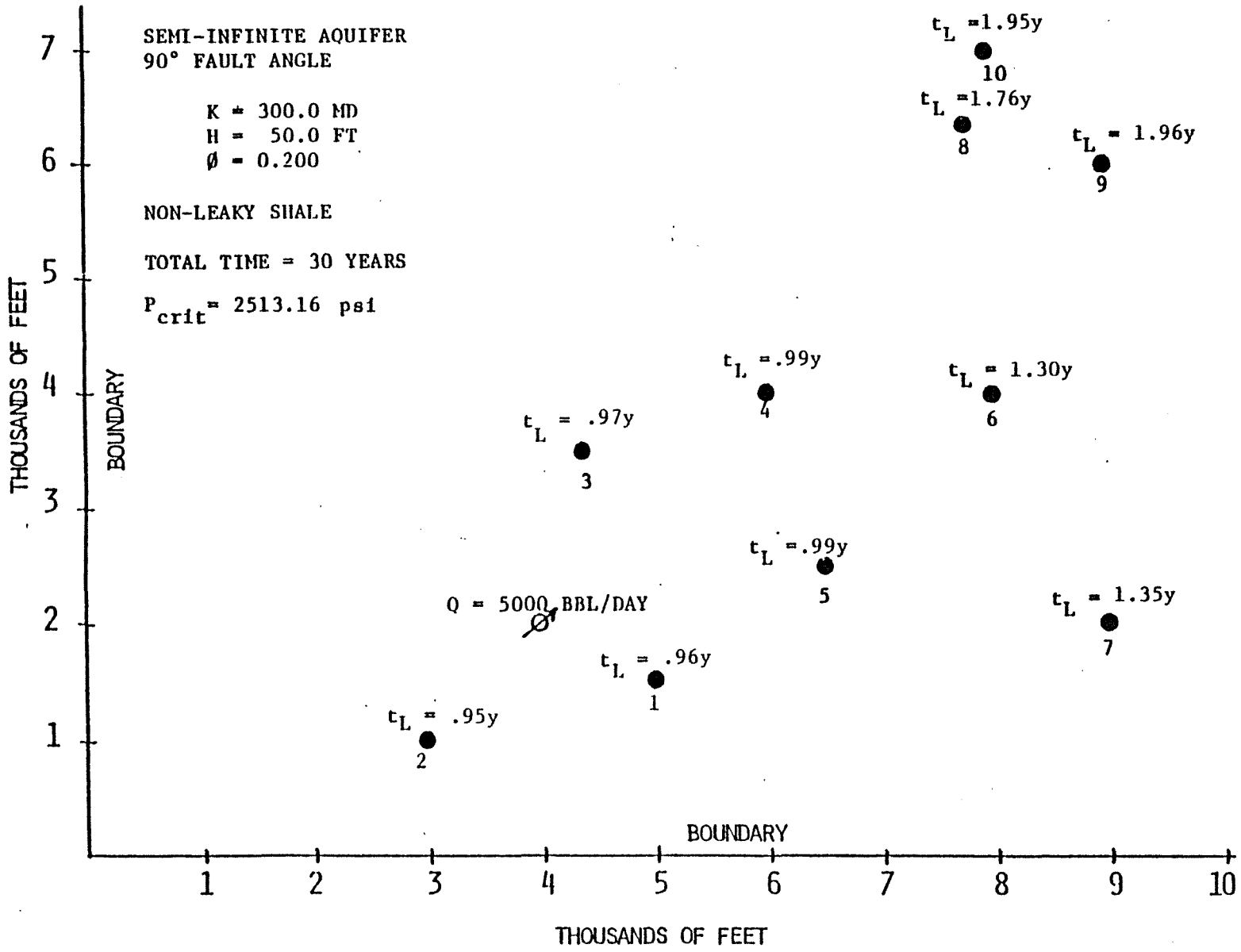

CASE I, GROUP 1, NO. 3

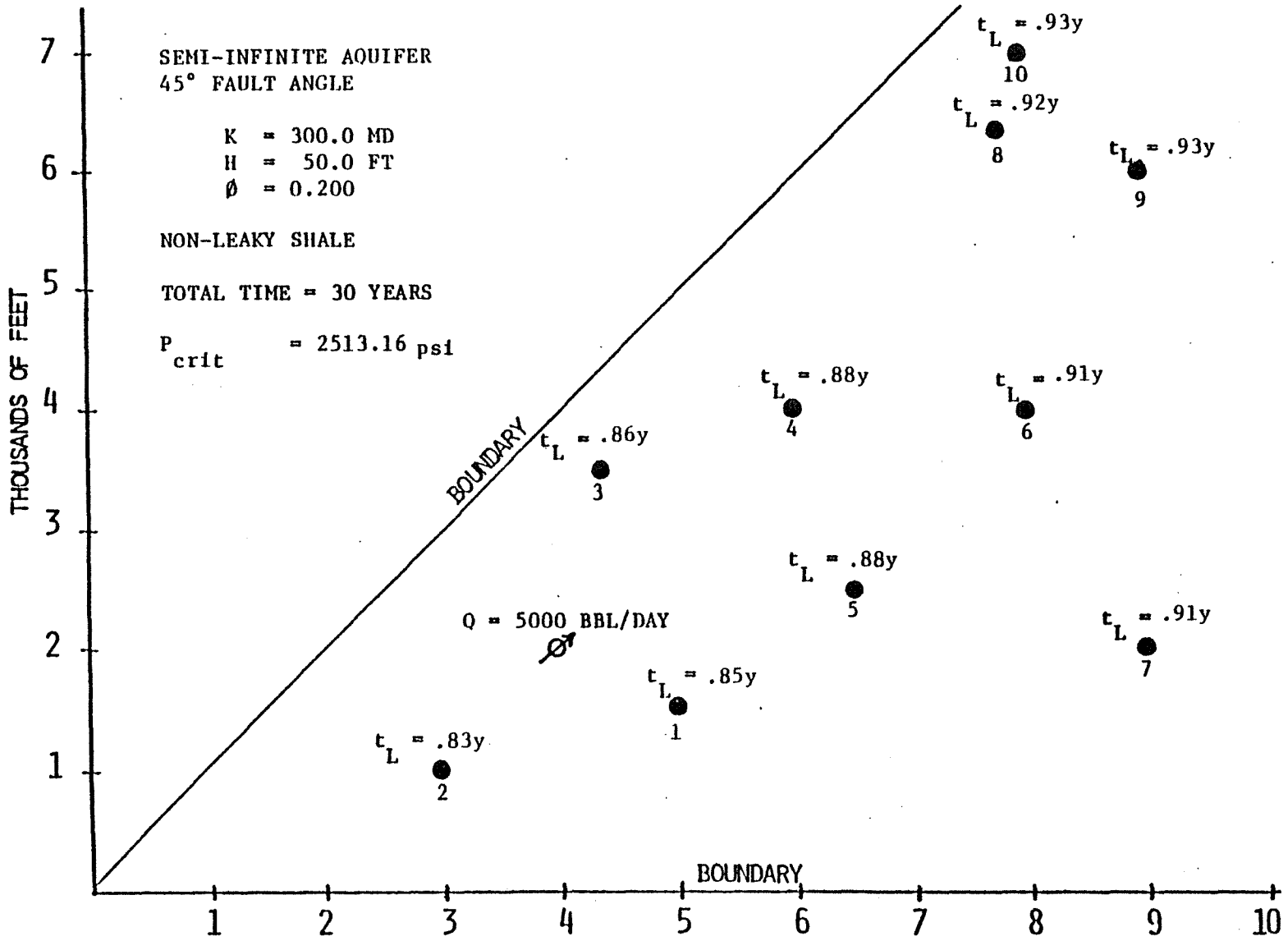

CASE 1 , GROUP 1, NO. 4

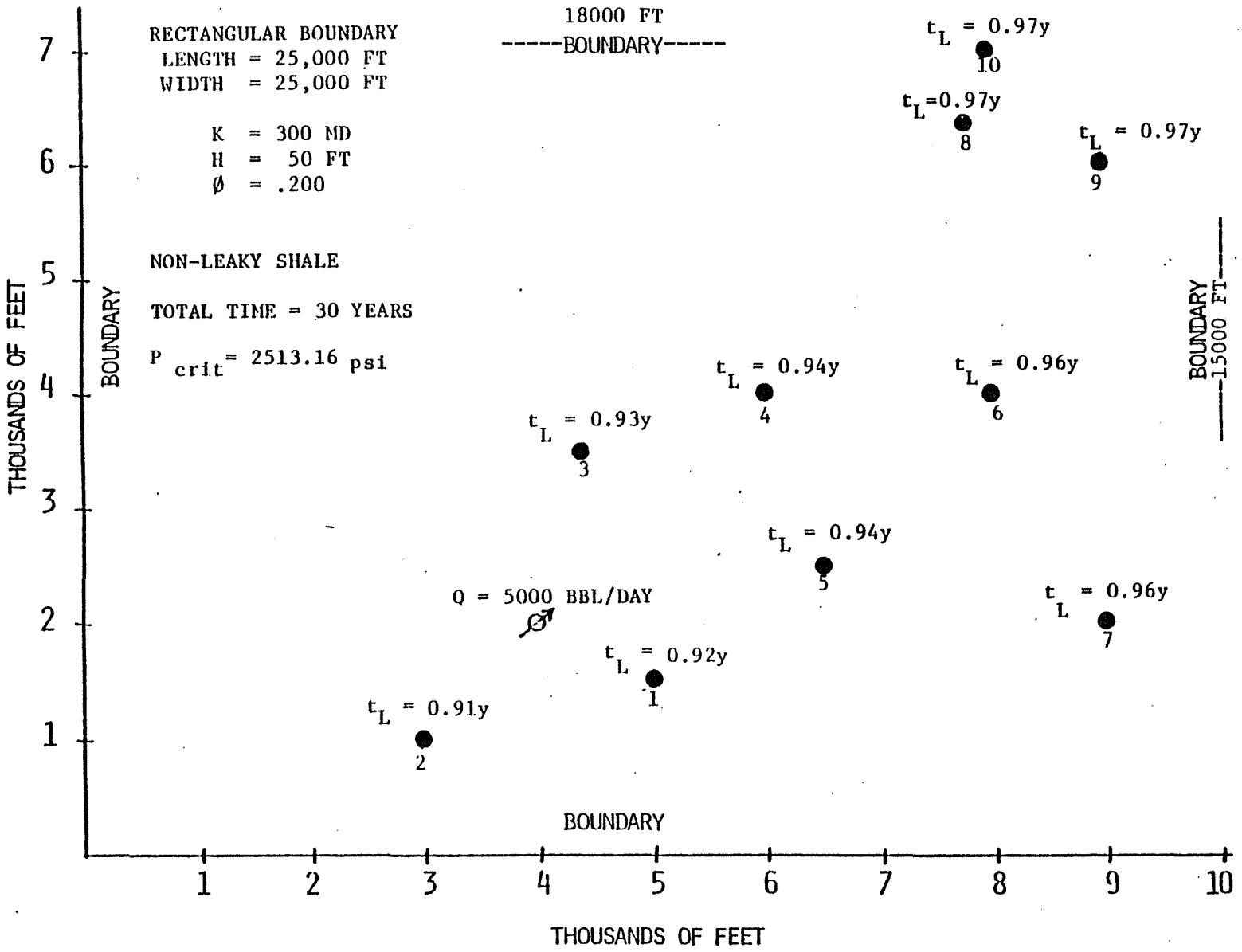

CASE I, GROUP 1, NO. 5

CASE I, GROUP 2

PROPERTIES OF THE DISPOSAL ZONE

COMPRESSIBILITY = 0.500E-05 1/PSI
PERMEABILITY = 300.000 MD
VISCOSITY = 1.000 CP
THICKNESS = 50.0 FT
POROSITY =0.200

PROPERTIES OF ABANDONED HOLES

ABAN WELL	WELL DIAM	DEPTH TO DISP ZONE	DEPTH TO H2O ZONE	MUD DENSITY	GEL STRENGTH	CRITIC PRESSU
	IN	FT	FT	LB/GAL	LB/100FT2	PSI
1	9.6	5000.00	600.0	9.000	100.00	2513.16
2	9.6	5000.00	600.0	9.000	100.00	2513.16
3	9.6	5000.00	600.0	9.000	100.00	2513.16
4	9.6	5000.00	600.0	9.000	100.00	2513.16
5	9.6	5000.00	600.0	9.000	100.00	2513.16
6	9.6	5000.00	600.0	9.000	100.00	2513.16
7	9.6	5000.00	600.0	9.000	100.00	2513.16
8	9.6	5000.00	600.0	9.000	100.00	2513.16
9	9.6	5000.00	600.0	9.000	100.00	2513.16
10	9.6	5000.00	600.0	9.000	100.00	2513.16

COORDINATES OF THE ABANDONED WELLS

WELL #	X FT.	Y FT.
1	5000.000	1500.000
2	3000.000	1000.000
3	4400.000	3600.000
4	6000.000	4000.000
5	6500.000	2500.000
6	8000.000	4000.000
7	9000.000	2000.000
8	7800.000	6400.000
9	9000.000	6000.000
10	8000.000	7000.000

COORDINATES OF THE INJECTION WELL

X= 2000.000 Y= 1500.000 FT.
INJECTION RATE =5000. BBL/DAY

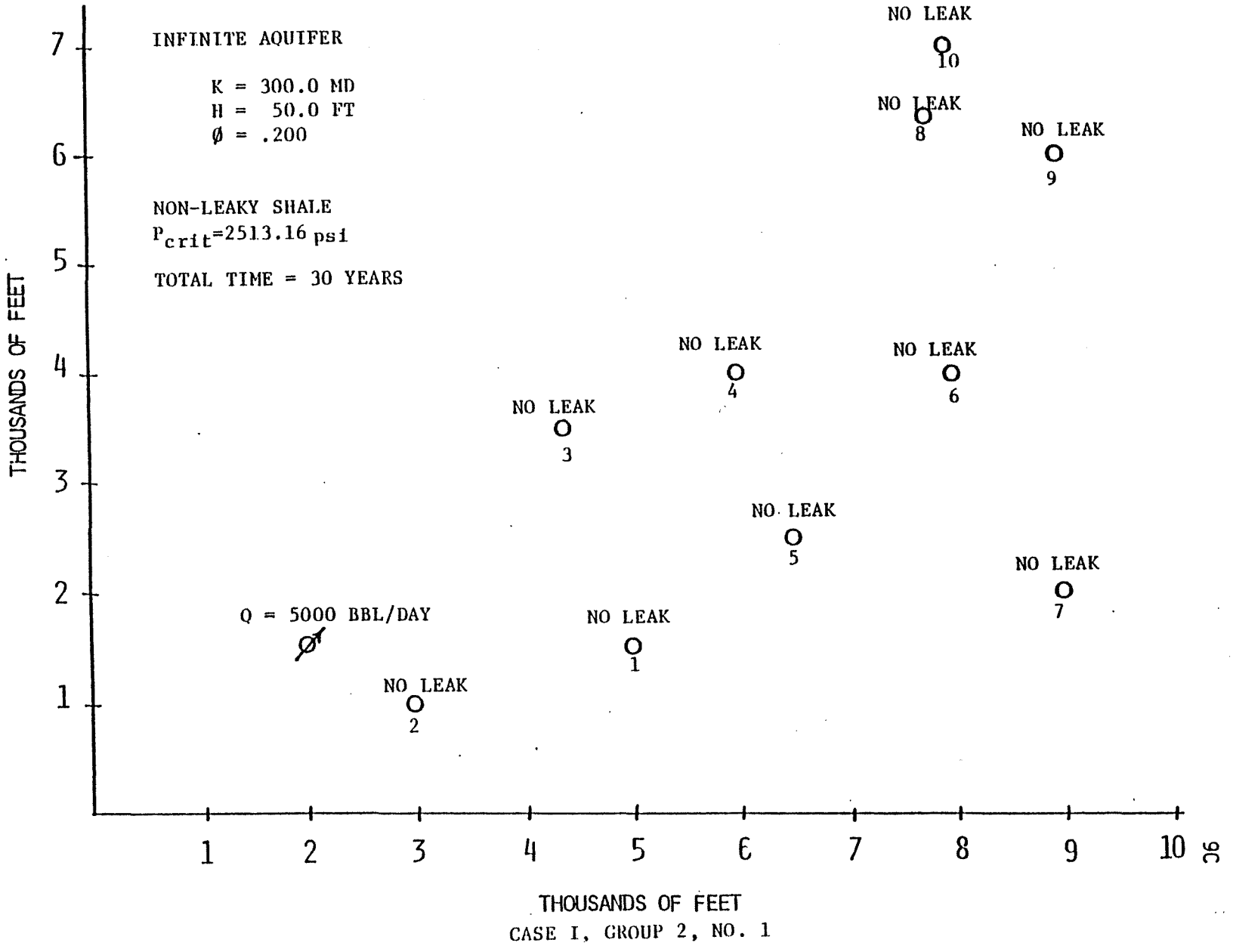

CASE I, GROUP 2, NO. 1

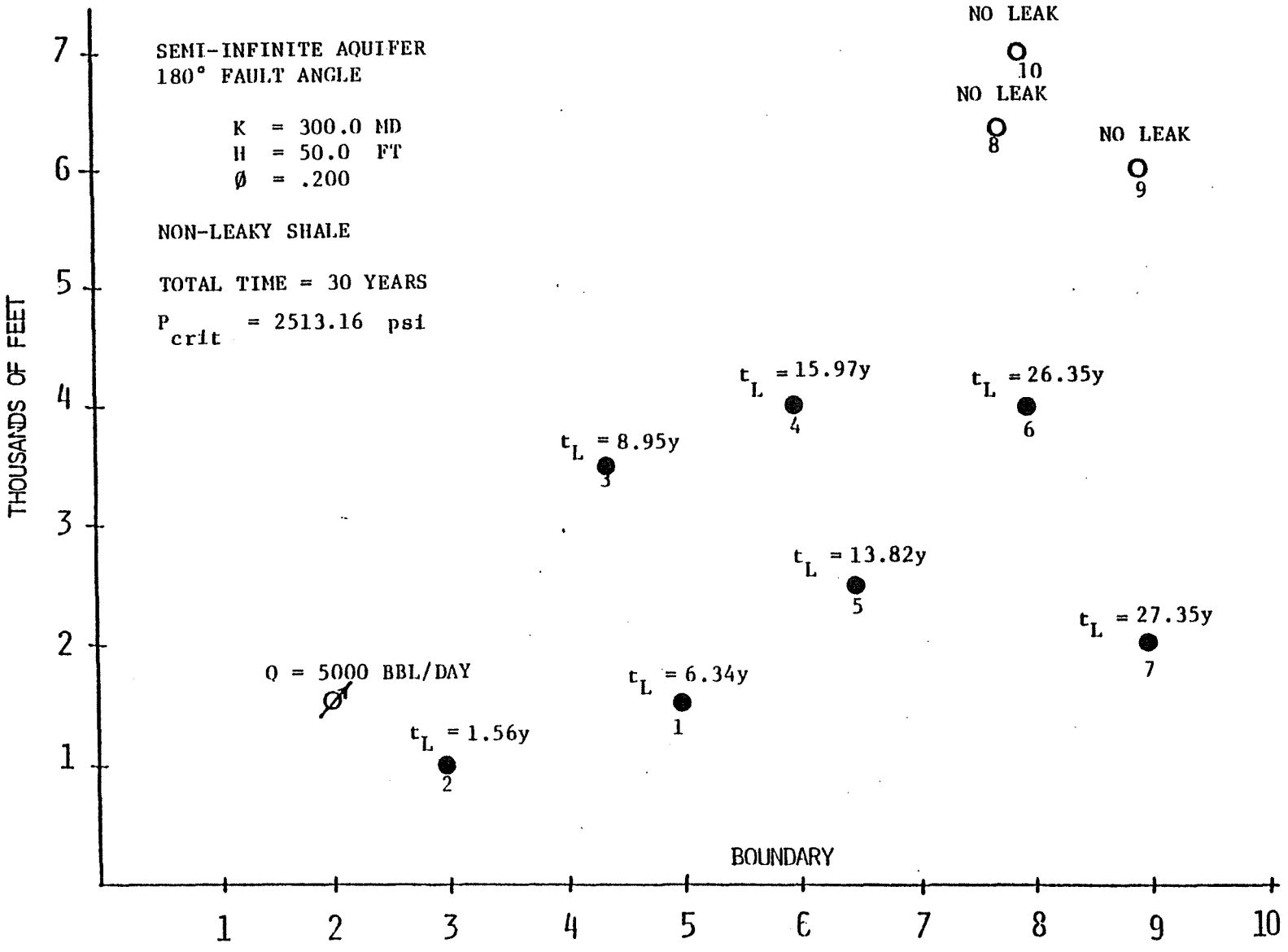

CASE 1, GROUP 2, NO. 2

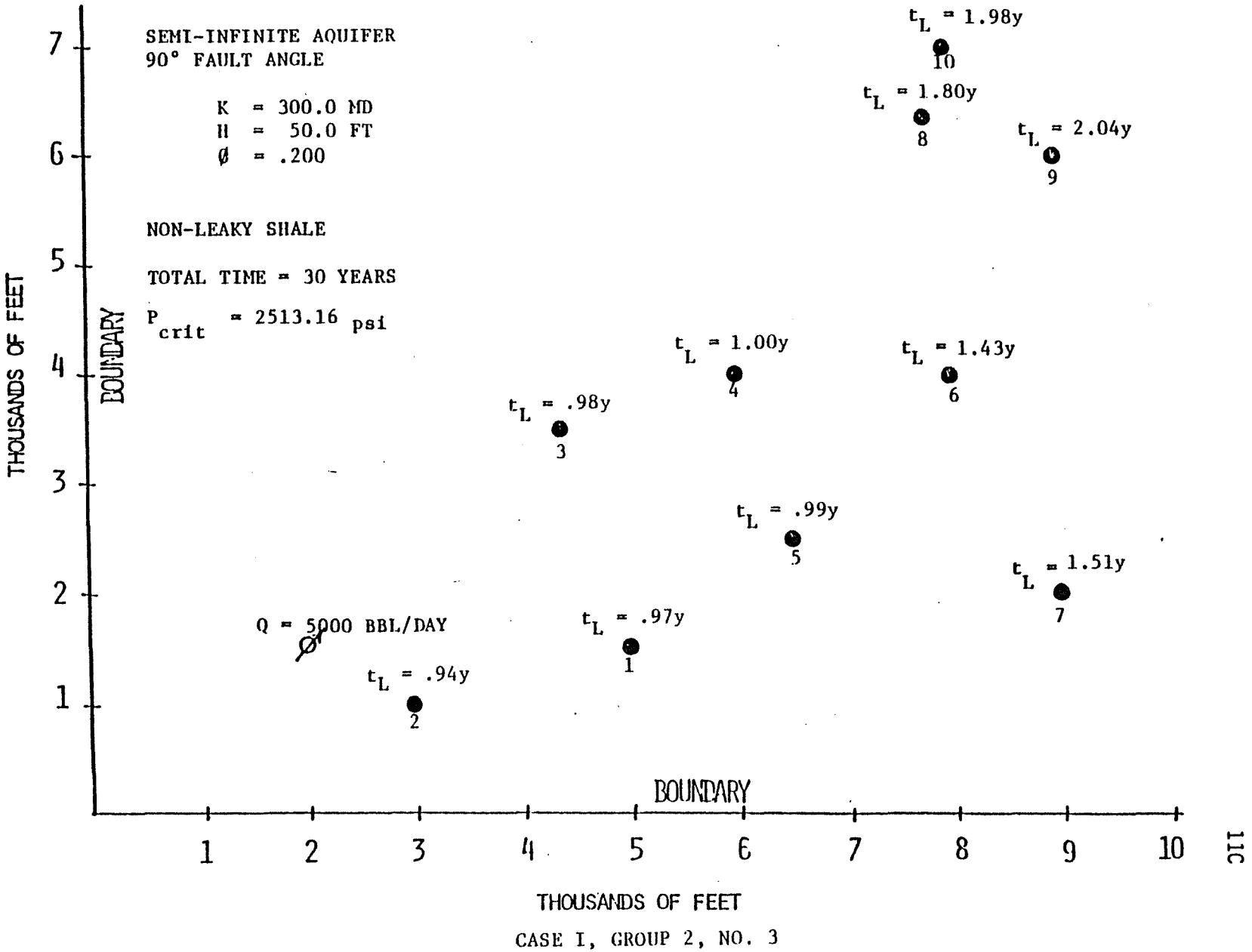

CASE I, GROUP 2, NO. 3

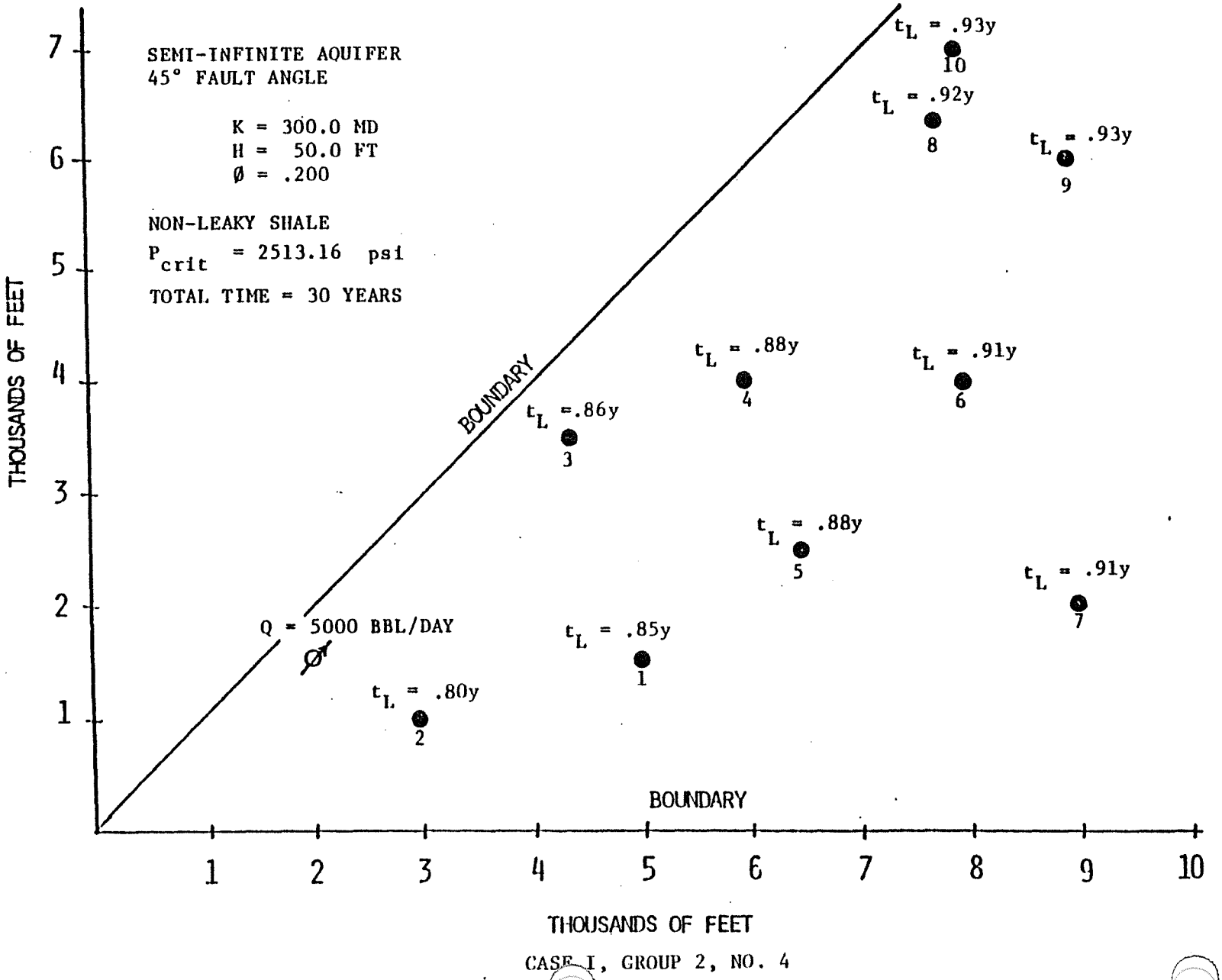

CASE I, GROUP 2, NO. 4

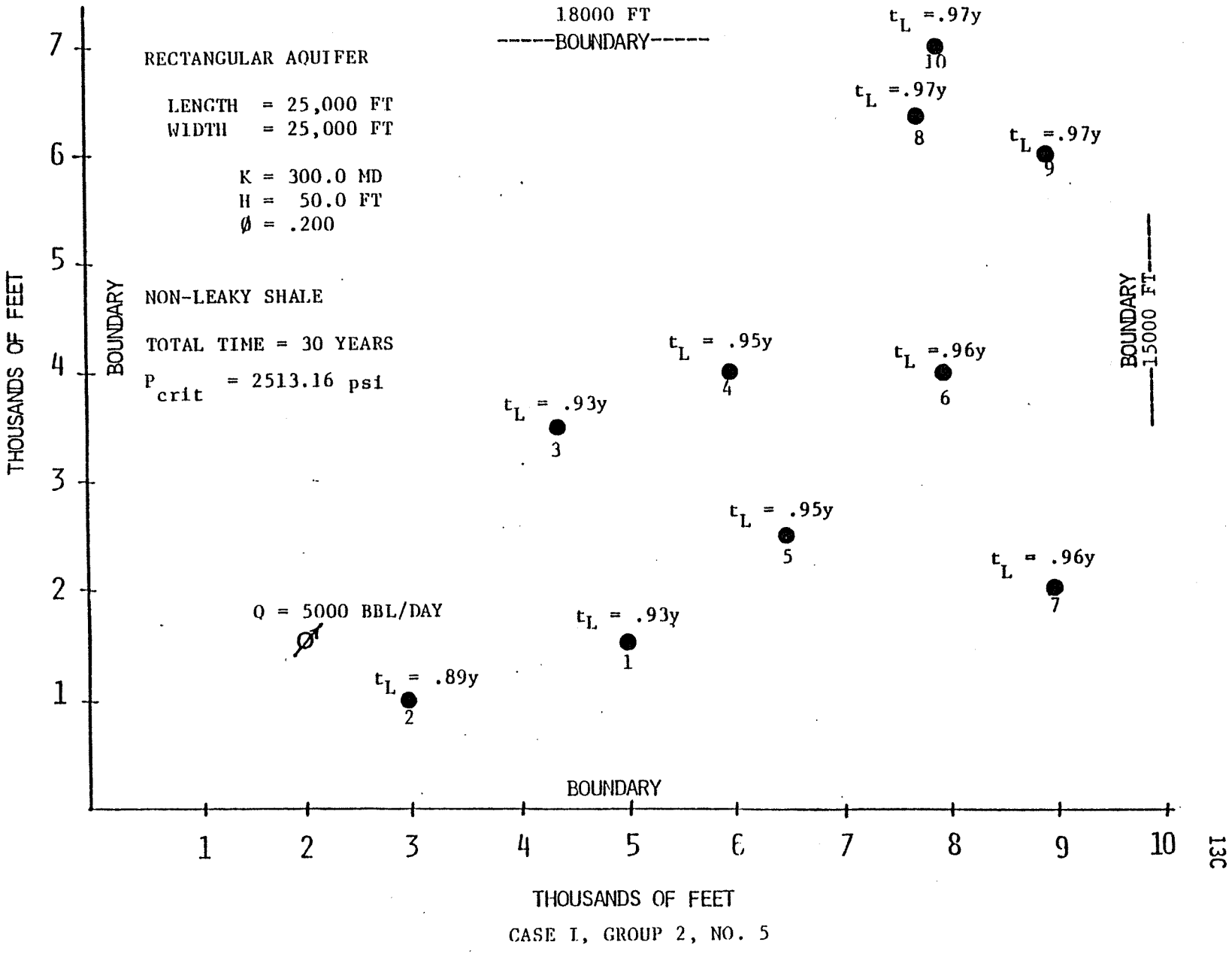

CASE I, GROUP 2, NO. 5

CASE I, GROUP 3

PROPERTIES OF THE DISPOSAL ZONE

COMPRESSIBILITY = 0.500E-05 1/PSI
PERMEABILITY = 300.000 MD
VISCOSITY = 1.000 CP
THICKNESS = 50.0 FT
POROSITY =0.200

PROPERTIES OF ABANDONED HOLES

ABAN WELL	DIAM	DEPTH TO DISP ZONE	DEPTH TO H2O ZONE	MUD DENSITY	GEL STRENGTH	CRITIC PRESSU
	IN	FT	FT	LB/GAL	LB/100FT2	PSI
1	9.6	5000.00	600.0	9.000	100.00	2513.16
2	9.6	5000.00	600.0	9.000	100.00	2513.16
3	9.6	5000.00	600.0	9.000	100.00	2513.16
4	9.6	5000.00	600.0	9.000	100.00	2513.16
5	9.6	5000.00	600.0	9.000	100.00	2513.16
6	9.6	5000.00	600.0	9.000	100.00	2513.16
7	9.6	5000.00	600.0	9.000	100.00	2513.16
8	9.6	5000.00	600.0	9.000	100.00	2513.16
9	9.6	5000.00	600.0	9.000	100.00	2513.16
10	9.6	5000.00	600.0	9.000	100.00	2513.16

COORDINATES OF THE ABANDONED WELLS

WELL #	X FT.	Y FT.
1	5000.000	1500.000
2	3000.000	1000.000
3	4400.000	3600.000
4	6000.000	4000.000
5	6500.000	2500.000
6	8000.000	4000.000
7	9000.000	2000.000
8	7800.000	6400.000
9	9000.000	6000.000
10	8000.000	7000.000

COORDINATES OF THE INJECTION WELL

X= 6000.000 Y= 3000.000 FT.
INJECTION RATE =5000. BBL/DAY

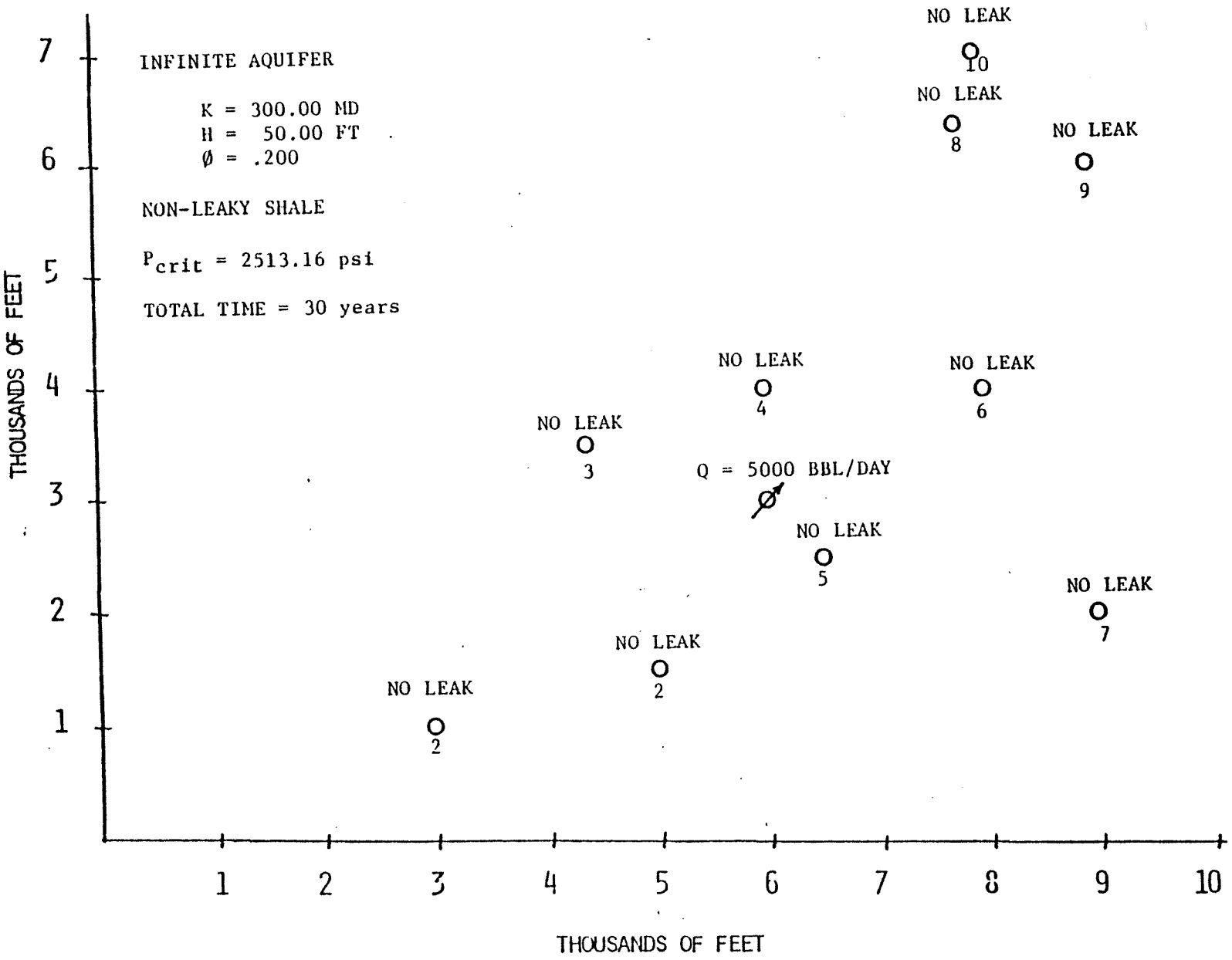

CASE I, GROUP 3, NO. 1

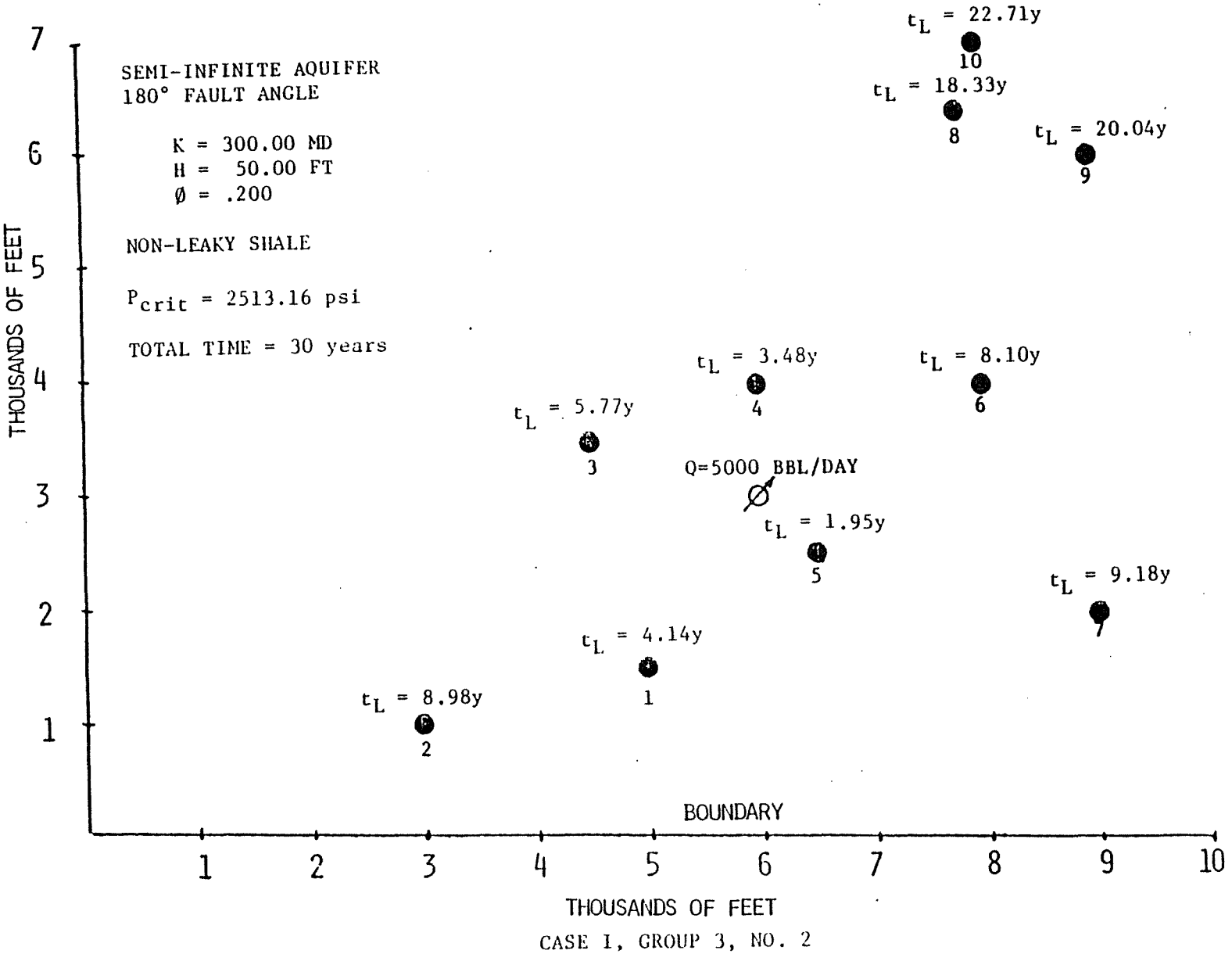

CASE I, GROUP 3, NO. 2

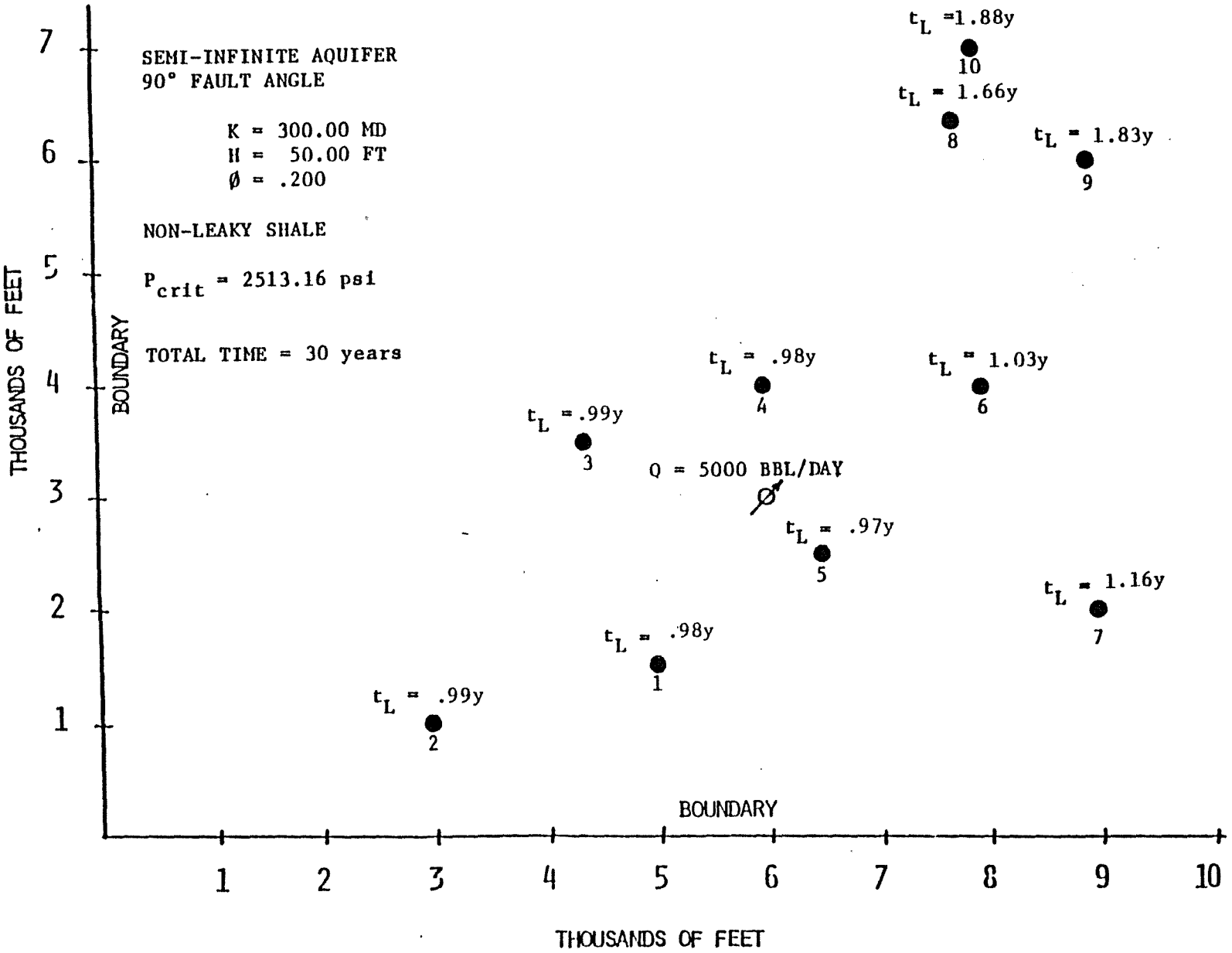

CASE I, GROUP 3, NO. 3

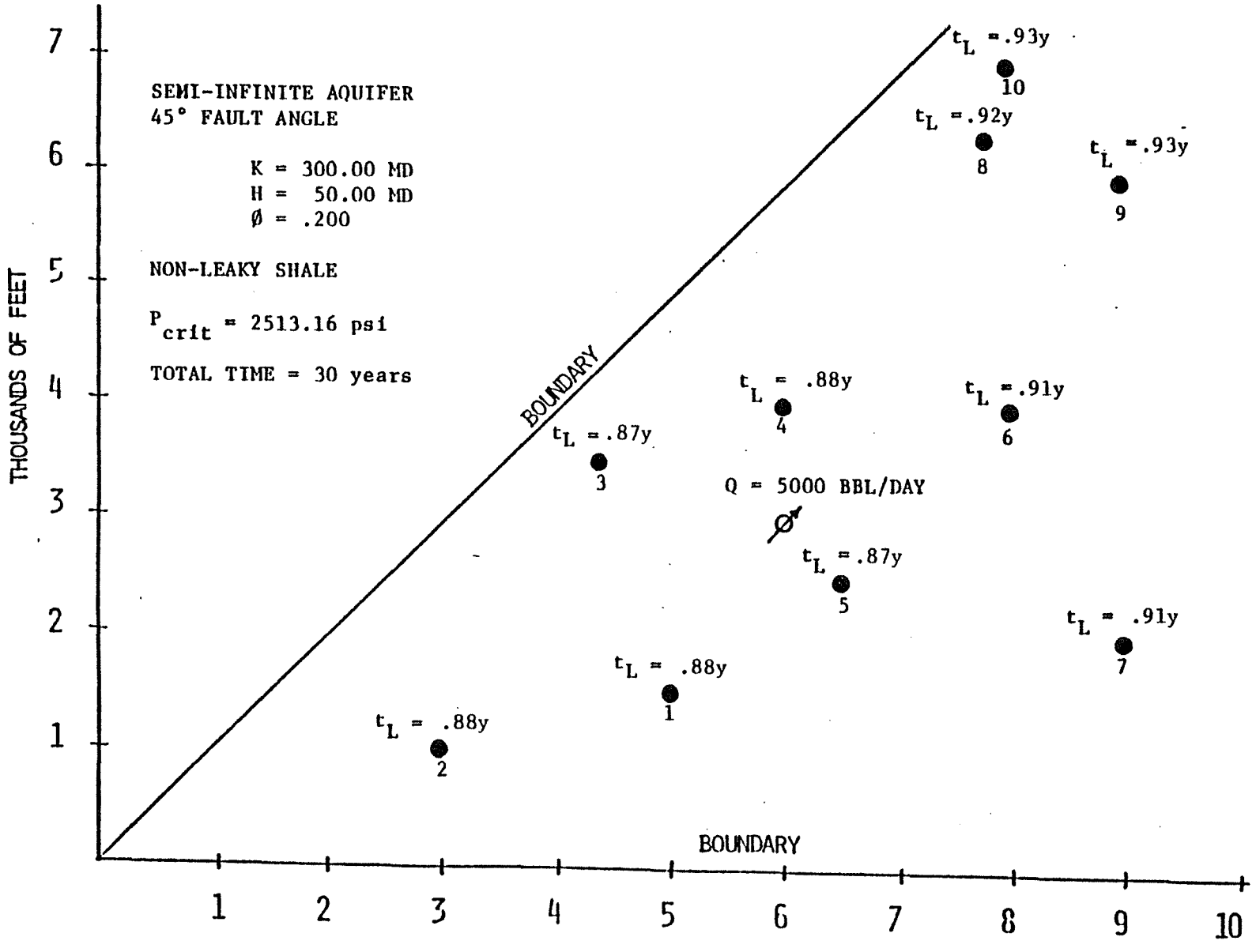

CASE I, GROUP 3, NO. 4

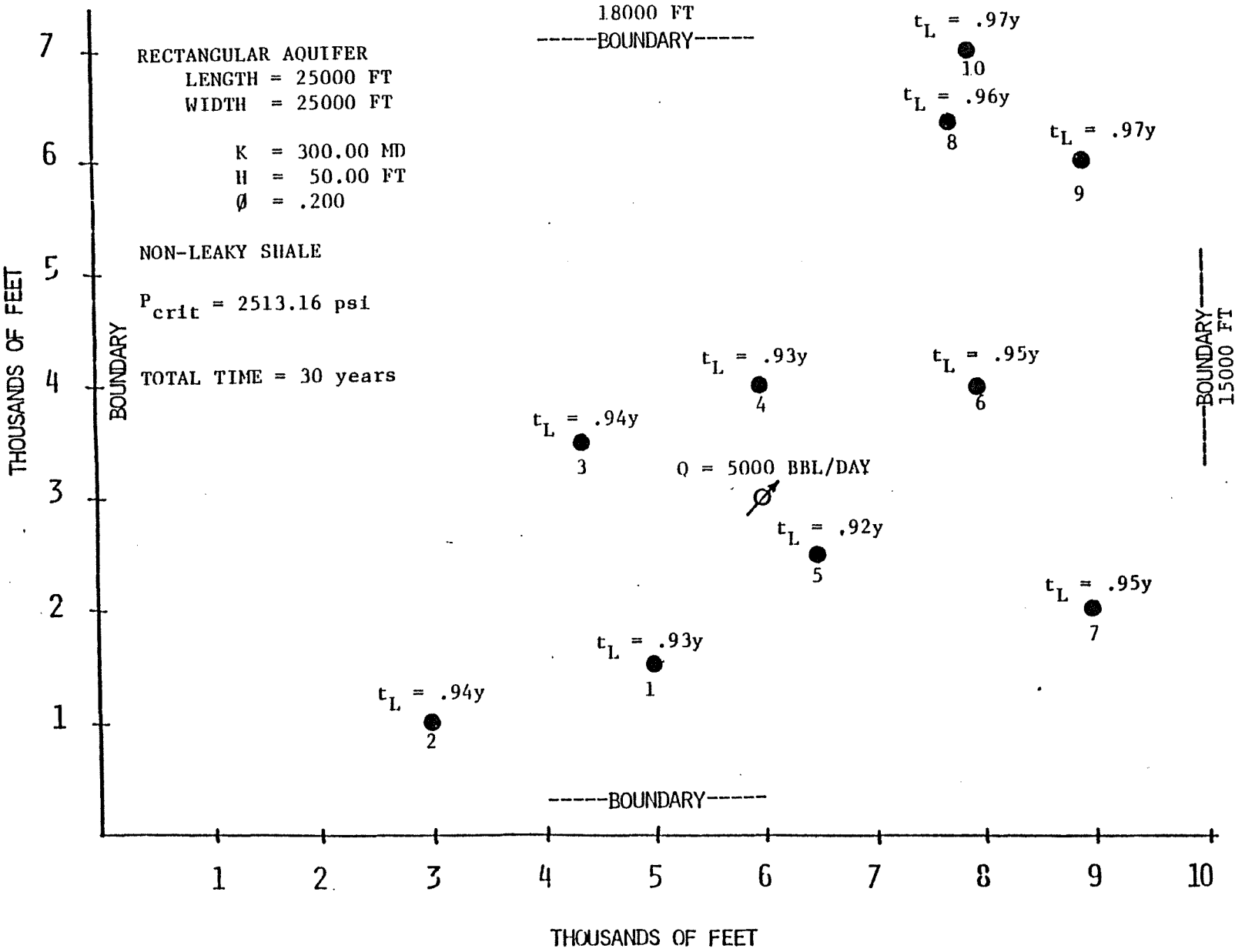

CASE I, GROUP 3, NO. 5

CASE I, GROUP 4

PROPERTIES OF THE DISPOSAL ZONE

COMPRESSIBILITY = 0.500E-05 1/PSI
PERMEABILITY = 100.000 MD
VISCOSITY = 1.000 CP
THICKNESS = 300.0 FT
POROSITY =0.200

PROPERTIES OF ABANDONED HOLES

ABAN WELL	DIAM IN	DEPTH TO DISP ZONE FT	DEPTH TO H2O ZONE FT	MUD DENSITY LB/GAL	GEL STRENGTH LB/100FT2	CRITIC PRESSU PSI
1	9.6	5000.00	600.0	9.000	100.00	2513.16
2	9.6	5000.00	600.0	9.000	100.00	2513.16
3	9.6	5000.00	600.0	9.000	100.00	2513.16
4	9.6	5000.00	600.0	9.000	100.00	2513.16
5	9.6	5000.00	600.0	9.000	100.00	2513.16
6	9.6	5000.00	600.0	9.000	100.00	2513.16
7	9.6	5000.00	600.0	9.000	100.00	2513.16
8	9.6	5000.00	600.0	9.000	100.00	2513.16
9	9.6	5000.00	600.0	9.000	100.00	2513.16
10	9.6	5000.00	600.0	9.000	100.00	2513.16

COORDINATES OF THE ABANDONED WELLS

WELL #	X FT.	Y FT.
1	5000.000	1500.000
2	3000.000	1000.000
3	4400.000	3600.000
4	6000.000	4000.000
5	6500.000	2500.000
6	8000.000	4000.000
7	9000.000	2000.000
8	7800.000	6400.000
9	9000.000	6000.000
10	8000.000	7000.000

COORDINATES OF THE INJECTION WELL

X= 2000.000 Y= 1500.000 FT.
INJECTION RATE =5000. BBL/DAY

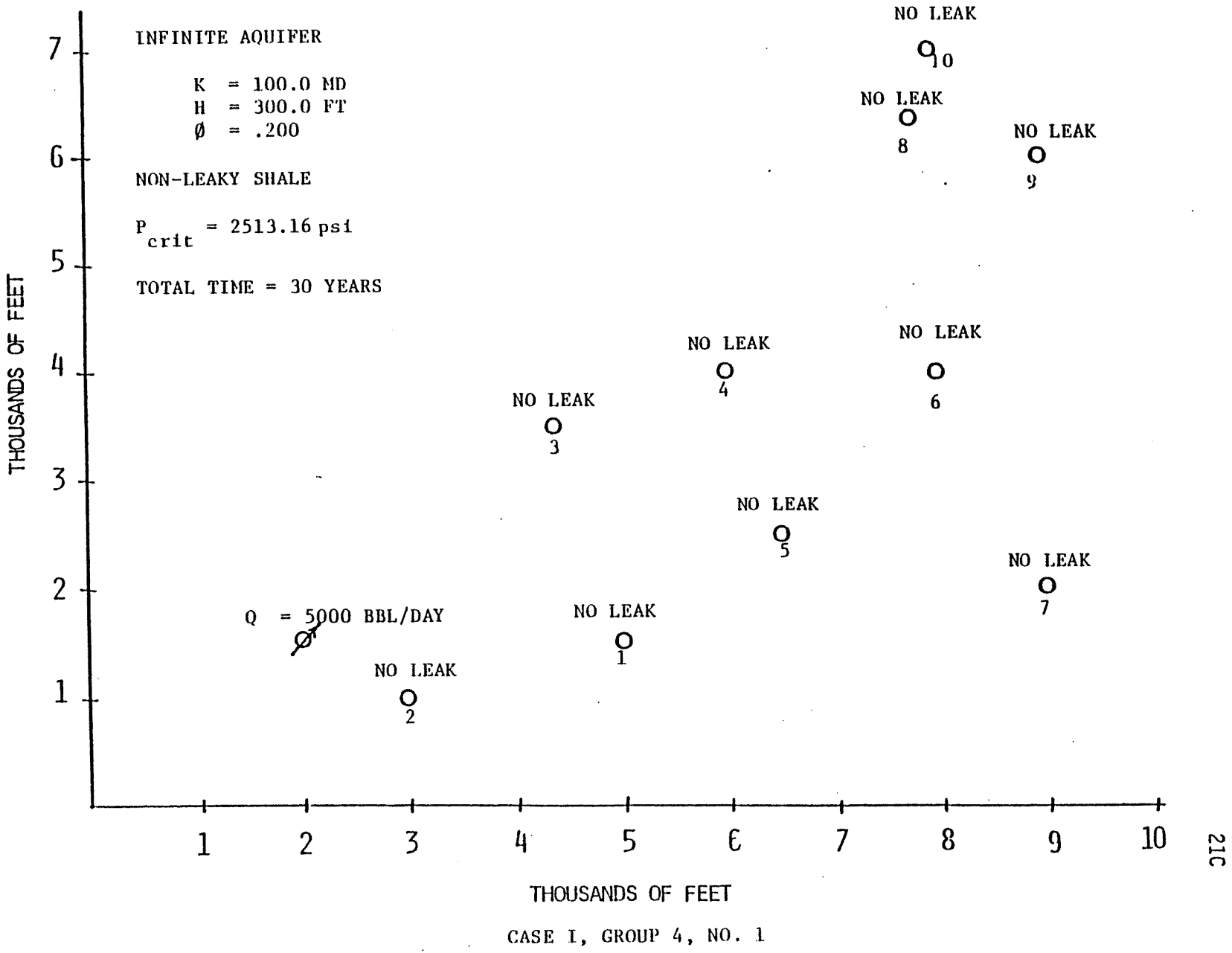

CASE I, GROUP 4, NO. 1

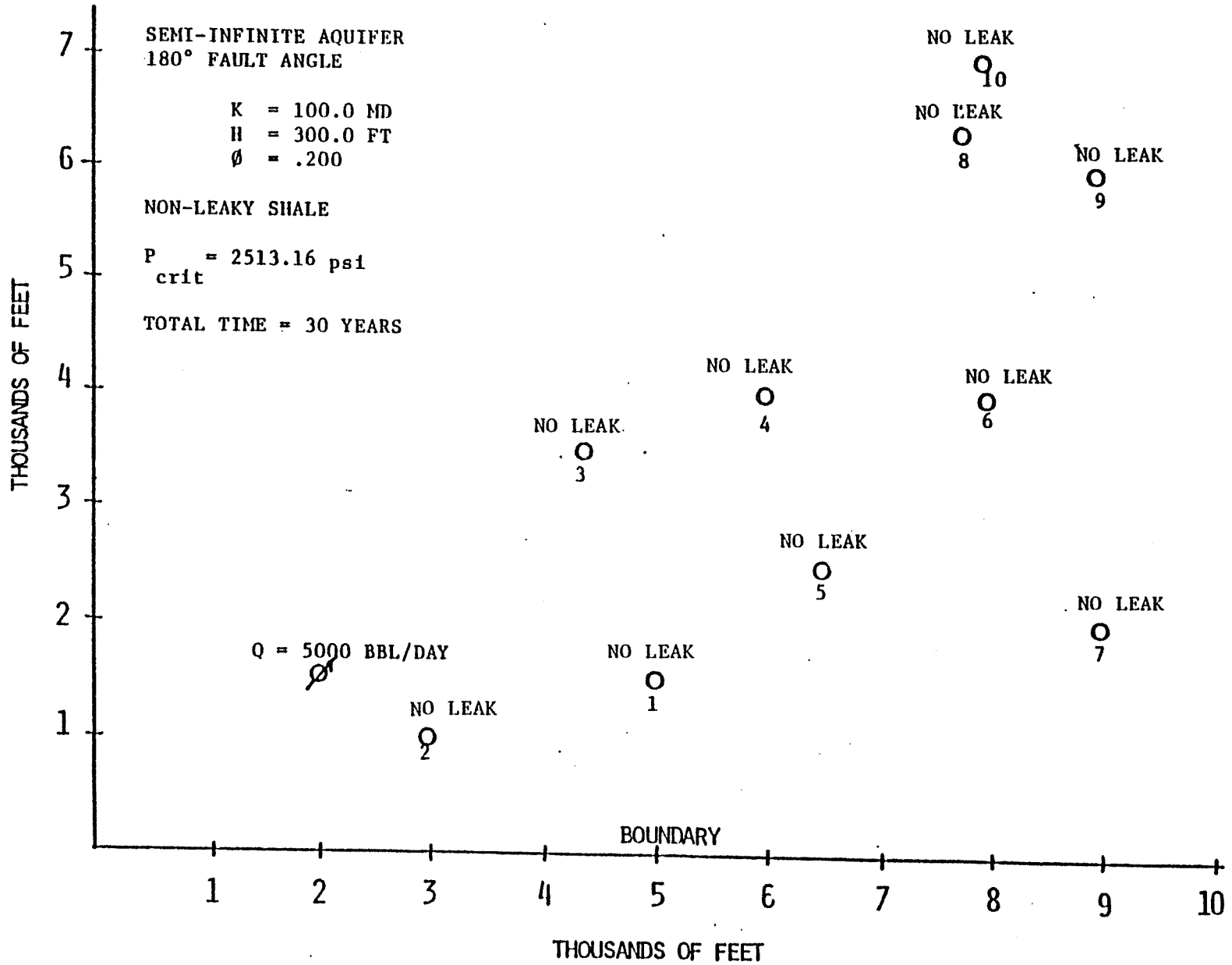

CASE I, GROUP 4. NO. 2

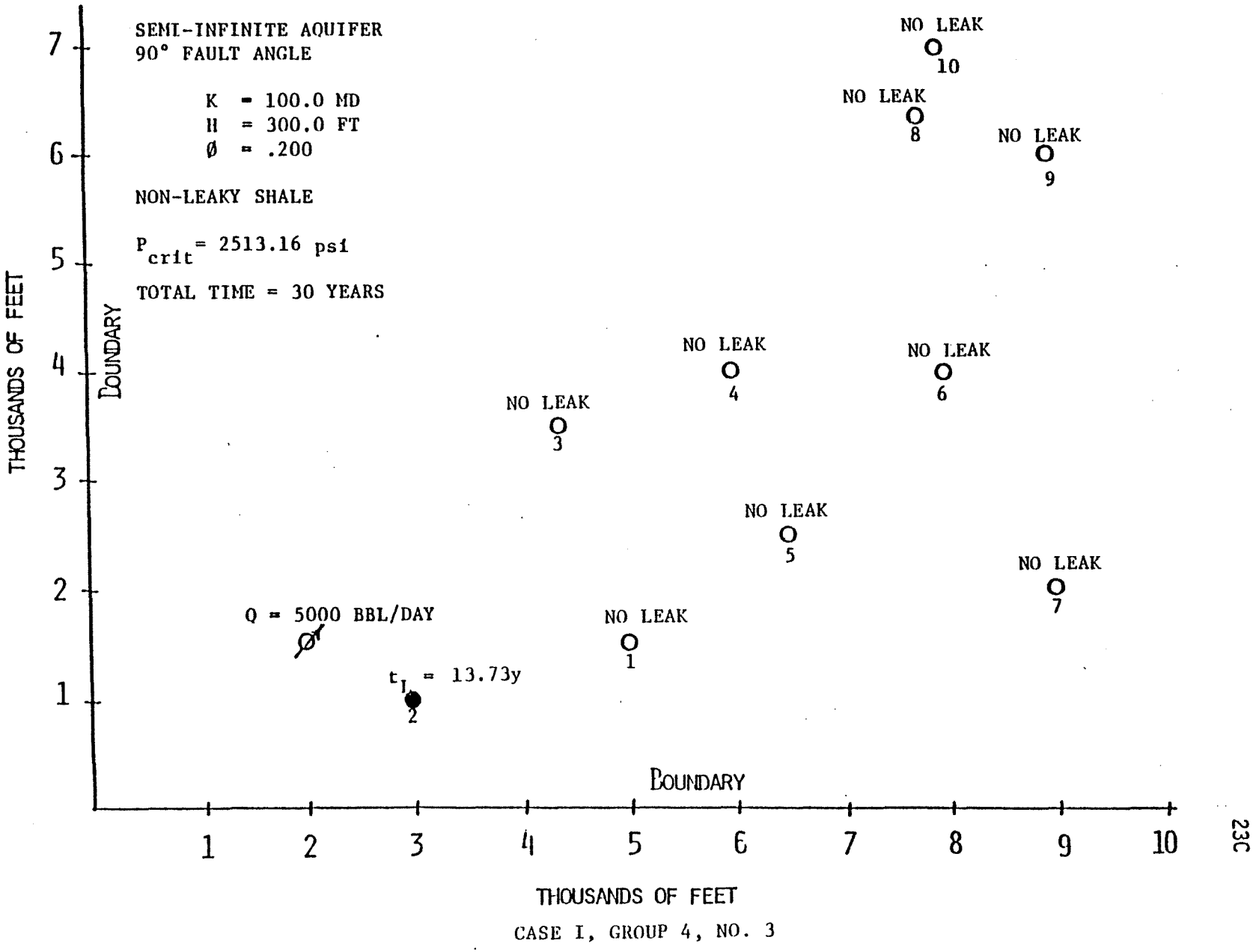

CASE I, GROUP 4, NO. 3

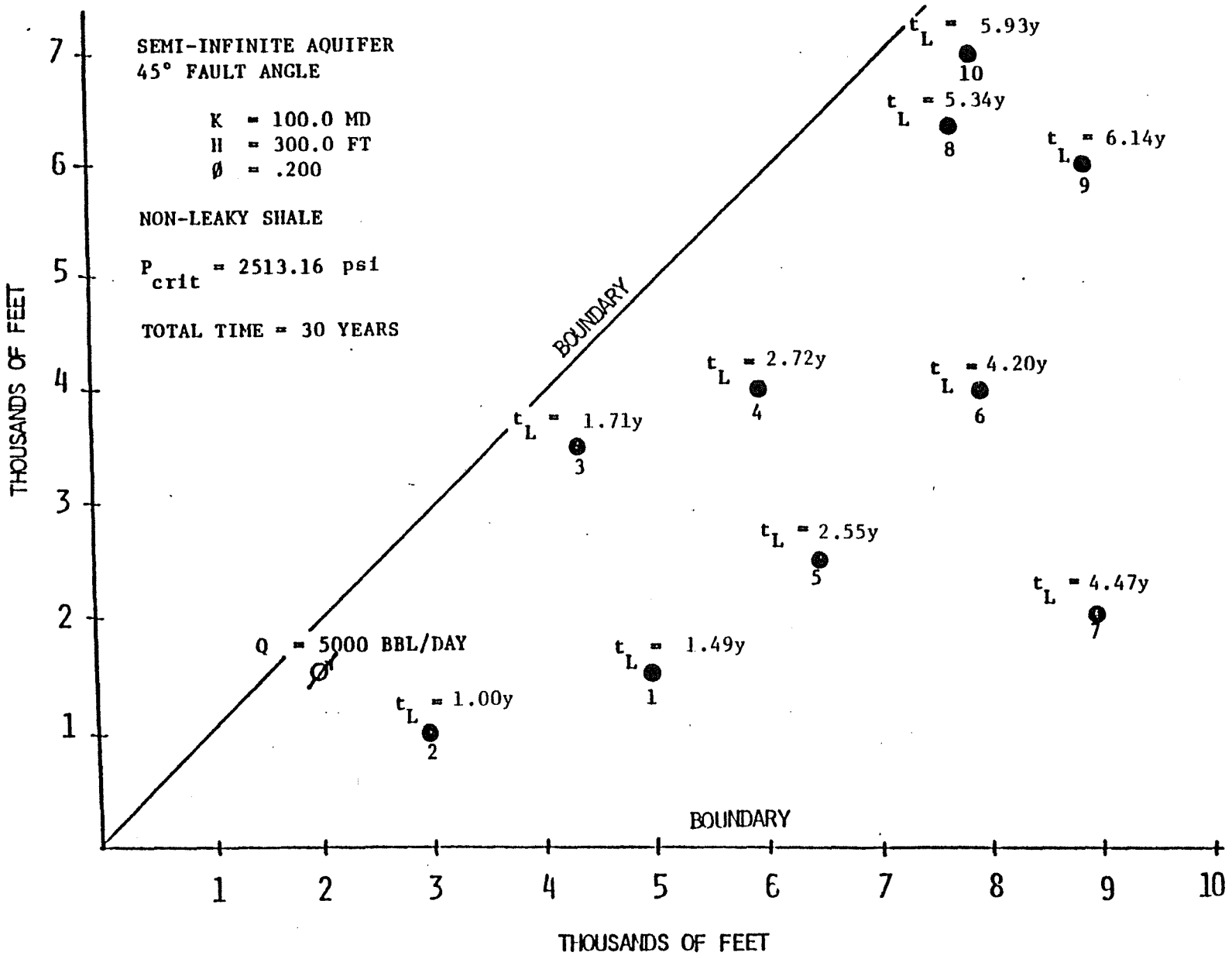

CASE I, GROUP 4, NO. 4

CASE I, GROUP 5

PROPERTIES OF THE DISPOSAL ZONE

COMPRESSIBILITY = 0.500E-05 1/PSI
PERMEABILITY = 100.000 MD
VISCOSITY = 1.000 CP
THICKNESS = 300.0 FT
POROSITY =0.200

PROPERTIES OF ABANDONED HOLES

ABAN WELL	DIAM	DEPTH TO DISP ZONE	DEPTH TO H2O ZONE	MUD DENSITY	GEL STRENGTH	CRITIC PRESSU
	IN	FT	FT	LB/GAL	LB/100FT2	PSI
1	9.6	5000.00	600.0	9.000	100.00	2513.16
2	9.6	5000.00	600.0	9.000	100.00	2513.16
3	9.6	5000.00	600.0	9.000	100.00	2513.16
4	9.6	5000.00	600.0	9.000	100.00	2513.16
5	9.6	5000.00	600.0	9.000	100.00	2513.16
6	9.6	5000.00	600.0	9.000	100.00	2513.16
7	9.6	5000.00	600.0	9.000	100.00	2513.16
8	9.6	5000.00	600.0	9.000	100.00	2513.16
9	9.6	5000.00	600.0	9.000	100.00	2513.16
10	9.6	5000.00	600.0	9.000	100.00	2513.16

COORDINATES OF THE ABANDONED WELLS

WELL #	X FT.	Y FT.
1	5000.000	1500.000
2	3000.000	1000.000
3	4400.000	3600.000
4	6000.000	4000.000
5	6500.000	2500.000
6	8000.000	4000.000
7	9000.000	2000.000
8	7800.000	6400.000
9	9000.000	6000.000
10	8000.000	7000.000

COORDINATES OF THE INJECTION WELL

X= 4000.000 Y= 2000.000 FT.
INJECTION RATE =5000. BBL/DAY

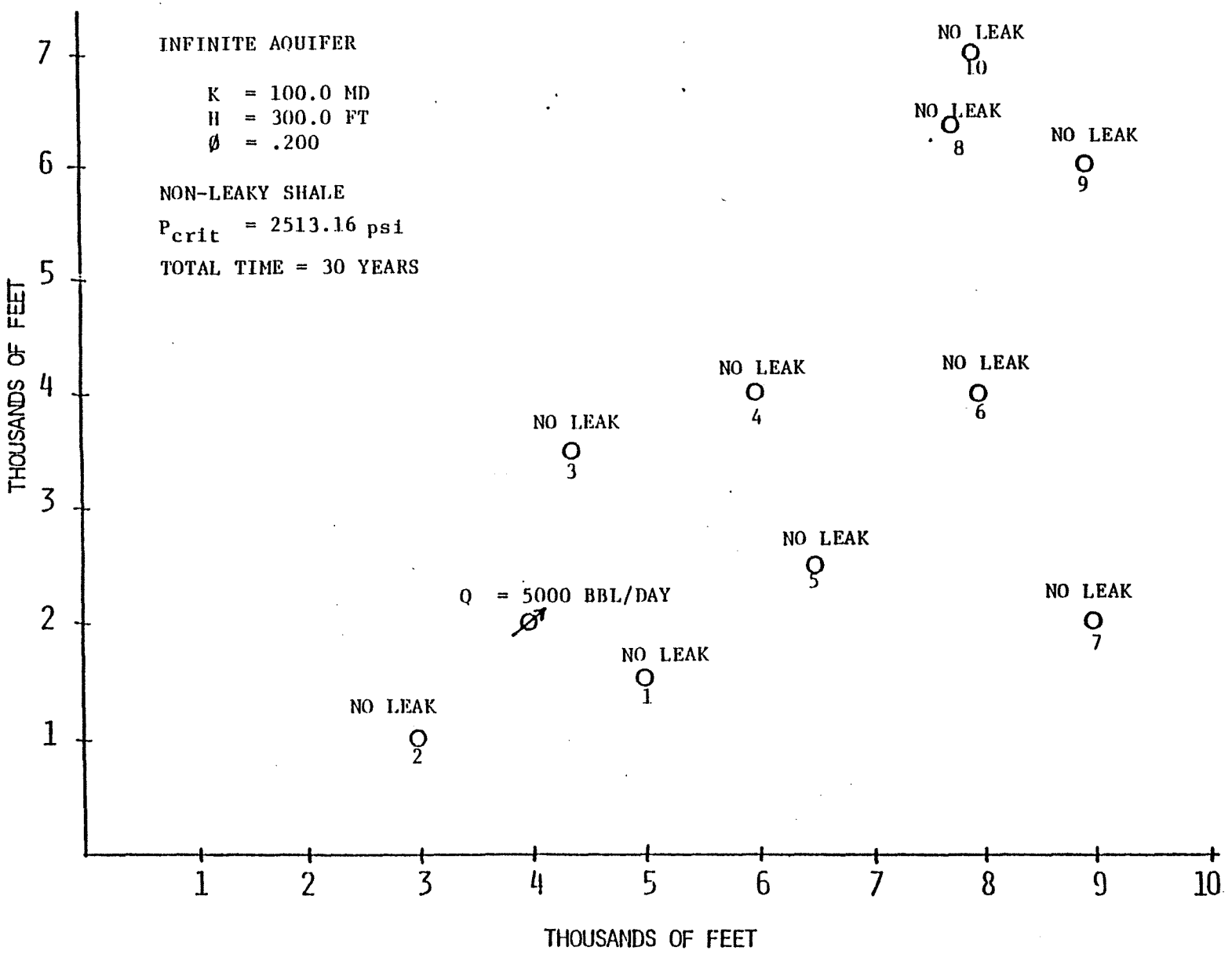

CASE I, GROUP 5, NO. 1

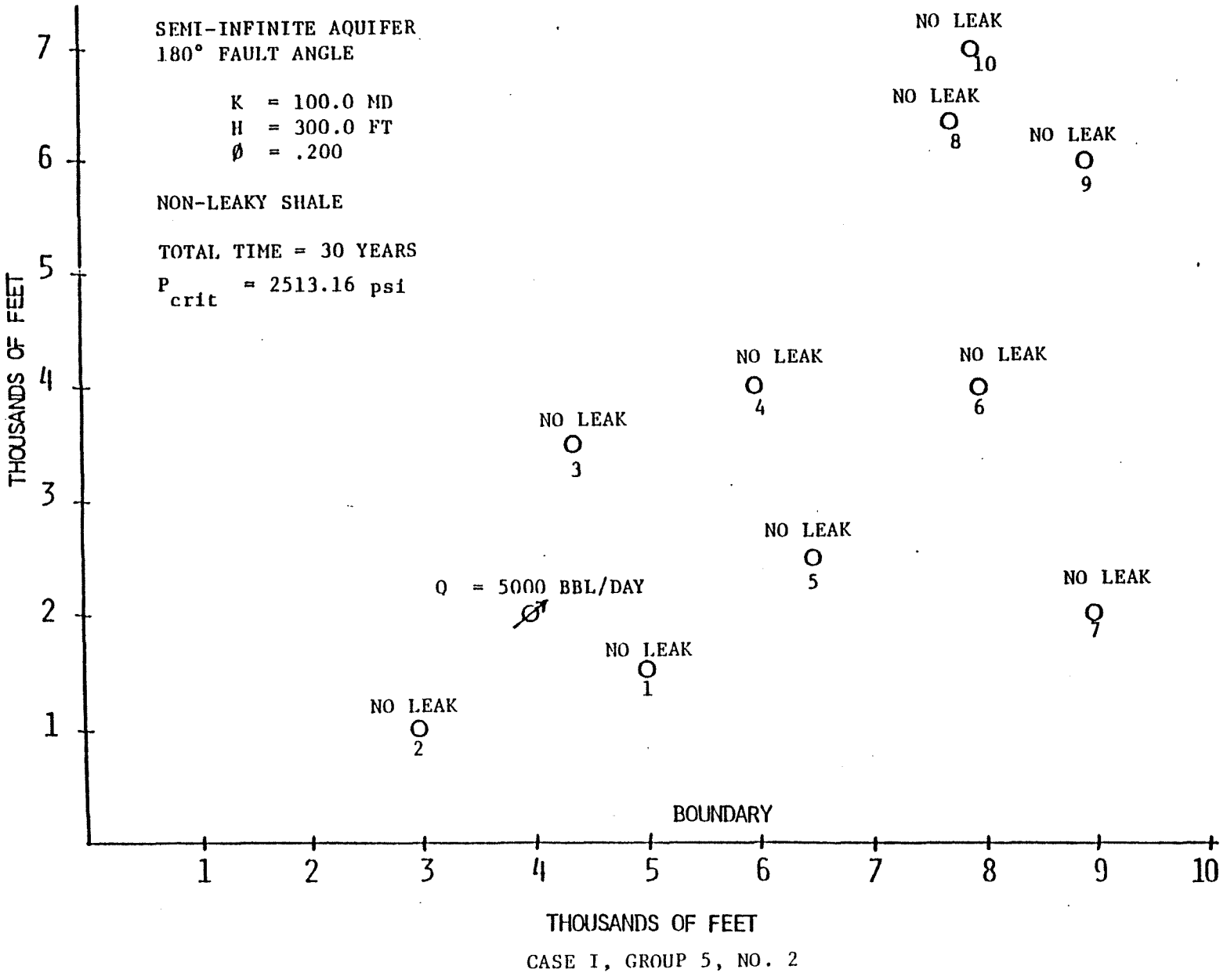

CASE I, GROUP 5, NO. 2

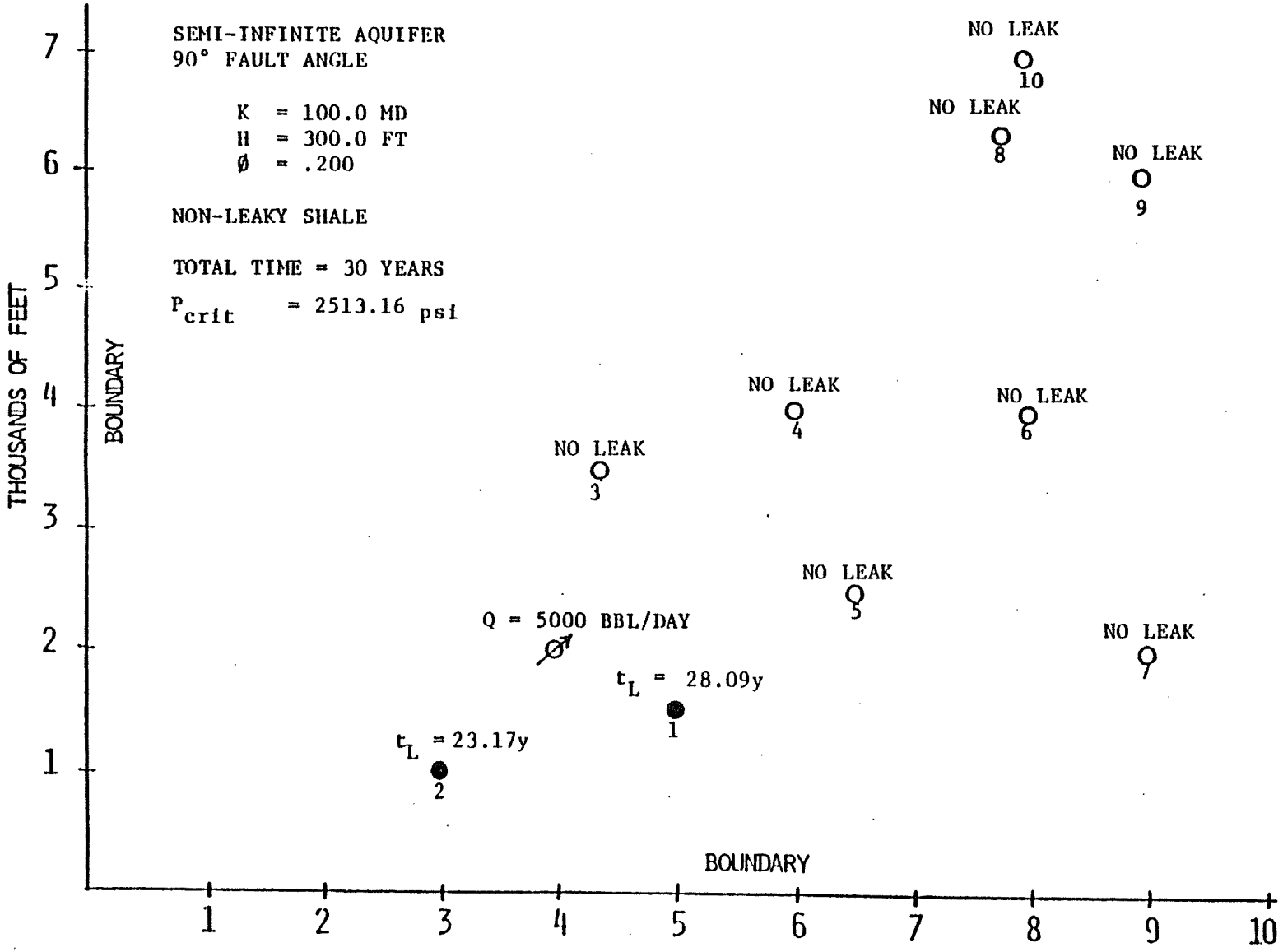

CASE I, GROUP 5, NO. 3

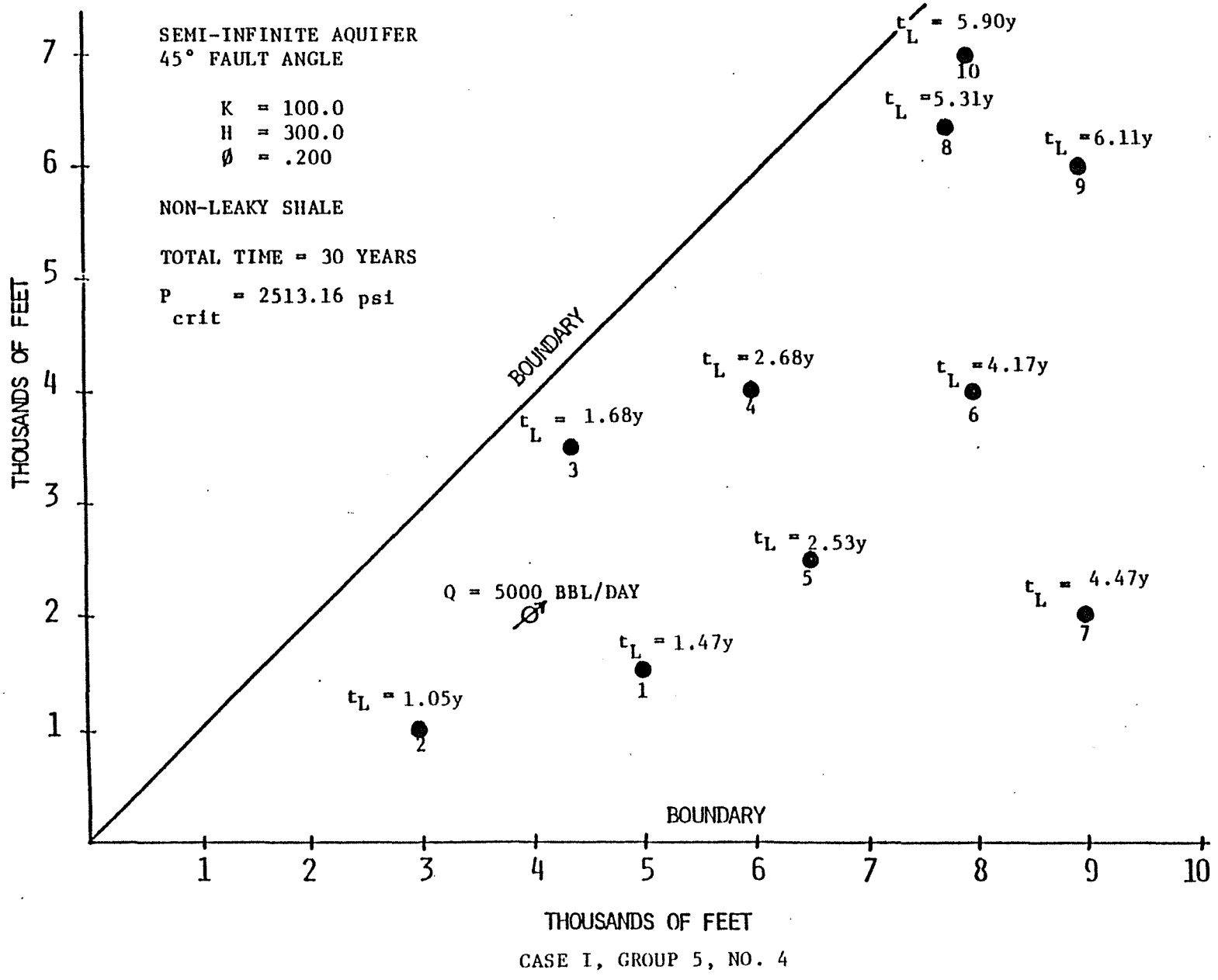

CASE I, GROUP 5, NO. 4

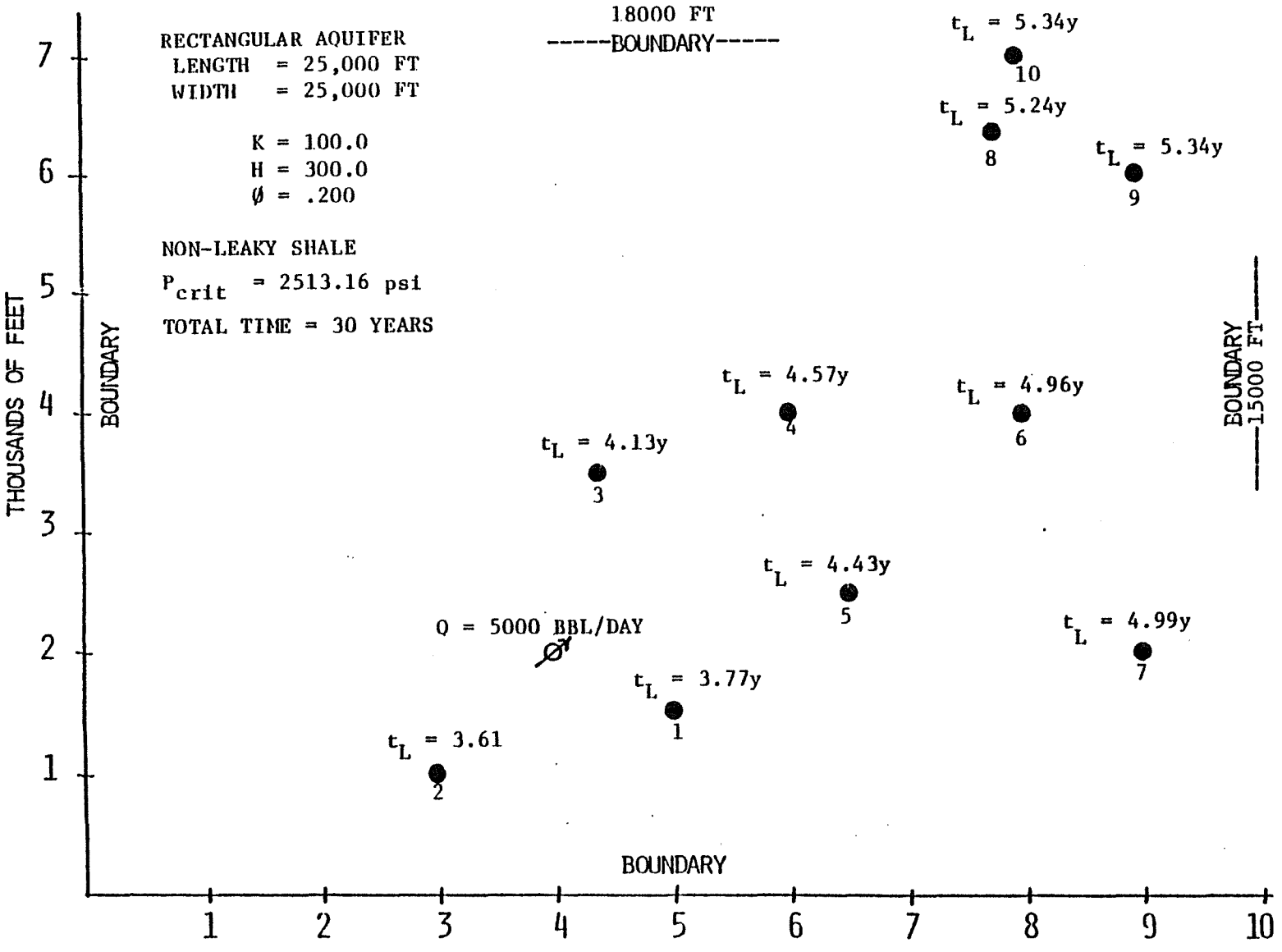

CASE I, GROUP 5, NO. 5

CASE I GROUP 6

PRESSURE HISTORIES
AT ABANDONED WELLS
CASE I, GROUP 1, NO. 2

TIME	WELL NUMBER (PRESSURES IN PSI)									
YEARS	1	2	3	4	5	6	7	8	9	10
1.0	2480.0	2475.5	2441.5	2410.6	2425.0	2383.1	2383.4	2359.5	2354.0	2352.1
2.0	2512.6	2508.1	2474.0	2443.0	2457.5	2415.4	2415.7	2391.7	2386.1	2384.1
3.0	2531.6	2527.2	2493.0	2462.0	2476.6	2434.4	2434.7	2410.6	2405.0	2403.0
4.0	2545.2	2540.7	2506.5	2475.5	2490.1	2447.9	2448.2	2424.0	2418.4	2416.4
5.0	2555.7	2551.2	2517.0	2486.0	2500.6	2458.3	2458.7	2434.5	2428.9	2426.9
6.0	2564.2	2559.8	2525.6	2494.6	2509.1	2466.9	2467.2	2443.0	2437.4	2435.4
7.0	2571.5	2567.0	2532.8	2501.8	2516.4	2474.1	2474.5	2450.3	2444.7	2442.6
8.0	2577.8	2573.3	2539.1	2508.1	2522.7	2480.4	2480.7	2456.5	2450.9	2448.9
9.0	2583.3	2578.9	2544.6	2513.7	2528.2	2485.9	2486.3	2462.1	2456.5	2454.4
10.0	2588.3	2583.8	2549.6	2518.6	2533.2	2490.9	2491.2	2467.0	2461.4	2459.4
11.0	2592.8	2588.3	2554.1	2523.1	2537.7	2495.4	2495.7	2471.5	2465.9	2463.9
12.0	2596.8	2592.4	2558.2	2527.2	2541.7	2499.5	2499.8	2475.6	2470.0	2467.9
13.0	2600.6	2596.2	2561.9	2530.9	2545.5	2503.2	2503.6	2479.3	2473.7	2471.7
14.0	2604.1	2599.7	2565.4	2534.4	2549.0	2506.7	2507.0	2482.8	2477.2	2475.2
15.0	2607.3	2602.9	2568.7	2537.7	2552.2	2510.0	2510.3	2486.1	2480.4	2478.4
16.0	2610.4	2605.9	2571.7	2540.7	2555.3	2513.0	2513.3	2489.1	2483.5	2481.5
17.0	2613.2	2608.8	2574.6	2543.6	2558.1	2515.8	2516.2	2492.0	2486.3	2484.3
18.0	2615.9	2611.5	2577.2	2546.3	2560.8	2518.5	2518.9	2494.6	2489.0	2487.0
19.0	2618.5	2614.0	2579.8	2548.8	2563.4	2521.1	2521.4	2497.2	2491.6	2489.5
20.0	2620.9	2616.4	2582.2	2551.2	2565.8	2523.5	2523.8	2499.6	2494.0	2491.9
21.0	2623.2	2618.7	2584.5	2553.5	2568.1	2525.8	2526.1	2501.9	2496.3	2494.2
22.0	2625.4	2620.9	2586.7	2555.7	2570.3	2528.0	2528.3	2504.1	2498.5	2496.4
23.0	2627.5	2623.0	2588.8	2557.8	2572.4	2530.1	2530.4	2506.2	2500.5	2498.5
24.0	2629.5	2625.0	2590.8	2559.8	2574.4	2532.1	2532.4	2508.2	2502.5	2500.5
25.0	2631.4	2626.9	2592.7	2561.7	2576.3	2534.0	2534.3	2510.1	2504.5	2502.4
26.0	2633.2	2628.8	2594.5	2563.6	2578.1	2535.8	2536.2	2511.9	2506.3	2504.3
27.0	2635.0	2630.6	2596.3	2565.3	2579.9	2537.6	2537.9	2513.7	2508.1	2506.1
28.0	2636.7	2632.3	2598.0	2567.0	2581.6	2539.3	2539.7	2515.4	2509.8	2507.8
29.0	2638.4	2633.9	2599.7	2568.7	2583.3	2541.0	2541.3	2517.1	2511.4	2509.4
30.0	2640.0	2635.5	2601.3	2570.3	2584.9	2542.6	2542.9	2518.7	2513.0	2511.0

CASE II

EFFECTS OF ABANDONED WELL PARAMETERS

Group 1, Only boundaries are varied, P_{crit} = 2668.9 psi

Group 2, Same as Group 1 but with P_{crit} = 2409.16 Psi, "box" boundaries omitted (all leaked early)

Group 3, Same as Group 1 but with P_{crit} = 2322.58 Psi and a different injection well location

Group 4, Two examples same as Case I, Group 1, No. 1 but with a leaky shale aquiclude and P_{crit} values of 2365.87 and 2409.16 Psi respectively

CASE II, GROUP 1

PROPERTIES OF THE DISPOSAL ZONE

COMPRESSIBILITY = 0.500E-05 1/PSI
PERMEABILITY = 300.000 MD
VISCOSITY = 1.000 CP
THICKNESS = 50.0 FT
POROSITY =0.200

PROPERTIES OF ABANDONED HOLES

ABAN WELL	DIAM IN	DEPTH TO DISP ZONE FT	DEPTH TO H2O ZONE FT	MUD DENSITY LB/GAL	GEL STRENGTH LB/100FT2	CRITIC PRESSU PSI
1	9.6	5000.00	600.0	8.600	250.00	2668.90
2	9.6	5000.00	600.0	8.600	250.00	2668.90
3	9.6	5000.00	600.0	8.600	250.00	2668.90
4	9.6	5000.00	600.0	8.600	250.00	2668.90
5	9.6	5000.00	600.0	8.600	250.00	2668.90
6	9.6	5000.00	600.0	8.600	250.00	2668.90
7	9.6	5000.00	600.0	8.600	250.00	2668.90
8	9.6	5000.00	600.0	8.600	250.00	2668.90
9	9.6	5000.00	600.0	8.600	250.00	2668.90
10	9.6	5000.00	600.0	8.600	250.00	2668.90

COORDINATES OF THE ABANDONED WELLS

WELL #	X FT.	Y FT.
1	5000.000	1500.000
2	3000.000	1000.000
3	4400.000	3600.000
4	6000.000	4000.000
5	6500.000	2500.000
6	8000.000	4000.000
7	9000.000	2000.000
8	7800.000	6400.000
9	9000.000	6000.000
10	8000.000	7000.000

COORDINATES OF THE INJECTION WELL

X= 6000.000 Y= 3000.000 FT.
INJECTION RATE =5000. BBL/DAY

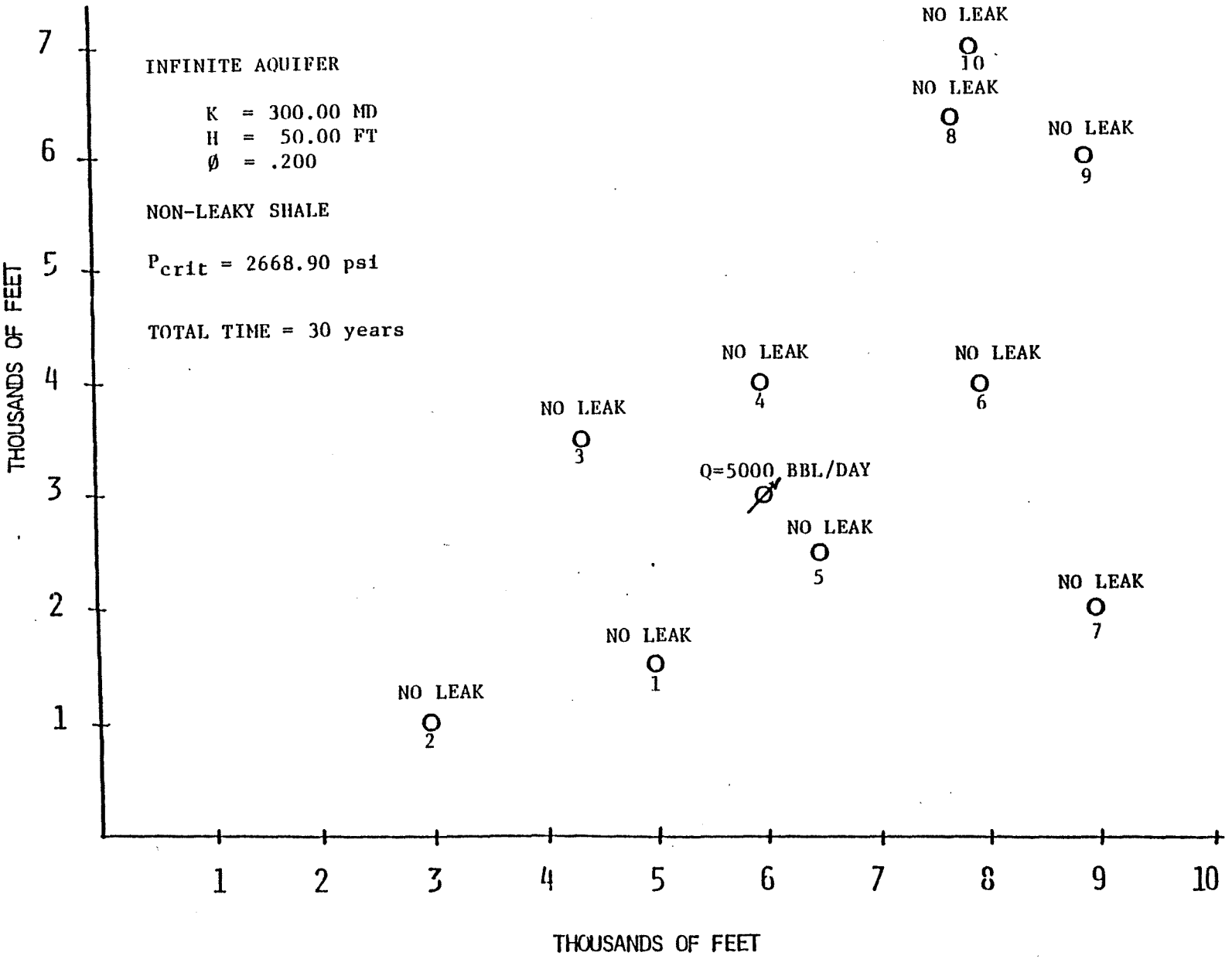

CASE II, GROUP 1, NO. 1

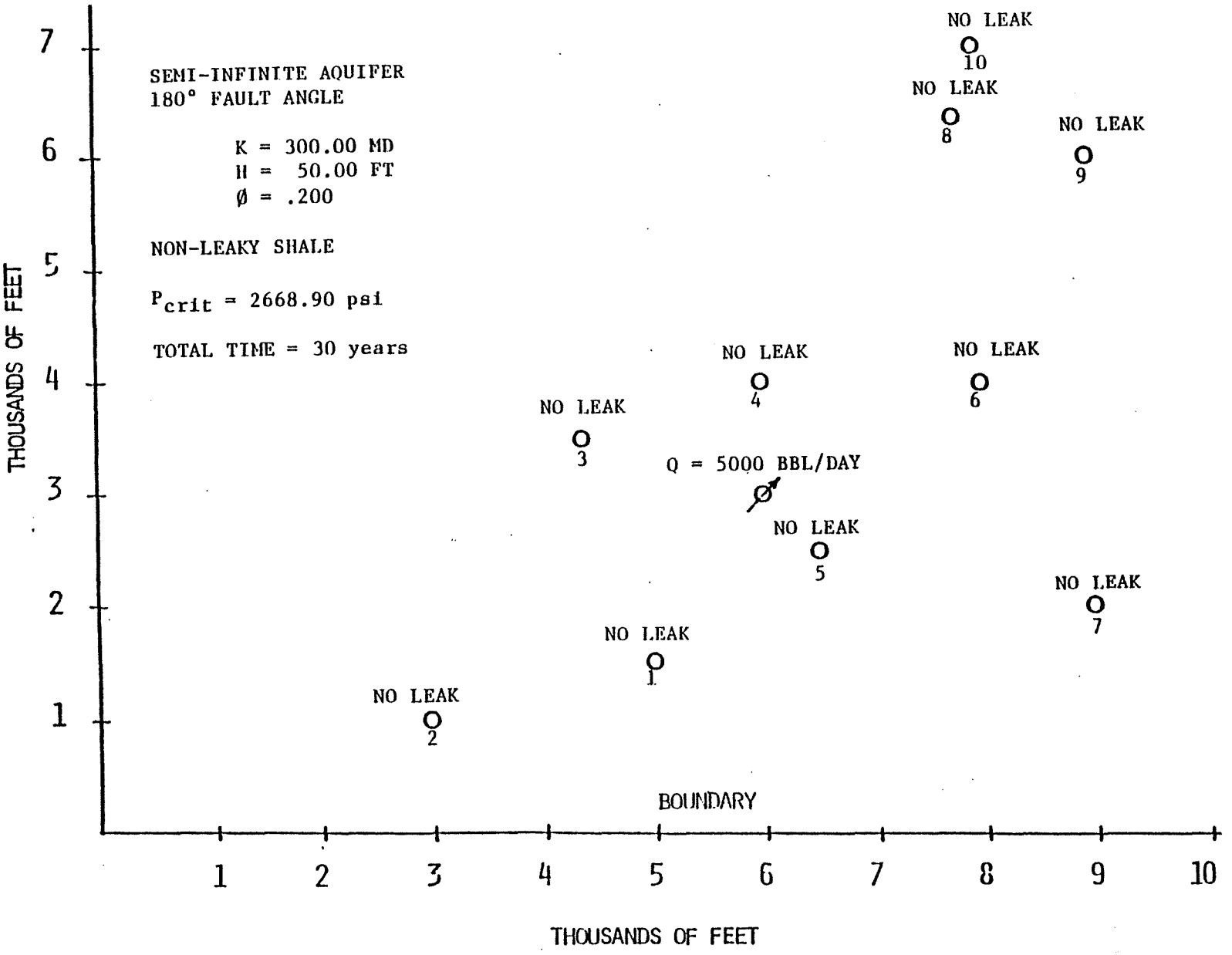

CASE 11, GROUP 1, NO. 2

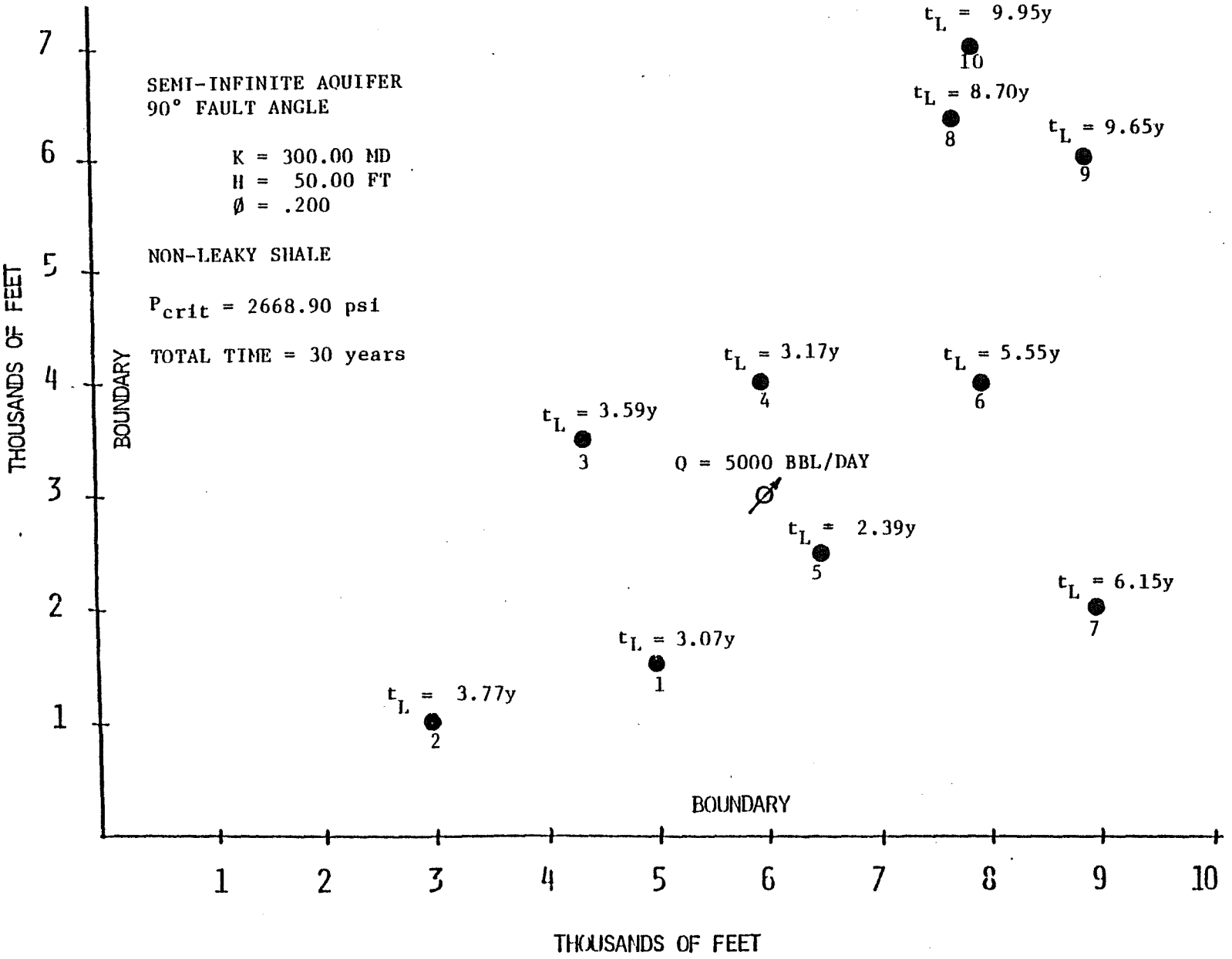

CASE II, GROUP 1, NO. 3

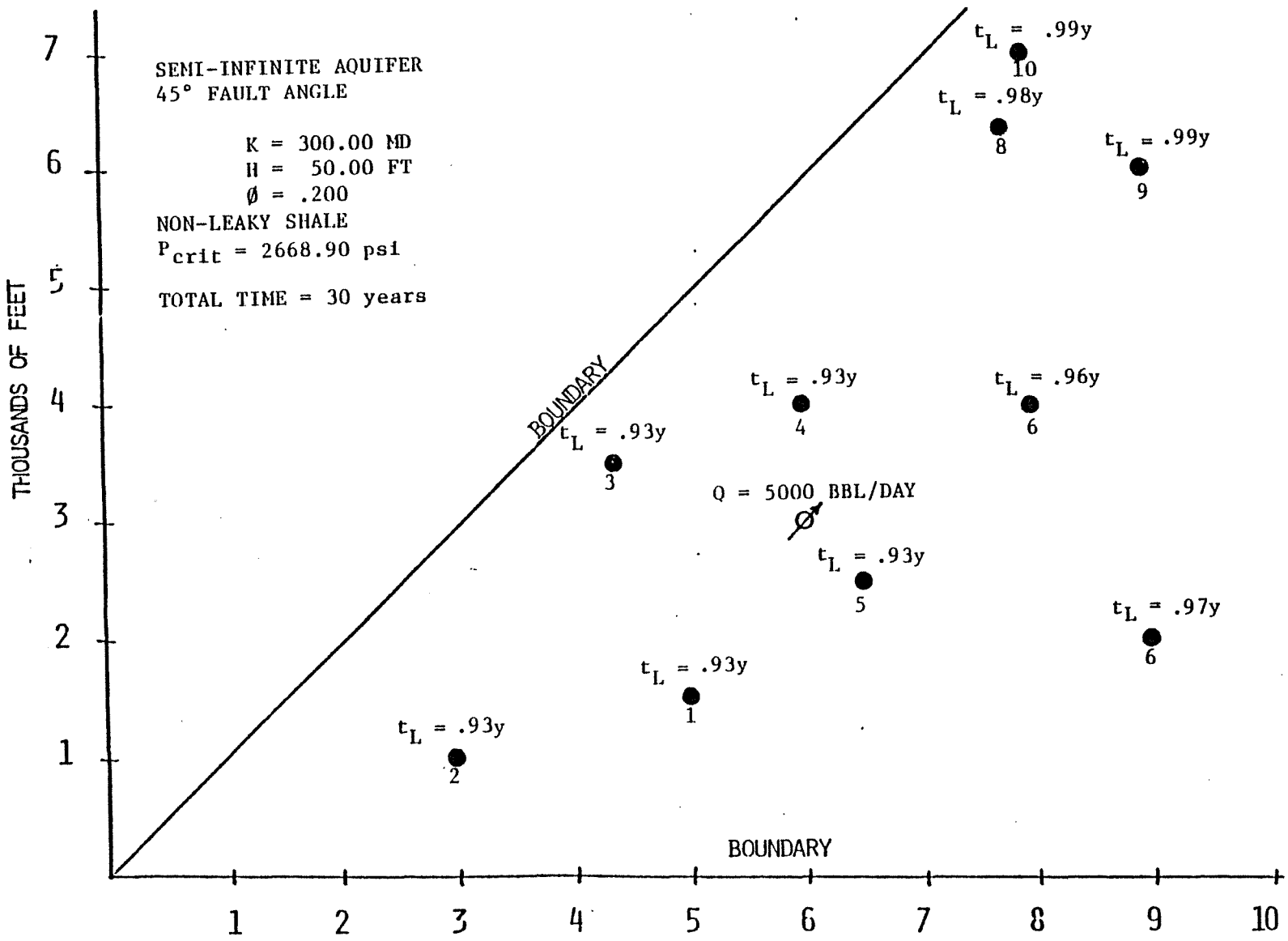

CASE II, GROUP 1, NO. 4

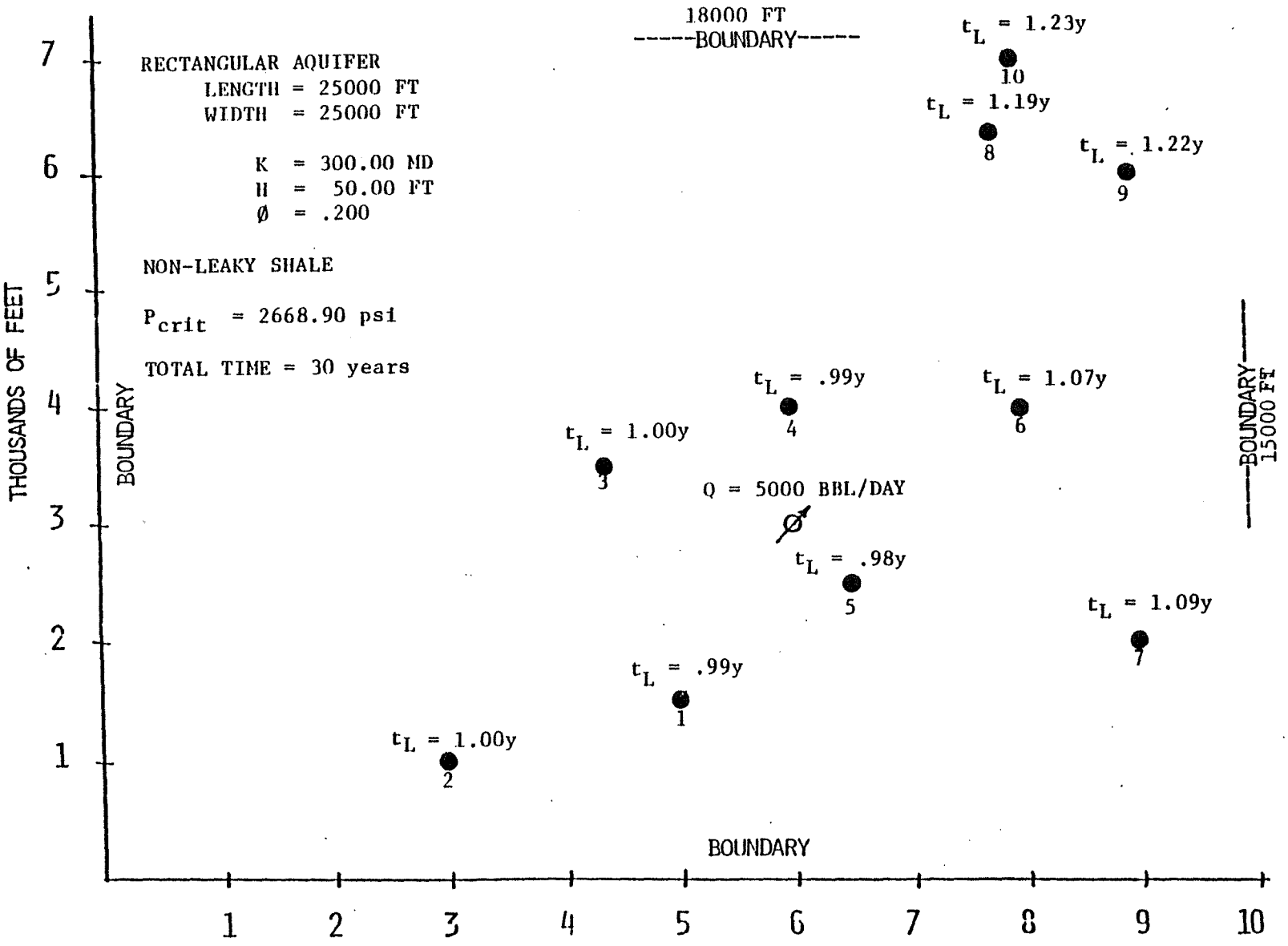

CASE II, GROUP 1, NO. 5

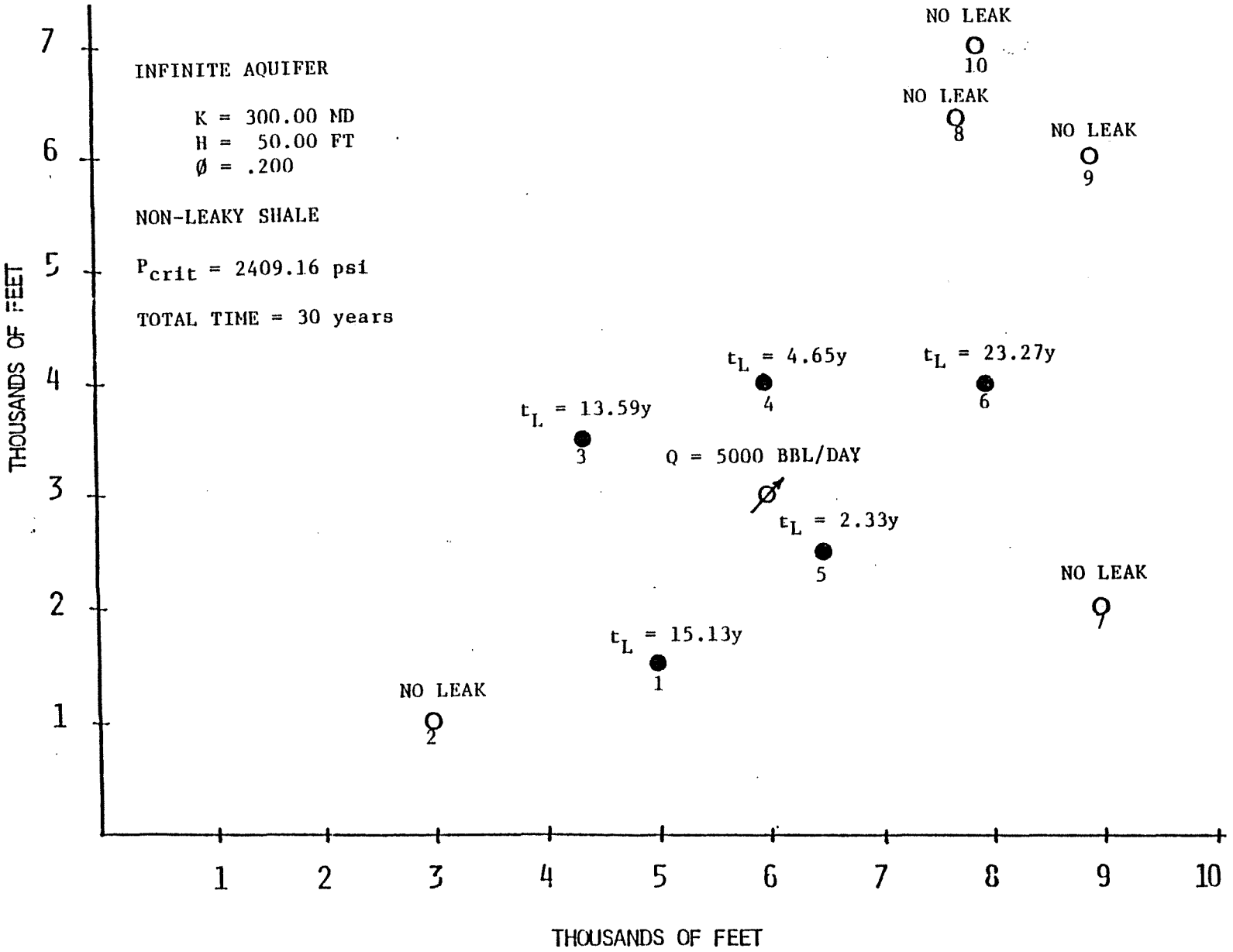

CASE II, GROUP 2, NO. 1

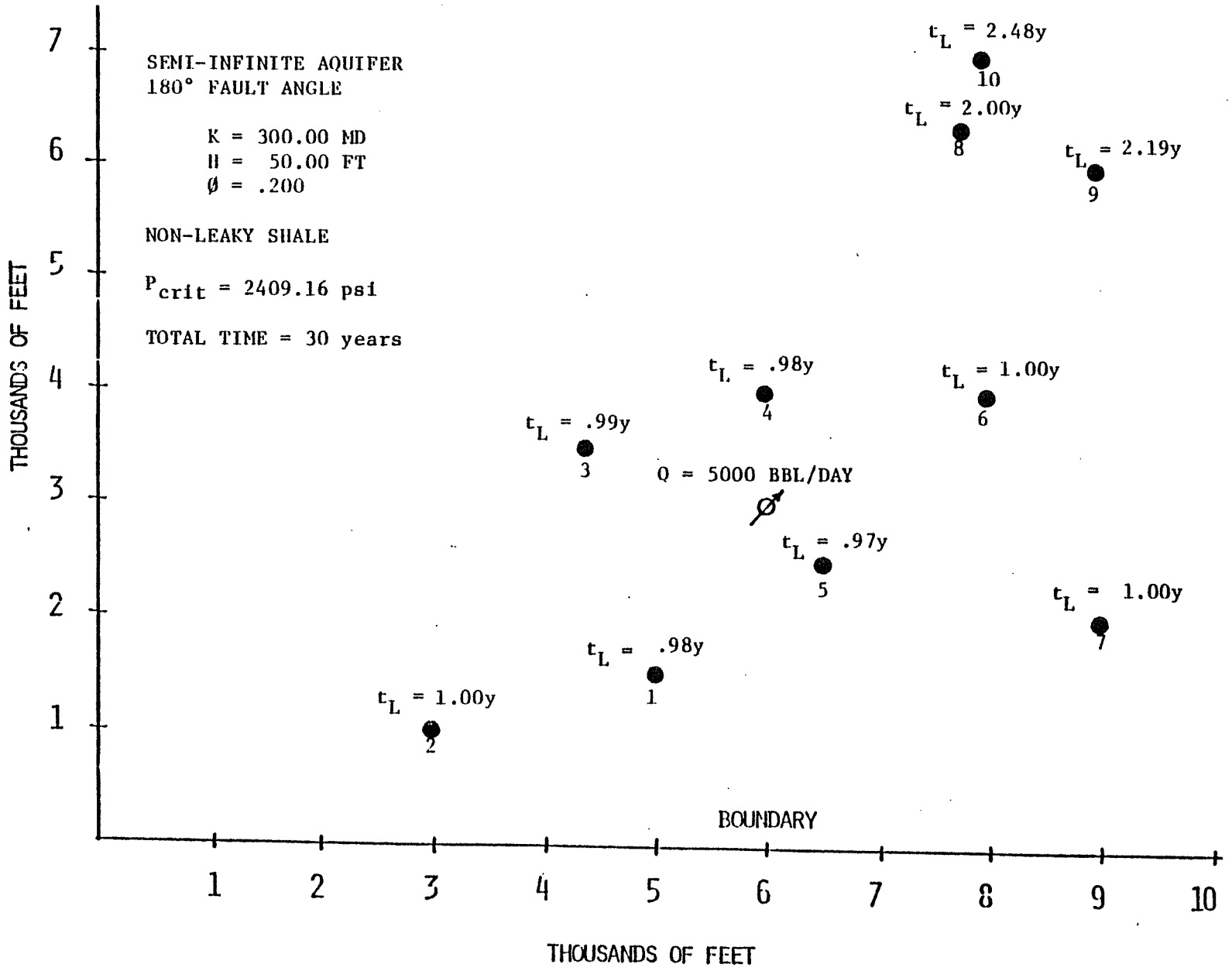

CASE II, GROUP 2, NO. 2

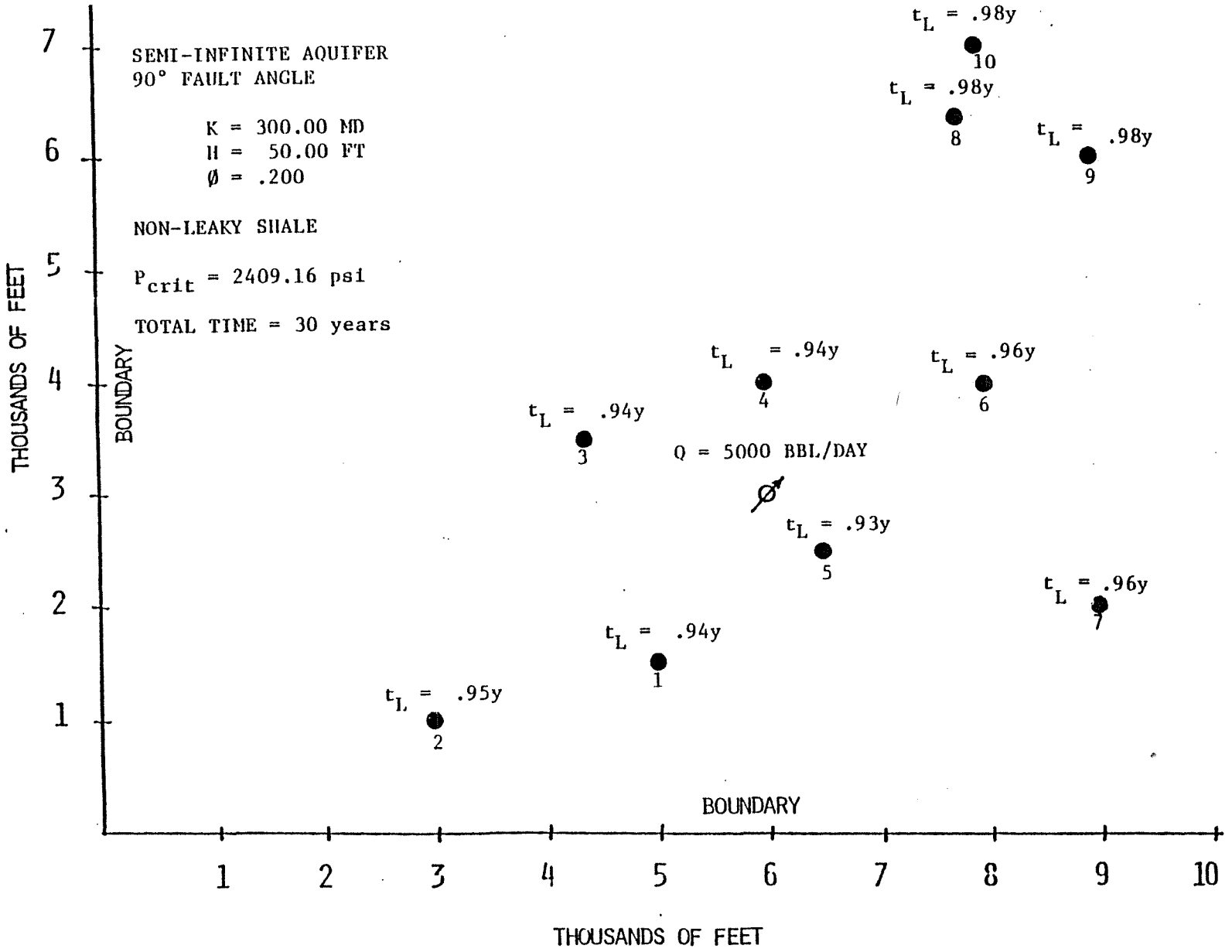

CASE II, GROUP 2, NO. 3

THIS PAGE

INTENTIONALLY

LEFT BLANK

CASE II

PROPERTIES OF THE DISPOSAL ZONE
****
COMPRESSIBILITY = 0.500E-05 1/PSI
PERMEABILITY = 300.000 MD
VISCOSITY = 1.000 CP
THICKNESS = 50.0 FT
POROSITY =0.200
****

PROPERTIES OF THE FRESH WATER ZONE
****
COMPRESSIBILITY = 0.100E-04 1/PSI
PERMEABILITY = 30.000 MD
VISCOSITY = 1.000 CP
THICKNESS = 50.0 FT
POROSITY =0.200

PROPERTIES OF THE SHALE LAYER
****

SHALE PERMEABILITY =0.10000E-02 MD
SHALE THICKNESS = 1.00000 FT

PROPERTIES OF ABANDONED HOLES

ABAN WELL	DIAM	DEPTH TO DISP ZONE	DEPTH TO H2O ZONE	MUD DENSITY	GEL STRENGTH	CRITIC PRESSU
	IN	FT	FT	LB/GAL	LB/100FT2	PSI
1	9.6	5000.00	600.0	8.600	75.00	2365.87
2	9.6	5000.00	600.0	8.600	75.00	2365.87
3	9.6	5000.00	600.0	8.600	75.00	2365.87
4	9.6	5000.00	600.0	8.600	75.00	2365.87
5	9.6	5000.00	600.0	8.600	75.00	2365.87
6	9.6	5000.00	600.0	8.600	75.00	2365.87
7	9.6	5000.00	600.0	8.600	75.00	2365.87
8	9.6	5000.00	600.0	8.600	75.00	2365.87
9	9.6	5000.00	600.0	8.600	75.00	2365.87
10	9.6	5000.00	600.0	8.600	75.00	2365.87

COORDINATES OF THE ABANDONED WELLS

WELL #	X FT.	Y FT.
1	5000.000	1500.000
2	3000.000	1000.000
3	4400.000	3600.000
4	6000.000	4000.000
5	6500.000	2500.000
6	8000.000	4000.000
7	9000.000	2000.000
8	7800.000	6400.000
9	9000.000	6000.000
10	8000.000	7000.000